Constructive methods for estimation and control of nonlinear dynamical systems with applications to HCI modeling

THESIS PREPARED AT INRIA BY

ANATOLII KHALIN

TO BE DEFENDED ON DECEMBER 16TH, 2022 IN FRONT OF THE JURY:

M.	MOHAMED DAROUACH	Professor, CRAN, University of Lorraine	(Reviewer)
M.	GIORDANO SCARCIOTTI	Lecturer, Imperial College, UK	(Reviewer)
M.	MAMADOU MBOUP	Professor, CReSTIC, University of Reims Champagne Ardenne	(Examiner)
M.	GÉRY CASIEZ	Professor, CRIStAL, University of Lille	(Co-adviser)
M.	DENIS EFIMOV	Research Director, Inria	(Co-supervisor)
Mme.	ROSANE USHIROBIRA	Researcher, Inria	(Supervisor)
M.	STANISLAV ARANOVSKIY	Associate Professor CentraleSupélec Rennes	(Invited)

A thesis submitted in fulfillment of the requirements
for the degree of Doctor of Philosophy in Computer Science and Automatic Control

DOCTORAL SCHOOL MADIS 631

THÈSE

POUR OBTENIR LE GRADE DE

DOCTEUR DE L'UNIVERSITÉ DE LILLE

DANS LA SPÉCIALITÉ

"GÉNIE INFORMATIQUE, AUTOMATIQUE ET TRAITEMENT DU SIGNAL"

PAR

ANATOLII KHALIN

MÉTHODES CONSTRUCTIVES POUR L'ESTIMATION ET LE CONTRÔLE DES SYSTÈMES DYNAMIQUES NON LINÉAIRES AVEC APPLICATIONS À LA MODÉLISATION EN IHM

THÈSE À SOUTENIR LE 16 DÉCEMBRE 2022 DEVANT LE JURY COMPOSÉ DE:

M.	MOHAMED DAROUACH	Professeur, CRAN, Université de Lorraine	(Rapporteur)
M.	GIORDANO SCARCIOTTI	Lecturer, Imperial College, UK	(Rapporteur)
M.	MAMADOU MBOUP	Professeur, CReSTIC, Université de Reims Champagne Ardenne	(Examinateur)
M.	GÉRY CASIEZ	Professeur, CRIStAL, Université de Lille	(Co-encadrant de Thèse)
M.	DENIS EFIMOV	Directeur de Recherche, Inria	(Co-Directeur de Thèse)
Mme.	ROSANE USHIROBIRA	Chargée de Recherche, Inria	(Directeur de Thèse)
M	STANISLAV ARANOVSKIY	Maître de Conferénces, CentraleSupélec Rennes	(Invité)

THÈSE PRÉPARÉE À INRIA LILLE - NORD EUROPE

ECOLE DOCTORALE MADIS 631

Abstract

This work presents results for modeling, estimating, and controlling particular classes of nonlinear dynamical systems, focusing on simplifying the practical implementation of these methods. The thesis is divided into two main parts. The first part is motivated by applying control theory to human-computer interaction (HCI) problems, with the modeling and parameter identification for computer mouse navigation.
Chapter 2 proposes a simplified pointing model as a dynamic feedback-based system incorporating humans and computers in a single loop. Then, the model parameter identification is used to develop an online endpoint prediction algorithm. The mouse position increment signal from noisy experimental data is used for validation.
The second part presents advances in the estimation and control of nonlinear systems using the notion of an attractive steady-state solution of the system driven by a signal generator, often used in model reduction or output regulation frameworks. This notion is applied to two different classes of nonlinear systems. For the first class of models studied in Chapter 3, a simple analytical expression of the steady-state is obtained as a solution of linear matrix inequalities and equalities without any partial differential equations used in classical theory. The advantage of these results is demonstrated in two applications. The first application is the design of robust reduced-order observers and tracking control for the case of two interconnected systems of the same class. The second application, presented in Chapter 3, is the design of robust reduced-order observers in both continuous and discrete time for time-varying systems, which also incorporates adaptive linear and nonlinear regression.
Chapter 4 considers the second class of nonlinear systems based on a triangular structure, i.e., upper triangular, lower triangular, or a mix between the two. It is shown that, in this case, the nonlinear steady-state solution can be found analytically using techniques similar to backstepping or forwarding. The result is applied to the design of a robust reduced-order observer with the corresponding system input.
Numerical simulations validate the applications of the second part of the thesis based on real-world dynamic models and benchmark examples: an anaerobic digestion bioreactor model, Chua networks, a two-mass spring system, and a mechanical arm.

Résumé

Ce travail présente des résultats de modélisation, d'estimation et contrôle de classes particulières de systèmes dynamiques non linéaires en se concentrant sur la simplification de l'implémentation pratique de ces méthodes. La thèse est divisée en deux parties principales. La première partie est motivée par l'application de la théorie du contrôle aux problèmes d'interaction humain-machine (IHM), avec la modélisation et l'identification des paramètres pour la navigation de la souris d'ordinateur.
Le chapitre 2 propose un modèle de pointage simplifié en tant que système dynamique basé sur la rétroaction incorporant l'humain et l'ordinateur dans une seule boucle. Ensuite, l'identification des paramètres du modèle est utilisée pour développer un algorithme de prédiction de pointage en ligne. Le signal d'incrémentation de la position de la souris provenant de données expérimentales bruitées est utilisé pour la validation.
La deuxième partie présente les avancées dans l'estimation et le contrôle des systèmes non linéaires en utilisant la notion de solution attractive en régime permanent du système piloté par un générateur de signaux, souvent utilisée dans les cadres de réduction de modèle ou de régulation de sortie. Cette notion est appliquée à deux classes différentes de systèmes non linéaires. Pour la première classe de modèles étudiés dans le chapitre 3, une expression analytique simple de l'état stationnaire est obtenue comme une solution d'inégalités et d'égalités matricielles linéaires sans aucune implication des équations différentielles partielles utilisées dans la théorie classique. L'avantage de ces résultats est démontrée dans deux applications. La première application est la conception d'observateurs robustes d'ordre réduite et la commande de suivi pour le cas de deux systèmes interconnectés de même classe. La deuxième application, présentée dans le chapitre 3, est la conception d'observateurs robustes d'ordre réduite, à la fois en temps continu et en temps discret, pour des systèmes variant dans le temps, qui intègre également la régression linéaire et non linéaire adaptative. Dans le chapitre 4, la deuxième classe de systèmes non linéaires est considérée, basée sur une structure triangulaire, c'est-à-dire triangulaire supérieure, triangulaire inférieure, ou d'un mélange entre les deux. Il est démontré que, dans ce cas, la solution non linéaire en régime permanent peut être trouvée analytiquement en utilisant des techniques similaires au backstepping ou au forwarding. Le résultat est appliqué à la conception d'un observateur robuste d'ordre réduit avec l'entrée correspondante du système.
Des simulations numériques valident les applications de la deuxième partie de la thèse sur la base de modèles dynamiques du monde réel et d'exemples de référence, à savoir un modèle de bioréacteur de digestion anaérobie, les réseaux de Chua, un système de ressort à deux masses et un bras mécanique.

Contents

List of Figures

Notation

$\mathbb{R}$	The sets of real numbers
$\mathbb{N}$	The sets of natural numbers
$\mathbb{R}_+ := \{t \in \mathbb{R} \mid t \geq 0\}$	The set of positive real numbers
$\mathbb{R}^n$	The space of real vectors of dimension n
$\mathbb{R}^{n\times m}$	The space of real matrices of dimension $n \times m$
$u : \mathbb{R}_+ \to \mathbb{R}^n$	A Lebesgue measurable function
$\|\cdot\|$	Euclidean norm in $\mathbb{R}^n$
$\|u\|_{[t_1,t_2)} = \text{ess sup}_{t\in[t_1,t_2)} \|u(t)\|$	The norm of a function, for $[t_1, t_2) \subset \mathbb{R}_+$
$\mathcal{L}^n_\infty$	The set of functions $u : \mathbb{R}_+ \to \mathbb{R}^n$ such that $\|u\|_\infty = \|u\|_{[0,+\infty)} < +\infty$
$A^\top$	The transpose of matrix $A \in \mathbb{R}^{n\times n}$
$\lambda_{\min}(A)$ and $\lambda_{\max}(A)$	The minimal and maximal eigenvalue of a symmetric matrix A, respectively.
I_n	The $n \times n$ identity matrix
Λ_j	A diagonal matrix with $\Lambda_j \in \mathbb{R}$ with $j = 1, \ldots, r$
$\Lambda = \text{diag}(\Lambda_j)_{j=1}^r \in \mathbb{R}^{r\times r}$	The main diagonal of the matrix
$\|u\|_\infty = \sup_{k\in\mathbb{N}} \|u_k\|$	The norm for a sequence $u = (u_k)_{k\in\mathbb{N}} \subset \mathbb{R}^n$
L^n_∞	The set of sequences with the finite norm $\|u\|_\infty < +\infty$
$\underline{\xi}_i$	The subvector $(\xi_1\ \xi_2\ \ldots\ \xi_i)^\top \in \mathbb{R}^i$ of a vector $\xi = (\xi_1\ \ldots\ \xi_n)^\top \in \mathbb{R}^n$
$\overline{\xi}_i$	The subvector $(\xi_i\ \xi_{i+1}\ \ldots\ \xi_n)^\top \in \mathbb{R}^{n-i+1}$ of a vector $\xi = (\xi_1\ \ldots\ \xi_n)^\top \in \mathbb{R}^n$

List of Abbreviations

HCI	**H**uman **C**omputer **I**nteraction
LME	**L**inear **M**atrix **E**qualities
LMI	**L**inear **M**atrix **I**nequalities
PDE	**P**artial **D**ifferential **E**quations
LTI	**L**inear **T**ime **I**nvariant
ISS	**I**nput-to-**S**tate **S**tability
IOS	**I**nput-to-**O**utput **S**tability
HOMD	**HOM**ogeneous **D**ifferentiator
DREM	**D**ynamic **R**egressor **E**xtension and **M**ixing
δ**ISS**	Incremental **I**nput-to-**S**tate **S**tability
PTF	**P**ointing **T**ransfer **F**unction
KEP	**K**inematic **E**ndpoint **P**rediction
MAE	**M**ean **A**bsolute **E**rror
ANOVA	**AN**alysis **O**f **VA**riance
PE	**P**ersistent **E**xcitation
CPI	**C**ounts **P**er **I**nch
KTM	**K**inematic **T**emplate **M**atching
VITE	**V**ector **I**ntegration **T**o **E**ndpoint
ID	**I**ndex of **D**ifficulty

Chapter 1

General Introduction

1.1 Motivation and goals

This first section is dedicated to describing the background of the thesis. The main ideas on which the research was based and developed are expressed here. We start from the problem of human behavior modeling, analyzing and simplifying models of human behavior prediction during the fulfillment of basic tasks, such as pointing. Continuing in this direction, we investigate several challenging nonlinear control and estimation problems trying to find a way to restate them for possible applications. Therefore, one of the thesis's key motivations is simplifying a complex nonlinear analysis or design problem regarding control and estimation.

1.1.1 Human behavior modeling

Modeling human behavior is a complicated issue for several causes: its nonlinearity, the uniqueness of the person's behavior, the decision-making process, and the noise presence, usually of unknown nature. For these reasons, the dynamics of human motion is challenging to model and to predict.

Especially nowadays, since computer and information technologies have conquered a big part of our everyday lives, the optimization in a smooth and pleasurable manner of Human-Computer Interaction (HCI) processes has become an important issue. There are different approaches to analysis and design of HCI algorithms, some of them are based on the control theory. According to [Oulasvirta et al., 2018], it allows the user and computer systems to be linked by describing the communication between the parts and the process dynamics as a whole. In such an approach, human-computer interaction can be presented as a feedback interconnection. An experimental comparison of different methods demonstrates that control theory applications are up-and-coming in the HCI domain [Müller, Oulasvirta, and Murray-Smith, 2017]. For instance, casual and well-known human movements, such as indirect (pointing, dragging, tracking) or direct tasks (swipes, flicks, taps, *etc*.), can be modeled and approximated with coupled dynamical systems and feedback laws, using the automatic control theory approach.

Control theory is an important framework allowing the design and analysis of models for dynamical systems in general. In practical cases, these systems are artificial. Nevertheless, automatic control theory methods can still be applied to the case of human behavior. A prominent application case lies in computational technology, where the development of algorithms and mathematical models can be used to elucidate and improve human-computer interactions. The use of control theory methods in this field allows a vital way to formalize the interaction as a dynamical system with a feedback loop. The user in this system is seen as the controller who adapts its behavior to the feedback and can then alter a control signal to the desired reference level. The outputs of the considered system are the observed transformations. An advantage of a closed-loop system lies in the ability of the user to compensate for possible disturbances that might affect the system. This way, dynamical modeling enables a continuous insight into the consequences of changes in the user's behavior or the system's one.

Various methods in control theory do exist to estimate transfer functions of dynamical systems of different complexities by identifying parameters or performing numerical derivation. Nowadays, novel system identification techniques allow estimating the state and parameters of complex dynamical systems in finite time. In this spirit, the problem considered was the modelization and parameter identification of the indirect pointing

task. This thesis's first goal was to improve the dynamical model for pointing tasks proposed in [Aranovskiy et al., 2020] using experimental data. An important goal was a task's endpoint estimation using a finite-time observer and linear regression estimation techniques. This procedure allowed designing a controller to answer the human decision process in real-time and facilitate the interaction.

Therefore, the first part of the thesis is dedicated to the automatic control theory application to HCI and technical and theoretical analysis related to modeling and prediction. One of the tasks of this manuscript is to improve the dynamical model for pointing tasks with appropriate choices of transfer functions.

1.1.2 Estimation of feedback interconnected systems

There are many real-world scenarios in nature and technology where we have a model describing dynamical processes, which can be observed through the output of another uncertain dynamical system. Often, these systems take feedback from each other: they are interconnected. Continuing the analysis of the control and estimation problem for nonlinear systems in the second part of the thesis, we study how the system states and outputs in these interconnections influence each other and can be linked through some expression as a gain or a mapping. The nature of such mapping can differ for every case; for instance, it is a gain between the cursor and mouse velocity and position in a pointing task. Another example, which will be given in the thesis, is the model representing a two-stage anaerobic digestion process [Bernard et al., 2001], where we have two sets of bacteria. The link between their states (population and substrate concentrations) appears to be a linear combination of yield coefficients (the amount of cell mass or product related to the consumed substrate) and their ratios (for details, see the Example 1 of 3.2.4 in Chapter 3). However, in most cases for nonlinear interconnected systems, this mapping is nonlinear and not simple to find in practice. Most frameworks that try to determine this mapping (such as the output regulation theory for nonlinear systems [Isidori and Byrnes, 1990] or the nonlinear model reduction theory based on moment matching [Astolfi, 2010]) provide general theoretical results to find the relation between the so-called steady-states of both systems. Although the basic procedure is provided in these frameworks, it usually requires solving PDEs and nonlinear function inversions, making it challenging for applications in some cases. Therefore, a more straightforward and better approach for certain classes of systems could be researched and applied.

The mapping mentioned above between the systems is essential in analyzing control problems. In an observation problem, where we do not have access to all states of the second system, we can estimate them through mapping from the first system. Another problem is the tracking control synthesis, where we have to design the input from one system (with no accessible states) to another (the output of which is available for measurements), so the latter will follow the reference dynamics. In such a setting, an additional question arises: how to design such a controlling input while simultaneously simplifying the state estimation for both dynamics? Another relevant question is: for which classes of nonlinear systems is it possible to solve the problem by minimizing the use of resources and computational power?

Similar ideas appear in the case where the second system can also be presented as an observer for the original system. The link between them can help in the estimation problem and reduce the order of the observer. A more detailed explanation of all the scenarios considered in this thesis can be found in the introduction of Chapter 3.

All challenges just described motivate us to investigate the mentioned problems and simplify the analysis when possible. The series of issues studied in this thesis is not exhaustive but rather demonstrative that the methods adapted to a particular class of models can still be more beneficial for nonlinear problems than a general approach.

1.2 State of the Art

1.2.1 Pointing Task

Modeling

The first concept related to the modeling of a pointing task was the Fitts law [Fitts, 1954], which states that the pointing time has a logarithmic relation to the ratio of distance and the target's width, also called the Index of Difficulty (ID). The Fitts law has been experimentally validated many times [Zhai, Kong, and Ren, 2004, Chapuis, Blanch, and Beaudouin-Lafon, 2007]. However, the Fitts law can model pointing time in relation to the ID of the task, but it does not allow modeling of the dynamics of the movement.

The so-called surge model in [Costello, 1968] was the first attempt to provide a dynamical pointing model. It tried to model the task in two modes: the constant-coefficient model and the second-order controller model, representing open-loop and closed-loop phases correspondingly. Later, VITE (Vector Integration to Endpoint) model was introduced in [Bullock and Grossberg, 1988] as a linear time-invariant system describing the motion, controlled by an agonist-antagonist pair of muscles (wrist rotation). Simultaneously, [Meyer et al., 1988] established that the pointing task contains two phases: a ballistic (supposed to be an open-loop process of the initial movement towards the target) and a correction phase (that finishes the task by closed-loop visual guidance until the target is reached). This concept was called Meyer's optimized initial impulse model [Meyer et al., 1988]. Another feature of this model was the possibility of modeling the multiple open-loop phases (also called sub-movements). More recently, based on this principle and the VITE model, a united switched dynamical model was created in [Aranovskiy et al., 2020], verified by experimental data of [Casiez and Roussel, 2011], and whose closed-loop stability has been proven. Another line of research was based on Todorov's optimal feedback control of motor coordination [Todorov and Jordan, 2002, Todorov, 2004, Todorov and Li, 2005]. The main idea was to apply stochastic optimal control to model a human movement [Qian et al., 2013, Rigoux and Guigon, 2012, Izawa et al., 2008]. The latest result of such an approach can be found in [Berret et al., 2021], where, besides feedback, the authors also consider feedforward control, which models the part of the process with motor planning to generate a command (before the movement begins). Another recent idea was based on the so-called intermittent control [Martín et al., 2021]. The key feature of the latter framework was a built-in event-based trigger, which allowed the model to switch between closed- and open-loop control depending on the error between the goal point and the one observed by the user. Such an approach appeared to be compatible with current physiological and psychological theories. A different view on modeling worth mentioning is the information theory. In the recent work of [Gori and Rioul, 2020], the two-phase process is viewed as a communication problem where the information is transmitted from a source (initial/current point) to a destination (endpoint) over a so-called channel, perturbed by Gaussian noise with a presence of feedback (in a second phase). Despite the diversity of approaches for modeling the pointing task, we believe that searching for a simple and, at the same time, accurate model is yet a relevant research direction.

Parameter Identification

Several papers have been published on endpoint prediction, but few algorithms in this area have been proposed. In [Lank, Cheng, and Ruiz, 2007], the kinematic endpoint prediction (KEP) model was introduced. This model is based on the minimum jerk law, formulated in [Hogan, 1984], and the proposed prediction relies on a polynomial curve fitting (based on a fourth-order polynomial). The model showed the best performance at 80% of the path and distances of more than 600 pixels. Another idea was presented in [Asano et al., 2005], where a simple regression-based extrapolation was used, making the endpoint guess at the peak of the velocity. The prediction technique based on the inverse optimal control model was introduced in [Ziebart, Dey, and Bagnell, 2012], where a probabilistic model and machine learning were combined. It performed better than previously proposed models, especially during short-distance trials. The kinematic template matching concept was introduced in [Pasqual and Wobbrock, 2014], where the template matching algorithm compares the velocity profile and decides which distance the user wants to cover based on previous trials. The algorithm showed a better performance for the 2D task than the KEP model and reasonable general accuracy.

We can formally divide all existing endpoint prediction algorithms into two groups:
group I) algorithms with knowledge about previous trials (memory), and
group II) without any knowledge (no memory).

In the first group, we can put the algorithms based on linear regression [Asano et al., 2005], any machine learning tools [Ziebart, Dey, and Bagnell, 2012], and the recently introduced KTM algorithm [Pasqual and Wobbrock, 2014] because they all require several trials of the same user or on the same setup to identify the endpoint online. The algorithms without memory, such as KEP [Lank, Cheng, and Ruiz, 2007], rely on more general rules and assumptions about the motion, and they can be applied from the first try.

Another innovative idea for facilitating the target acquisition for the user was presented in [Rozado, 2013]. The author used a target prediction approach with the eye-gaze device, and the idea was to skip the ballistic phase entirely by cursor warping (moving the pointer directly to the area of users' sight). The results of the experiments showed a significant decrease in the pointing time. In this thesis, we will follow the classical pointing task setup, using only the computer mouse for our prediction algorithm since it is the typical case for most users.

Despite all these achievements, the current state of the art can still be improved in many ways. For example, since all algorithms mentioned above do not utilize a dynamical pointing model representing both sides of the process (human and the computer) in the interconnection, the results are less general and less accessible for analysis. Algorithms based on machine learning or probability techniques do not explain the nature of the movement well, and their results are unreliable in unusual setups and situations.

1.2.2 Steady-state Estimation

Nonlinear Model Reduction

One of the mentioned frameworks for the behavior analysis of complex nonlinear systems is called nonlinear model reduction by moment matching. It was recently introduced in [Astolfi, 2010, Scarciotti and Astolfi, 2017a, Padoan and Astolfi, 2020]. The model reduction by moment matching for nonlinear systems is based on the output regulation theory and the center manifold theory. The output regulation theory is a concept dedicated to controlling a nonlinear dynamical plant using another system [Francis and Wonham, 1976, Isidori and Byrnes, 1990]. The center manifold theory asserts that under certain assumptions, any nonlinear system must have a central manifold, meaning an invariant subspace containing the steady-state solution of the system that can be used to replicate its behavior (i.e., by frequency response).

Recently developed, the theory of model reduction by moment matching for nonlinear systems expresses more general conditions on the existence of such a solution. However, despite the theoretical approach presented in [Astolfi, 2010], the problem of calculating this response for nonlinear systems is not an easy task and must be solved for different classes of systems separately.

In this thesis, we borrow some tools from the nonlinear model reduction by moment matching theory and the *invariant manifold approach* to look for the expression of steady-state solutions of some particular classes of nonlinear systems, which are later used to solve estimation and control problems for particular classes of systems.

Reducer-order observer

Reducing the order of the observer is a relevant sub-problem, the main idea being to separate the dynamics of measured states from unmeasured ones and disregard the estimate of known variables. This approach greatly simplifies systems analysis, modeling, and real-life applications. First stated in [Luenberger, 1964], such an idea presented for the linear case had many continuations in nonlinear analysis, some of them using linearization techniques [Sundarapandian, 2006b] and others based on solutions of partial differential equations (PDEs). Reduced-order observers were also studied for discrete-time systems in linear [Leondes and Novak, 1974] and nonlinear settings [Boutayeb and Darouach, 2000, Sundarapandian, 2006a].

1.3 Preliminaries

The following section presents the baseline mathematical concepts and definitions used in the thesis.

1.3.1 Dynamical systems

The scientific community broadly accepts the concept of a dynamical system as the basis to describe any artificial or real-life processes. Therefore, there are plenty of different definitions in the literature, based on the area of interest, describing the same phenomenon.

One of the most commonly used is a dynamical system in *the implicit form*:

$$\Sigma_1 : \begin{cases} \dot{x}(t) = f\left(x(t), u(t)\right), \\ y(t) = h(x(t)), \end{cases} \tag{1.1}$$

where $x : \mathbb{R}_+ \to \mathbb{R}^n$ is the *state* of a dynamical system Σ_1, n is the *order* of the system, $u : \mathbb{R}_+ \to \mathbb{R}^m$ is the *input* of Σ_1 (for example, a signal in $\mathcal{L}_\infty^m$), $y : \mathbb{R}_+ \to \mathbb{R}^p$ is the *output* of the system Σ_1, $f : \mathbb{R}^n \times \mathbb{R}^m \to \mathbb{R}^n$, $h : \mathbb{R}^n \to \mathbb{R}^p$ are continuous *functions*. There are two key assumptions on continuous dynamical systems: the *existence* and *uniqueness* of a solution and *forward completeness*. More precisely, the former properties imply that (1.1), with *initial conditions* $x_0 \in \mathbb{R}^n$ and an admissible input u is assumed to have a *solution* $x(t, x_0, u)$ defined on an interval of time $[0, T)$ for some $T \geq 0$.

Definition 1.3.1. *The system* (1.1) *is forward complete if for all initial conditions $x_0 \in \mathbb{R}^n$ and inputs u, the solution $x(t, x_0, u)$ is uniquely defined for all $t \geq 0$.*

The system (1.1) is called a *continuous-time system*, and t takes values from $\mathbb{R}_+$ (positive real values). However, in some cases (especially in practice) another description of the system is useful: when $t \in \mathbb{N}$ (takes integer values), this system is called a *discrete-time system*. It can be expressed as follows:

$$\Sigma_1^d : \begin{cases} x_{k+1} = f(x_k, u_k), \\ y_k = h(x_k), \end{cases} \tag{1.2}$$

where $x_k \in \mathbb{R}^n$, $u_k \in \mathbb{R}^m$, $y_k \in \mathbb{R}^p$ are the state, bounded external input and the output vector at time instant $k \in \mathbb{N}$, respectively and $f : \mathbb{R}^n \times \mathbb{R}^m \to \mathbb{R}^n$, $h : \mathbb{R}^n \to \mathbb{R}^\ell$ are nonlinear functions as defined before. Throughout most of the thesis, the analysis for continuous-time systems as (1.1) will be considered. However, in some practical cases, the discrete-time analysis will be presented, for instance, in parameter identification and signal processing.

Generally, the problems of dynamical systems can be grouped into three categories: *Modeling*, *Analysis*, and *Estimation and Control*. All three will be partially covered in this thesis.

1.3.2 Modeling

The term *model* of a system refers to the representation of the evolution of a dynamical system, approximated from known data or the system behavior. There are different ways to approach the model design, like the *graphical model* (which consists of impulse or step frequency responses), the *software model* (which consists of look-up tables, coded algorithms, *etc.*), and others. This thesis uses the term model for a mathematical model, representing strictly analytical methods expressed with differential or difference equations. According to Ljung, 1999, well-designed mathematical models are instrumental for simulations and prediction, extensively used in all fields, including nontechnical areas, like the economy, ecology, and biology. Generally, there are two ways to obtain a mathematical model: *modeling* and *system identification* or a mixture of both. The latter is the one that will be used in the thesis. We will rely on the existing results and methods in terms of modeling, but for example, in part I, we will use tools from system identification to correct the model parameters based on the experimental data.

On the other hand, an *algorithm* is a less strict formalization and modeling method, which can represent a sequence of actions and contain a mixture of difference or differential equations, to solve a specific task.

Part I of the thesis aims to obtain a simple model and algorithm for a highly nonlinear process (the pointing task) using experimental data. In part II, models are given and the focus is on the analysis of the interconnection, state estimation, and control.

1.3.3 Stability analysis

The key property of the dynamical system analysis is the concept of *stability*. The most popular notion was introduced by Lyapunov [Lyapunov, 1992], it evolved in more than a century to obtain more advanced tools and methods of defining the stability of the system.

In order to use the different definitions of stability, we first have to define two classes of *comparison functions*. A function $\alpha : \mathbb{R}_+ \to \mathbb{R}_+$ is of *class* $\mathcal{K}_\infty$ if it is continuous, strictly increasing, unbounded, and satisfies $\alpha(0) = 0$. A function $\beta : \mathbb{R}_+ \times \mathbb{R}_+ \to \mathbb{R}_+$ is of *class* $\mathcal{KL}$ if $\beta(\cdot, t) \in \mathcal{K}_\infty$ for each t and $\beta(r, t)$ decreases to zero with $t \to \infty$, for each fixed r.

Using these two classes, several definitions are formulated.

Definition 1.3.2. *The system* (1.1) *without inputs* u *(*$u = 0$*) is* globally asymptotically stable (GAS) *if there exists a function* $\beta \in \mathcal{KL}$ *such that*

$$|x(t, x_0)| \leq \beta(|x_0|, t), \tag{1.3}$$

holds for every $x_0 \in \mathbb{R}^n$ *and every* $t \geq 0$.

Definition 1.3.3. *The system* (1.1) *is* input-to-state stable (ISS) *if there exist* $\beta \in \mathcal{KL}$ *and* $\gamma \in \mathcal{K}_\infty$ *such that*

$$|x(t)| \leq \beta(|x_0|, t) + \gamma(\|u\|_\infty) \tag{1.4}$$

holds for all $t \geq 0$*, all inputs* $u \in \mathcal{L}_\infty^m$*, and all initial conditions* $x_0 \in \mathbb{R}^n$.

Definition 1.3.4. *The system* (1.1) *is* uniformly bounded input bounded state (UBIBS) *if there exists* $\sigma \in \mathcal{K}_\infty$ *such that, for every input* $u \in \mathcal{L}_\infty^m$ *and every initial state* $\xi \in \mathbb{R}^n$*, the solution* $x(t, \xi, u)$ *is defined for all* $t \geq 0$ *and*

$$|x(t, \xi, u)| \leq \max \sigma(|\xi|), \sigma(\|u\|), \tag{1.5}$$

holds for all $t \geq 0$.

Definition 1.3.5. *The system* (1.1) *is* input-to-output stable (IOS) *if:*

- *it is UBIBS, and*
- *there exist* $\beta \in \mathcal{KL}$ *and* $\gamma \in \mathcal{K}$ *such that*

$$|y(t, \xi, u)| \leq \beta(|\xi|, t) + \gamma(\|u\|) \tag{1.6}$$

holds for all $t \geq 0$*, all* $u \in \mathcal{L}_\infty^m$ *and all* $\xi \in \mathbb{R}^n$.

Another important area of analysis of the dynamical system used in this thesis is the one of *convergence*, which was introduced by Demidovich, and used in nonlinear output regulation theory [Isidori and Byrnes, 1990, Pavlov, Wouw, and Nijmeijer, 2005].

Definition 1.3.6. *[Pavlov, Wouw, and Nijmeijer, 2005] For a given input* $u \in \mathcal{L}_\infty^m$*, system* (1.1) *is said to be* convergent *if there is a solution* $\bar{x}(t)$*, defined and bounded for all* $t \in \mathbb{R}_+$*, which is globally asymptotically stable. Such a solution* $\bar{x}$ *is called the* limit solution.

This limit solution $\bar{x}$, if it is unique, is called the *steady-state solution* (or the steady-state response) x^{ss} of system (1.1) under input u. In other words, convergence is a property of the system to "forget" its initial conditions and asymptotically converge to some solution.

Stability is important as an intrinsic property of the system, which assures the boundedness of all solutions, neglecting possible external disturbances acting on the system. Therefore, the signal u in (1.1) can be considered as a control input and also as a disturbance (usually denoted as $d \in \mathcal{L}_\infty^n$). The thesis also includes the robustness analysis of the stability property, as the goal is to deal with real-life dynamical systems and focus on practical implementation.

Therefore, let us consider system (1.1) with exogenous inputs $u \in \mathcal{L}_\infty^m$.

Definition 1.3.7. *[Angeli, 2002] System* (1.1) *is* incrementally input-to-state stable (δISS) *if there exist $\beta \in \mathcal{KL}$ and $\gamma \in \mathcal{K}_\infty$ such that for any $t \geq 0$, any $\xi_1, \xi_2 \in \mathbb{R}^n$ and any couple of inputs $u_1, u_2 \in \mathcal{L}_\infty^m$, the following is true:*

$$\|x(t,\xi_1,u_1) - x(t,\xi_2,u_2)\| \leq \beta(\|\xi_1 - \xi_2\|, t) + \gamma(\|u_1 - u_2\|_\infty).$$

This property is a robust version of the convergence given in Definition 1.3.6.

The steady-state response is often used in problems with a second system, which has to generate an input forcing the original system to converge to the required signal or trajectory effectively. Therefore, let us consider a second nonlinear continuous-time system, which is called the *signal generator* or *exosystem*:

$$\Sigma_2 : \begin{cases} \dot{\omega}(t) = s(\omega(t)), \\ u(t) = \ell(\omega(t)), \end{cases} \tag{1.7}$$

where $\omega : \mathbb{R}_+ \to \mathbb{R}^q$ is the state variable, $s : \mathbb{R}^q \to \mathbb{R}^q$, $\ell : \mathbb{R}^q \to \mathbb{R}^m$ are analytic functions with $s(0) = 0$ and $\ell(0) = 0$. The *interconnected system* is given by (1.1) and (1.7)[1]:

$$\dot{x} = f(x, \ell(\omega)), \quad \dot{\omega} = s(\omega), \quad y = h(x). \tag{1.8}$$

Next, to obtain the relation of steady-state response of (1.1) to the signal generator system (1.7), the following conditions should be imposed:

Assumption 1.3.1. *[Scarciotti and Astolfi, 2017b] System* (1.1) *is* minimal, *and the zero equilibrium is locally exponentially stable. The signal generator system* (1.7) *is observable and* neutrally stable.

The minimality condition implies the *observability* and *accessibility* of the system, notions well introduced for linear dynamical systems but rather complex to define for nonlinear cases. In [Scarciotti and Astolfi, 2017b], they are defined as follows.

Definition 1.3.8. *Two states x_1 and x_2 are said to be* indistinguishable *for* (1.1) *if for every input function u the output function $h(x_1)$ of the system for the initial state $x(0) = x_1$, and the output function $h(x_2)$ of the system for the initial state $x(0) = x_2$, coincide on their common domain of definition. The system is* observable *if it has the property that if the states x_1 and x_2 are indistinguishable then $x_1 = x_2$.*

Let us define two neighborhoods of the origins, $\mathcal{X} \subset \mathbb{R}^n$ and $W \subset \mathbb{R}^q$, for the systems (1.1) and (1.7), respectively.

Definition 1.3.9. *Let V be a neighborhood of $x(0)$ and $R^V(x(0),T)$ be the reachable set from $x(0)$ at time $T \geq 0$, following trajectories which remain in the neighborhood V of $x(0)$, for $t \leq T$, (*i.e. *all points x for which there exists an input u such that the evolution of* (1.1) *from $x(0)$ satisfies $x(t) \in V$, for $0 \leq t \leq T$, and $x(T) \in R^V(x(0),T)$). Let $R_T^V(x(0)) = \bigcup_{\tau \leq T} R^V(x(0),\tau)$. A system is* locally accessible from $x(0)$ *if $R_T^V(x(0))$ contains a non-empty open subset of $X \subset \mathbb{R}^n$ for all non-empty neighborhoods V of $x(0)$ and all $T > 0$. If this holds for all $x(0) \in \mathcal{X}$, then the system is* locally accessible.

[1] Throughout the thesis, we simplify the notation by writing, for instance, x in place of $x(t)$ when the time dependency is clear.

Next, the assumptions on system generator (1.7) are also required. We call the function $\omega(t) = \Phi_t^s(\omega_0) \in \mathcal{N} \subset \mathbb{R}^q$ a *flow*, if it is a solution (1.7) with initial condition $\omega(0) = \omega_0$.

Definition 1.3.10. *Consider the signal generator* (1.7)*. A point $\omega \in W$ is* Poisson stable *if the flow $\Phi_t^s(\omega)$ of the vector field s is defined for every $t \in \mathbb{R}$, and if for every neighborhood $\mathcal{N}$ of ω and every constant $T \in \mathbb{R}_{\geq 0}$ there exist constants $t_- < T$ and $t_+ > T$ such that $\Phi_{t_-}^s(\omega_0) \in \mathcal{N}$ and $\Phi_{t_+}^s(\omega_0) \in \mathcal{N}$. The signal generator* (1.7) *is* Poisson stable *if there exists a dense set of Poisson stable initial points in W.*

Definition 1.3.11. *The signal generator* (1.7) *is neutrally stable if it is* Poisson stable *and the zero equilibrium is stable.*

Under this hypothesis, the steady-state behavior of (1.8) can be characterized as follows.

Lemma 1.3.1. *(Lemma 2.1 in [Scarciotti and Astolfi, 2017b]) Consider the system* (1.1) *and the signal generator* (1.7)*. Suppose Assumption 1.3.1 holds. Then there is a mapping $\pi : \mathbb{R}^q \to \mathbb{R}^n$, locally defined in a neighborhood $\mathcal{W} \subset \mathbb{R}^q$ of $\omega = 0$, with $\pi(0) = 0$, which solves the partial differential equation:*

$$\frac{\partial \pi}{\partial w}(w)s(w) = F(\pi(w), \ell(w)), \quad \forall w \in \mathcal{W}. \tag{1.9}$$

In addition, the steady-state response of system (1.8) *is $x^{ss}(t) = \pi(\omega(t))$, for any $x(0)$ and $\omega(0)$ sufficiently small.*

Note that other results and definitions regarding nonlinear *moments* accompanying the theory of nonlinear model reduction can be found in [Scarciotti and Astolfi, 2017b]. This thesis focuses on the practical applicability and solution of (1.9).

To complement the theory presented above, let us define the solution of a particular partial derivative equation. Consider a quasi-linear partial differential equation of the first order [Evan, 2010] (a variant of (1.9)):

$$\frac{\partial \chi}{\partial w}\sigma(\chi, w) = \phi(\chi, w), \tag{1.10}$$

where $\chi : \mathbb{R}^q \to \mathbb{R}$ is a function, $\sigma : \mathbb{R}^{q+1} \to \mathbb{R}^q$ and $\phi : \mathbb{R}^{q+1} \to \mathbb{R}$ are real analytic functions ($\sigma(0,0) = 0$ and $\phi(0,0) = 0$), with initial or boundary conditions

$$\chi(w) = 0, \ \forall w \in \Gamma = \{w \in \mathcal{W} : w_q = 0\}, \tag{1.11}$$

where $\mathcal{W} \subset \mathbb{R}^q$ is a neighborhood of the origin and w_q denotes the q-th component of $w \in \mathbb{R}^q$. The Cauchy problem (1.10), (1.11) is called *non-characteristic* if

$$\sigma_q(0, w) \neq 0, \ \forall w \in \Gamma \setminus \{0\},$$

where the origin is excluded since, in such a case, the trivial solution $\chi(0) = 0$ exists by construction. The conditions for the existence of a solution χ to (1.10), (1.11) are given by the Cauchy-Kowalevski theorem:

Theorem 1.3.1. *[Kowalevsky, 1875] The Cauchy problem* (1.10)*,* (1.11) *has a unique real analytic solution χ on $\mathcal{W}$ if the Cauchy problem is non-characteristic.*

In the case when σ and ϕ are continuously differentiable functions, analogs of this theorem can be found, for example in [Evan, 2010; Han and Park, 2015], providing a continuously differentiable solution χ.

A solution of (1.9) represents an invariant trajectory for (1.8). In addition, if we ask for such a solution to be attractive for the surrounding trajectories in some region, we return to the concept of convergence [Pavlov, Wouw, and Nijmeijer, 2005]. Alternatively, to take into account the presence of uncertainties, we return to the concept of δISS, defined earlier. If the δISS property is satisfied, all system trajectories (1.8) converge to a solution of (1.9), and stay close to it in case of additive perturbations. The definition is given for the global stability scenario, and the local version can be obtained by restricting the set of admissible values for initial

conditions and inputs. The definition of conventional (local) input-to-state stability (ISS) property can be found in [Sontag and Wang, 1995; Khalil, 2002].

Another concept that will be used in the thesis, especially in signal-based estimation and linear-like regression, is the property of *Persistent Excitation* (or PE), which can be defined as follows.

Definition 1.3.12. *A function* $\phi : \mathbb{R}_+ \to \mathbb{R}^n$ *is* persistently exciting (or ϕ is PE)*, if there exist* $T, \mu > 0$ *such that for all* $t \in \mathbb{R}_+$*,*

$$\int_t^{t+T} \phi(s)\phi(s)^\top ds > \mu I_n,$$

where $\phi(s)^\top$ *denotes the function* $\mathbb{R}_+ \to \mathbb{R}^{1\times n}$*,* $t \mapsto \phi(t)^\top$*.*

Definition 1.3.13. *Two PE functions* $\phi : \mathbb{R}_+ \to \mathbb{R}^n$ *,* $\psi : \mathbb{R}_+ \to \mathbb{R}^m$ *are* linearly independent*, if there exists* $T > 0$ *such that for all* $t \in \mathbb{R}_+$*, the following matrix functions are not constant:*

$$\left(\int_t^{t+T} \phi(s)\phi(s)^\top ds\right)^{-1} \int_t^{t+T} \phi(s)\psi(s)^\top ds \text{ and}$$
$$\left(\int_t^{t+T} \psi(s)\psi(s)^\top ds\right)^{-1} \int_t^{t+T} \psi(s)\phi(s)^\top ds.$$

1.3.4 Estimation and Control

Designing control or estimation algorithms for nonlinear systems is a rather complex issue [Khalil, 2002], which needs properly selected assumptions and positioning hypotheses. Designing *observers* is one of the central problems in modern control theory and dynamical systems analysis. Once presented for linear setting [Luenberger, 1964], the problem of observer design was vastly applied and studied for nonlinear cases (*e.g.*, [Khalil, 2002, Fridman et al., 2008, Besançon, 2007, Thau, 1973]) and became a popular research subject in the field. Initially, the idea of the observer was based on the measured output inclusion into the replicated system, with a gain matrix to be found. This idea was innovative for dynamical systems analysis and provided a ground for new frameworks and fields in control theory.

The nonlinear dynamical system

$$\dot{\hat{z}} = \mathcal{F}(\hat{z}, y, t), \tag{1.12}$$
$$\hat{x} = \mathcal{T}(\hat{z}, y, t), \tag{1.13}$$

with state $\hat{z} \in \mathbb{R}^{n_z}$ for $n_z \in \mathbb{N}_{>0}$ and maps $\mathcal{F} : \mathbb{R}^{n_z} \times \mathbb{R}^p \times \mathbb{R} \to \mathbb{R}^{n_z}$, $\mathcal{T} : \mathbb{R}^{n_z} \times \mathbb{R}^p \times \mathbb{R} \to \mathbb{R}^n$ is called an *asymptotic observer* for system (1.1) if there exist $\mathcal{Z}_0 \subset \mathbb{R}^{n_z}$ such that for any solution $x(t, x_0, y)$ to (1.1) defined on $[0, +\infty)$ with $x(0) \in \mathcal{X}_0$, $y(t) = h(x(t), t)$ is also defined on $[0, +\infty)$, any solution $\hat{z}(t, \hat{z}_0, y)$ to (1.12) with $\hat{z}(0) \in \mathcal{Z}_0$ is defined on $[0, +\infty)$ and verifies

$$\lim_{t\to\infty} |\hat{x}(t) - x(t)| = 0 \tag{1.14}$$

with $\hat{x}(t) = \mathcal{T}(\hat{z}, y(t), t)$.

The *observer design* problem is therefore to establish proper mappings $\mathcal{F}$ and $\mathcal{T}$, so the system (1.12), (1.13) converges to (1.1).

Generally, in the observation problem, it is assumed that we measure the signal that the system generates (the output), and the system is partially observed for any external input signal (from a bounded set), meaning that the system is uniformly observable. However, there are cases in practice when the system can be observed only under particularly designed inputs, and this complex scenario is not frequently covered by the observer design theory (for instance, see [Moreno and Besancon, 2021]). Therefore, a more relaxed assumption than minimality for system (1.1), which is local and implies non-uniform observability, can be stated as follows:

Assumption 1.3.2. *System* (1.1) *is accessible and it is observable only for* $x_0 \in \mathcal{X}$ *and for* $u \in \mathcal{U}$*, where* $\mathcal{X} \subset \mathbb{R}^n$ *and* $\mathcal{U} \subset \mathcal{L}_\infty^m$ *denote the sets of admissible initial conditions and inputs, respectively.*

The concept of observability of the dynamical system is indirectly tied to the concept of stability [Angeli, 2002], and the input design in such a case must be based on the ISS concept.

In this thesis, we are particularly interested in the observer design based on the steady-state response. One example of such an approach can be found in Karagiannis, Carnevale, and Astolfi, 2008, where the setting can be expressed as follows. Consider a time-varying nonlinear system in general form:

$$\begin{cases} \dot{y}(t) = f_1(y(t), x(t), t), \ t \in \mathbb{R}_+ \\ \dot{x}(t) = f_2(y(t), x(t), t), \end{cases} \tag{1.15}$$

where $y(t) \in \mathbb{R}^m$ is the measured part of the state and $x(t) \in \mathbb{R}^n$ is the unmeasured part, and the functions f_1 and f_2 are assumed to guarantee the forward completeness of (1.15).

Definition 1.3.14. *The dynamical system*

$$\dot{\xi}(t) = \alpha(y(t), \xi(t), t), \ t \in \mathbb{R}_+ \tag{1.16}$$

with $\xi(t) \in \mathbb{R}^p$*,* $p \geq n$*, is called an* observer *for the system* (1.15)*, if there exist mappings*

$$\beta : \mathbb{R}^m \times \mathbb{R}^p \times \mathbb{R} \to \mathbb{R}^p \quad \text{and} \quad \phi_{y,t} : \mathbb{R}^n \to \mathbb{R}^p$$

where $\phi_{y,t}(\cdot)$ *is left-invertible such that the manifold*

$$\mathcal{M} = \{(y(t), x(t), \xi(t), t) \in \mathbb{R}^m \times \mathbb{R}^n \times \mathbb{R}^p \times \mathbb{R} \,|\, \beta(y(t), \xi(t), t) = \phi_{y,t}(x(t))\} \tag{1.17}$$

has the following properties:

- *all trajectories of the extended system* (1.15)*,* (1.16) *starting on* $\mathcal{M}$ *remain there for all future times,* i.e.*,* $\mathcal{M}$ *is forward invariant;*
- *all trajectories of the extended system* (1.15)*,* (1.16) *starting in a neighborhood of* $\mathcal{M}$ *asymptotically converge to* $\mathcal{M}$*.*

To find the mappings β, α, and $\phi_{y,t}$, consider the estimation error:

$$z(t) = \beta(y(t), \xi(t), t) - \phi_{y,t}(x(t))$$

the dynamics of which are given by

$$\dot{z} = \frac{\partial \beta}{\partial y} f_1 + \frac{\partial \beta}{\partial \xi} \alpha + \frac{\partial \beta}{\partial t} - \frac{\partial \phi_{y,t}}{\partial y} f_1 - \frac{\partial \phi_{y,t}}{\partial x} f_2 - \frac{\partial \phi_{y,t}}{\partial t}$$

and must admit the origin to be (locally) asymptotically stable. Existence conditions for these mappings are formulated in terms of PDE, and a more detailed description of the approach can be found in [Karagiannis, Carnevale, and Astolfi, 2008].

1.4 General problem statement and gaps to fill

1.4.1 Pointing task

Since this thesis is on automatic control theory, practical problems are also viewed through this framework. Complex problems as an HCI can be represented in terms of a control loop. The conventional diagram, presented in Fig. 1, is simplistic but rather general. The loop consists of the system with the state ω, representing

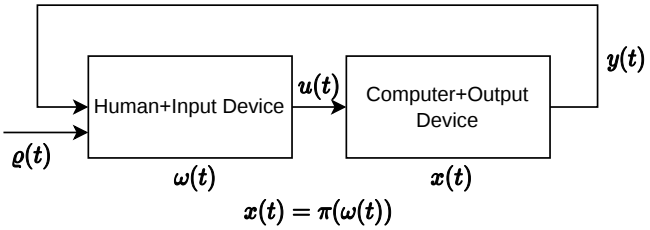

FIGURE 1.1: Control feedback loop for HCI

the human, and a device which he/she operates and the system with the state x, representing the computer with an output device, *i.e.*, a screen. The interaction in terms of feedback is represented through signals u and y, where ϱ describes the reference signal, possibly unknown, based on which the human makes a decision to alter the loop. The function π serves in this loop as a mapping connecting the states of both systems through some rule, usually based on software transformation of the physical signal inputted by system ω to the artificial interface system x.

The main challenge of such an approach is the complexity of unknown dynamics and decisions behind the human part, generally impossible to model. In some simple cases, one can attempt to design models and algorithms which represent the interaction rather well by modeling physical device dynamics instead, with the external input of the human, based on the reference. One such example is the so-called indirect *pointing task*, where the input device is the computer mouse, the output device is the screen, and the reference signal ϱ is the endpoint of the cursor which the human desires to reach.

Other than modeling such a system, another interesting problem is estimating and predicting of the reference endpoint. There are many existing approaches and models in place, which were discussed in Section 1.2. However, despite the broad interest in the subject, to the best of the author's knowledge, there is no single widely accepted dynamical pointing model (except for Fitts' law which does not provide dynamics, only statistical static relation). Moreover, it is worth highlighting that the existing literature is fragmented because most approaches do not consider the modeling and endpoint prediction together. Therefore, one of this thesis's goals is to show that the explicit model accurately representing the system can be designed, which also allows the endpoint estimation at the same time. Another possibility to be included in the model is the estimation of the function π, which will allow obtaining states of one system based on the states of the other.

1.4.2 Steady-state estimation based Estimation and Control

Following this line of thoughts, we look here at the idea of the dynamical systems analysis as the output regulation theory [Isidori and Byrnes, 1990] or other frameworks based on a similar concept, like model reduction by moment matching [Scarciotti and Astolfi, 2017b], synchronization theory [Nijmeijer and Mareels, 1997], immersion & invariance [Astolfi and Ortega, 2003], etc. The mentioned approaches consider a serial connection of two processes, the nominal dynamics and the ecosystem or signal generator or master system (names differ on the framework). The second system generates an input to the system in the study, in an advantageous way for the analysis. It could be either tracking control, estimation of so-called moments of the system, synchronization, stabilization, etc. Generally, the idea is to make the output of the original system follow a given reference signal, trajectory, or dynamics.

One of the ways how the system can be altered is to make the original system follow the so-called steady-state solution, meaning that both systems (original and generating the signal) can converge to the steady-states which can be linked through certain mapping. Take as an example the system presented in Fig. 1.2, where $x(t) \in \mathbb{R}^n$ is the state of a dynamical system Σ_1, $\omega(t) \in \mathbb{R}^q$ is the state of a dynamical system Σ_2, $u(t) \in \mathbb{R}^m$ is the input of Σ_1 and the output of Σ_2, and $y(t) \in \mathbb{R}^p$ is the measured output of system Σ_1.

The mapping $\pi : \mathbb{R}^q \to \mathbb{R}^n$ has to be set or found to analyze the connection. Such an approach can be used in different ways and for different scenarios, the most straightforward being system's model reduction or the estimation problem, based on such a scenario. The clear advantage of the observation of such a connection is that one can observe only the generating system to observe both, if the mapping π is known. In Fig. 1.3 this

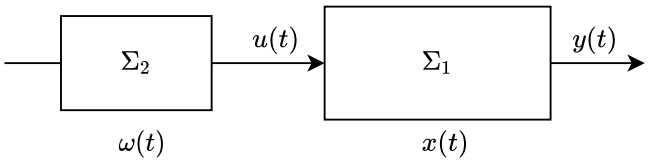

$$t \to \infty, x(t) \to \pi(\omega(t))$$

FIGURE 1.2: Connected systems

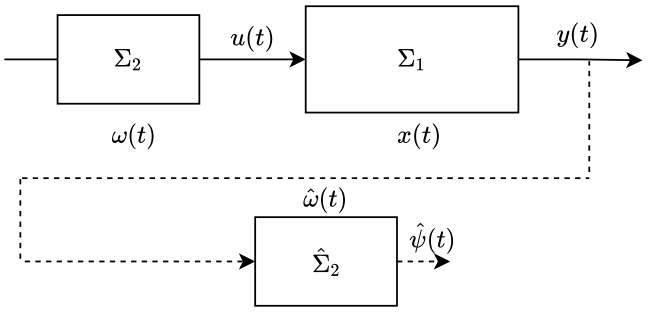

$$t \to \infty, \hat{x}(t) \to \pi(\hat{\omega})$$

FIGURE 1.3: Observer for connected systems

idea is demonstrated, where the measured output y of system Σ_1 is used in the observer $\hat{\omega}$ of $\hat{\Sigma}_2$ for Σ_2, and through the mapping π, the states of system Σ_1 can be estimated as $\hat{x}$. This way of state estimation is especially of interest if the master system is of lower order. This means that in practice, one can use less computational power, *etc*., to follow the big-scale original system Σ_1. This leads us to the reduced-order observation problem using steady-state:

Reduced-order observation problem using steady-state

For the input $u \in \mathcal{U}$, either designed or given, any initial conditions $\omega(0) \in \Omega(0)$ and $x(0) \in X(0)$, find an estimate $x(\hat{t}) = \pi(\hat{\omega}(t))$ of the state x based on the only knowledge of the input u, output y and steady-state mapping π, where the order of states $\omega(t)$ of system Σ_2 is smaller than x of Σ_1.

So the problem solution has a key intermediate step consisting of the computation of the mapping π, which we assume exists, or to design such an input u, generated by system Σ_2 that π can be defined.

One could also consider the reciprocal interconnection of two systems as shown in Fig. 1.4, where both systems receive an external reference signal ϱ, and the systems affect each other. The assumptions on the existence of the steady-state for such a case have to be more strict. In this case, the results are usually more local, so it is more difficult to ensure ISS and the observability of systems, and often the small-gain theorem is used for the stability analysis. However, it will be shown that for some cases, π exists in this case as well, at least locally, and can be found. In this situation, the estimation problem can be based on the same idea, where we build an observer (see Fig. 1.5) for one system, based on all available data, although the dynamics of the observer will differ, as it will be shown later.

The classical problem of the reduced-order observation, presented by Luenberger, can also be considered using steady-state mapping, as in Fig. 1.6. In particular, we consider the opposite problem of the one in Fig. 1.2, where we assume that we can alter the receiving system (in this case Σ_1 is our observer) so that the steady-state mapping π will connect both steady-states. It is beneficial to us to design the second system of a smaller dimension, so that for instance, we can estimate only the unmeasured states of Σ_2 (see, for example [Karagiannis, Carnevale, and Astolfi, 2008]). To estimate parameters or states of the Σ_1, the mapping π has to be inverted, which can be problematic for nonlinear systems and some applications.

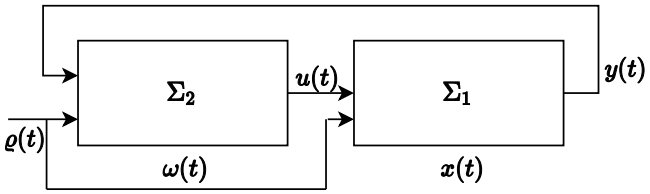

$$t \to \infty, x(t) \to \pi(\omega(t))$$

FIGURE 1.4: Interconnected systems with a reference signal

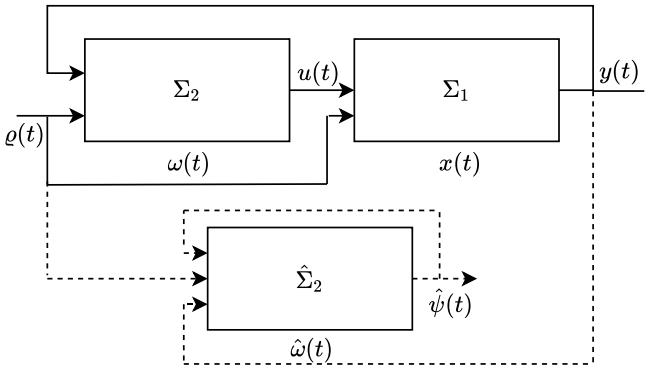

$$t \to \infty, \hat{x}(t) \to \pi(\hat{\omega}(t))$$

FIGURE 1.5: Observer for Interconnected systems

This second part of this thesis is therefore dedicated to investigating the different scenarios presented above. However, the research is limited to classes of nonlinear systems. In the general case, it is not easy to find the mapping π, especially without using linearization, function inversion, computational methods, *etc*. We will focus here on the scenarios where π could be found analytically and relatively easily, which would benefit possible applications. The presented cases are not the limit of the approach but rather an example how the problem can be solved based on the considered class of systems.

1.5 Outline of the thesis

The thesis is structured into two parts. Here, we briefly describe the scope and tools used in each chapter.

Chapter 2 in **Part I** proposes a new simplified pointing model as a feedback-based dynamical system, including both human and computer sides of the process. It considers the commutation between the correction and ballistic phases in pointing tasks. We use the mouse position increment signal from noisy experimental data to achieve our main objectives: to estimate the model parameters online and predict the task endpoint. Some estimation tools and validation results, applying linear regression techniques on experimental data are presented. For the modeling, we take the existing switched model [Aranovskiy et al., 2020] and simplify

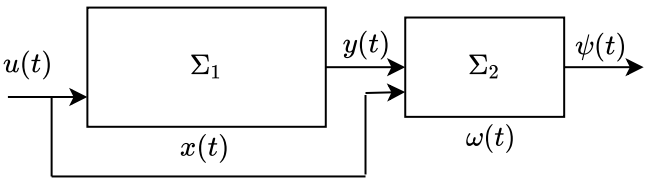

$$t \to \infty, x(t) \to \pi^{-1}(\omega(t))$$

FIGURE 1.6: Connected systems (reversed)

it for analysis. For model validation, we use data from [Antoine, Malacria, and Casiez, 2018] and apply a homogeneous differentiator to smoothen the signal for the identification. The modeling and identification are divided into two modes, where we use the DREM algorithm to find the unknown parameters in real time. We also compare with a similar prediction algorithm to show the potential of our algorithm's implementation.

Part II is divided into two parts based on the shape of the steady-state solution between interconnected systems: linear relations for **Chapter 3**, and nonlinear relations for **Chapter 4**. For each case, the considered class of nonlinear systems is also different. Section 3.2 proposes existence conditions for an observer of a particular class of nonlinear systems: an interconnection of two nonlinear models possessing relaxed non-uniform observability properties (dependent on the input choice). First, we apply the tools from nonlinear model reduction by moment matching, described in Section 1.3, to establish analytical expressions for steady-state solutions of the interconnected system. We then design reduced-order observers and a dynamical trajectory tracking regulator for such a system using this result. The stability and boundedness of the error dynamics under measurement noises and disturbances are established. Three real-world examples, an anaerobic bioreactor, Chua's circuit, and a one-link flexible arm, demonstrate the results' interest and applications. Later on, in Section 3.3, we present conditions on the existence and stability of a nonlinear observer for the same class of nonlinear systems based on the invariant manifold approach in both continuous- and discrete-time scenarios. The conditions are formulated using Linear Matrix Equations (LME) and Inequalities (LMI). We present two possible applications of the result, a reduced-order observer (e.g., an observer for unmeasured states) and regression in linear and nonlinear, continuous and discrete- time settings. With nonlinear regression being a sophisticated case, the parameter estimation problem for a particular output equation (when the fusion of linear and nonlinear sensors is weighted) is investigated. Two nonlinear examples demonstrating the efficiency of results are provided.

Chapter 4 deals with the mapping π which is found using tools from the nonlinear model reduction by moment matching for systems presented in lower-triangular or upper-triangular canonical forms. Next, this mapping helps design an excitation input and a corresponding reduced-order observer for interlaced systems, a combination of upper- and lower-triangular subsystems. A proposed global observer is proved to be robust to additive disturbance and measurement noise by applying the Lyapunov function method. An example involving a mass-spring system demonstrates the efficiency of the approach.

The final chapter is dedicated to the general conclusion of the thesis and discussion on future work.

1.6 List of publications

Published in international journals

- A. Khalin, R. Ushirobira, D. Efimov and G. Casiez, "On Computer Mouse Pointing Model Online Identification and Endpoint Prediction," in IEEE Transactions on Human-Machine Systems, vol. 52, no. 5, pp. 941-951, Oct. 2022, doi: 10.1109/THMS.2021.3131660.

Submitted international journals

- A. Khalin, R. Ushirobira, D. Efimov, "On robust reduced-order observer design and tracking control for a class of nonlinear systems", Automatica. (under review)
- —, "On robust observer design for a class of Persidskii time-varying continuous-time and discrete-time systems", Transactions on Automatic Control. (under review)

Presented in international conferences

- A. Khalin, R. Ushirobira and D. Efimov, "On steady-state based reduced-order observer design for interlaced nonlinear systems," 2022 European Control Conference (ECC), 2022, pp. 132-137, doi: 10.23919/ECC55457.2022.9838398.

- A. Khalin, D. Efimov and R. Ushirobira, "On observer design for a class of time-varying Persidskii systems based on the invariant manifold approach," 2022 European Control Conference (ECC), 2022, pp. 112-117, doi: 10.23919/ECC55457.2022.9838524.

Submitted to international conferences

- A. Khalin, D. Efimov, R. Ushirobira, "On observer design for a class of Persidskii systems based on steady-state estimation", IFAC World Congress 2023, Yokohama, JAPAN. (under review)

Part I

Application to HCI modeling

Chapter 2

Modeling and Parameter Identification for the Pointing Task

2.1 Introduction

This chapter is dedicated to the applied problem, the focus of several scientific communities for a long time. The relevance of the pointing task goes way back to the pre-computer times when human motor movement was a prominent topic in experimental psychology [Bryan, 1892]. The idea is that humans operate with their joints and limbs based on vision-based and muscle-based perception. Later, the HCI community adopted this problem for interface navigation.

Pointing is a fundamental task and has been a research subject for many years in the HCI field. A pointing task involves guiding some device in the control space (also called a motor) for navigating the cursor in the operating space (a display). There are some papers about hardware optimization (for instance, a recent study about the optimal sensor position in the mouse [Kim et al., 2020]), but the majority of papers in HCI with regards to pointing concern the so-called interaction techniques [Blanch, Guiard, and Beaudouin-Lafon, 2004, Grossman and Balakrishnan, 2005, Chapuis, Labrune, and Pietriga, 2009, Blanch and Ortega, 2009]. Despite the development of new devices, touchpads and computer mice are the most popular input devices for most users, and they are still widely used for such tasks as pointing, tracking, dragging, targeted-tracking [Senanayake, Goonetilleke, and Hoffmann, 2015], *etc*. That is why several models for direct and indirect pointing tasks are available in the literature, providing different levels of the process description.

Regarding the goals of this chapter, the considered problem can be divided into two parts: the first is **modeling a pointing task** and the second is the **endpoint prediction**. Indeed, it is possible to facilitate the interaction and shorten the movement time by predicting the user's desired destination.

Both problems are usually separated and not considered together in a single model-based prediction algorithm, which could be more advantageous for description and analysis. We fill the indicated gap in the present chapter, and an endpoint prediction algorithm is presented based on a new simplified version of the dynamical model given in [Aranovskiy et al., 2020]. The aim of simplifying the latter model is to improve the possibility of online parameter identification and allow the process characteristics to be adjusted or modified online. Another advantage of the presented model is its portability since we do not suppose to know the used surfaces that the computer mouse operates on, the Pointing Transfer Function (PTF) of the operating systems (which will be introduced later in the text) or other varying setup conditions. A recent adaptive observer technique in [Wang, Efimov, and Bobtsov, 2019] is used to adjust the model parameters and identify everything *on the fly*. It is suggested how to modify the PTF once the endpoint coordinates are derived. Experimental data with a computer mouse from [Casiez and Roussel, 2011; Antoine, Malacria, and Casiez, 2018] is applied for this chapter's model development and validation.

2.2 Problem Statement

The problem considered in this chapter is modeling and parameter identification of an indirect pointing task.

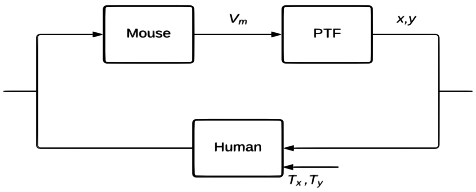

FIGURE 2.1: Closed-loop model, conventional block diagram

The main idea here is to use the automatic control theory to design the pointing model, where the user is a controller in the closed-loop whose behavior and decision we do not know exactly, but we can measure and estimate it indirectly and predict the desired position. The interaction and related input and output signals are presented in Fig. 2.1 for the x-direction displacement (there is also the y displacement in the 2-dimensional case). We suppose that the user positions the cursor on the screen having x and/or y as an input and transforms it with his decision into a wrist movement, producing the force that translates the mouse, which has the position x_m and y_m on the plane. So, the mouse output will be its velocity $V_m = \sqrt{V_{mx}^2 + V_{my}^2}$, where $\dot{x}_m = V_{mx}$ and $\dot{y}_m = V_{my}$ are the velocity projections on x and y axes, respectively. The term corresponding to the mass was omitted: we suppose that the mass of a mouse and a hand on it is a unit, and the mass normalizes all other parameters appearing in an equation. The basic equations for this process can be presented as follows:

$$\begin{aligned} \dot{x}_m(t) &= V_{mx}(t), \\ \dot{V}_{mx}(t) &= F_{\text{fr}}(t) - F_{\text{input}}(t), \\ \dot{x}(t) &= \frac{V_{mx}(t)}{V_m(t)} \,\text{PTF}(V_m(t)),\ \forall t \geq 0 \end{aligned} \tag{2.1}$$

where F_{fr} is the mouse friction force, and F_{input} is the force generated by the user, $\text{PTF} : \mathbb{R} \to \mathbb{R}$ is a pointing transfer function (see [Casiez and Roussel, 2011]), that transforms the mouse velocity V_m into the cursor velocity on the screen $V_c(t) = \frac{\partial}{\partial t}\sqrt{x^2(t) + y^2(t)}$, $\forall t \geq 0$ (usually, through look-up tables that realize a nonlinear function in all existing operating systems [Casiez and Roussel, 2011]), the ratio $\frac{V_{mx}}{V_m}$ is used to project the PTF effort on the corresponding movement direction. We assume that the human force F_{input} is proportional to the endpoint position T_x (in the ballistic phase) or the current error between x and T_x (in the correction phase).

Remark 2.2.1. *Our idea is to estimate the decision process online, predict the reference position T_x (which we originally do not know, only the user does), and improve PTF using the estimated value $\widehat{T}_x$ of the endpoint T_x. To this end, we introduce an additional feedback in the PTF block to adjust the navigation, shorten the pointing time, and possibly reduce the error rate (usually present in all known tests). Thus, we add a correction term $\varrho(x - \widehat{T}_x)$ with some tuning parameter $\varrho > 0$, so the last equations in* (2.1) *takes the form:*

$$\dot{x}(t) = \frac{V_{mx}(t)}{V_m(t)} \,\text{PTF}(V_m(t)) - \varrho\left(x(t) - \widehat{T}_x(t)\right),\ \forall t \geq 0.$$

It is also worth mentioning that we still do not know how a user will react to such a modification of PTF, will it be more optimal or not, but we will provide the related experiments to check it in a later future. An example of how users can react to a similar approach can be found in [Hourcade et al., 2010], where the endpoint prediction was used to help the elderly navigate on the screen.

For 2-D tasks, the equations for the vertical components y_m, V_{my}, y, T_y, $\widehat{T}_y$ can be presented in the same way.

So the motivating technical issue of this chapter is to estimate the cursor's wanted position T_x and T_y as fast as possible using the dataset obtained in the experiment of [Antoine, Malacria, and Casiez, 2018].

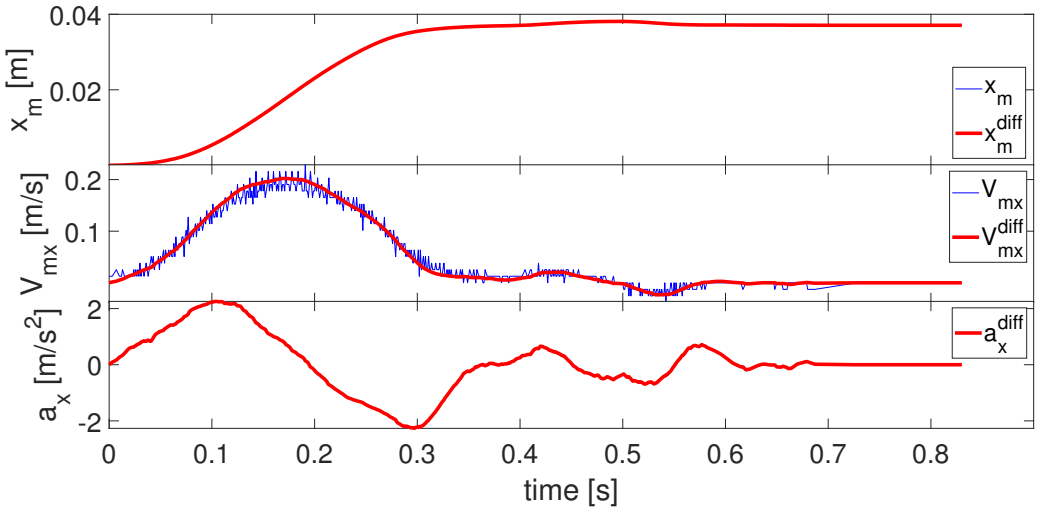

FIGURE 2.2: Position differentiation: a) t [s] vs x_m and x_m^{diff} [m]; b) t [s] vs V_{mx} and V_{mx}^{diff} [m/s]; c) t [s] vs a_x^{diff} [s]

2.3 Data Description and Processing

According to [Antoine, Malacria, and Casiez, 2018], a mouse with a frequency of 1 kHz and 2000 CPI (counts per inch) was used, and all measurements are provided at discrete instants of time t_k [s] with a varying sampling period $h^{k-1} = t_k - t_{k-1}$ for $k = 1, 2, \ldots$ and $t_0 = 0$ (the sampling is not exactly 0.001 [s] due to the event-based nature of the operating system). We have an optical sensor inside the mouse, that measures the integer value increment of the mouse displacement $\Delta x_m^k = x_m^k - x_m^{k-1}$ in counts (with a measurement noise that is skipped for brevity), where $x_m^k = x_m(t_k)$, which can be converted into velocity in [m/s] for the conformity, considering the mouse CPI and inches to meters ratio $\iota = 0.0254$:

$$V_{mx}(t_k) = V_{mx}^k = \frac{\iota\, \Delta x_m^k}{\text{CPI}\; h^{k-1}},\ k = 1, 2, \ldots.$$

The mouse position in [m] is obtained from the calculated velocity (scaled mouse displacement) by each time step accumulation:

$$x_m^k = x_m^{k-1} + h^{k-1} V_{mx}^k.$$

The cursor position on the screen $x^k = x(t_k)$ in [pixel] is available at the same time instants. Similarly, we have $y_m^k = y_m(t_k)$, $\Delta y_m^k = y_m^k - y_m^{k-1}$, $V_{my}(t_k)$ and $y^k = y(t_k)$.

2.3.1 Homogeneous Differentiator (HOMD)

The so-called homogeneous differentiator, which is used in order to obtain smooth velocity and acceleration signals, can be briefly described as follows.

Let a smooth signal $y(t) \in \mathbb{R}$ be available for measurements for all $t \geq 0$, and our goal is to estimate its derivatives.

To this end, we can use the homogeneous finite-time observer from [Perruquetti, Floquet, and Moulay, 2008], which in our case plays the role of a differentiator.

$$\begin{aligned} \dot{\widehat{z}}_1 &= \widehat{z}_2 - k_1 \lceil \widehat{z}_1 - y \rfloor^{1+\alpha}, \\ \dot{\widehat{z}}_2 &= \widehat{z}_3 - k_2 \lceil \widehat{z}_1 - y \rfloor^{1+2\alpha}, \\ &\vdots \\ \dot{\widehat{z}}_n &= -k_n \lceil \widehat{z}_1 - y \rfloor^{1+n\alpha}, \end{aligned} \tag{2.2}$$

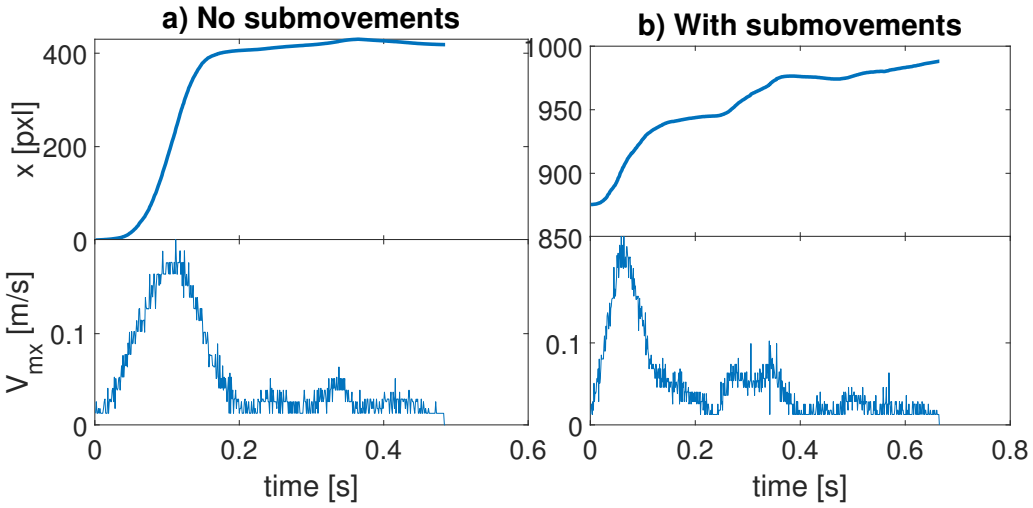

FIGURE 2.3: Trial with and without sub-movements: top sub-figures x [pxl] vs time, bottom sub-figures V_{mx} [m/s] vs time

where $\widehat{z}_i$ can be utilized as an estimate of $y^{(i-1)}$ derivative for $1 \leq i \leq n$ (here $y^{(0)} = y$), $\alpha \in \mathbb{R}$ and $k_i \in \mathbb{R}$ for $1 \leq i \leq n$ are tuning parameters. If $\alpha = \frac{-1}{n}$, then this differentiator becomes the high-order sliding-mode differentiator from [Levant, 2003].

For realization, the system (2.2) has to be discretized using, for example, the explicit Euler method at time instants $t_k = kh$ with a fixed step $h > 0$, and choosing the coefficients k_i in a way that ensures stability. For this purpose, for $n = 4$, taking the characteristic polynomial as $p(s) = (s+\lambda)(s+\lambda\xi)(s+\lambda\xi^2)(s+\lambda\xi^3)$, where $\lambda, \xi > 0$ are tuning parameters, we obtain:

$$k_1 = (1+\xi+\xi^2+\xi^3)\lambda,\ k_2 = (1+\xi+2\xi^2+\xi^3+\xi^4)\xi\lambda^2,$$
$$k_3 = (1+\xi+\xi^2+\xi^3)\xi^3\lambda^3,\ k_4 = \xi^6\lambda^4,$$

hence,

$$\begin{aligned}
\widehat{z}_1^{k+1} &= \widehat{z}_1^k + h\left(\widehat{z}_2^k - k_1\lceil \widehat{z}_1^k - y^k \rfloor^{1+\alpha}\right),\\
\widehat{z}_2^{k+1} &= \widehat{z}_2^k + h\left(\widehat{z}_3^k - k_2\lceil \widehat{z}_1^k - y^k \rfloor^{1+2\alpha}\right),\\
\widehat{z}_3^{k+1} &= \widehat{z}_3^k + h\left(\widehat{z}_4^k - k_3\lceil \widehat{z}_1^k - y^k \rfloor^{1+3\alpha}\right),\\
\widehat{z}_4^{k+1} &= \widehat{z}_4^k + hk_4\lceil \widehat{z}_1^k - y^k \rfloor^{1+4\alpha}
\end{aligned}$$

for $k = 0, 1, 2, \ldots$, where $\widehat{z}_i^k = \widehat{z}_i(t_k)$ and $y^k = y(t_k)$ for $1 \leq i \leq 4$, and $\alpha \in [-\frac{1}{4}; 0)$.

2.3.2 Signal Processing

Examples of obtained noisy signals are shown in Fig. 2.2 and demonstrate a bad velocity estimation due to the noise. To obtain a better velocity profile and the respective acceleration (which we need later for the mode identification) we applied a homogeneous differentiator to the mouse position (see [Perruquetti, Floquet, and Moulay, 2008], and Section 2.3.1 for the used equations). This type of differentiator's main advantage is that it possesses a finite-time convergence rate [Perruquetti, Floquet, and Moulay, 2008], which is faster than any exponential, and in addition, it is proven to be robust to the disturbances [Bernuau et al., 2013]. Finding a trade-off between smoothness and convergence accuracy, the parameters in (2.2) are tuned as

$$\lambda = 5,\ \xi = 2,\ \alpha = -0.2,$$

then $V_{mx} = \widehat{z}_2$ and $a_{mx} = \widehat{z}_3$ can be used for further parameter identification of the model. The filtered mouse position, velocity, and acceleration are derived by applying the homogeneous differentiator to the mouse position presented in Fig. 2.2. From these plots, we can conclude that this homogeneous differentiator filters well the noise and generates rather smooth estimates of the velocity and acceleration.

Remark 2.3.1. *The experiments of [Antoine, Malacria, and Casiez, 2018] included 10 users, which navigate the cursor on the screen using the mouse in a task with* 13 *targets positioned along a circle, following the norm ISO 9241-9 (§B.6.2.2). Two different distances (*150 *and* 75 *mm), target widths (*7 *and* 2 *mm), and two different PTFs were used. Depending on the velocity or position profile, it is possible to detect which user is more experienced with the setup and which. An experienced user makes a ballistic movement very close to the goal, and the motion is realized in one round without sub-movements (without additional ballistic corrections). A less-experienced user needs more attempts to reach the surrounding area and may produce several sub-movements to attain the goal (see Fig. 2.3 for illustrations). Another way to define experienced users is according to the movement time: the lower their time on completing the trial, the more experienced they are. In this chapter, we will rely on the first definition since our prediction algorithm will generalize to the cases with sub-movements. The performance also depends on the target width and the number of trials with the current setup. Therefore, it makes sense to evaluate the model on the trials without additional sub-movements because when a user utilizes his/her personal setup (PC and mouse), the movements are much more precise than with an unfamiliar one. This will be done first, and next, the model presented in this chapter is generalized, considering all possible cases.*

2.4 Modeling

2.4.1 Pointing Transfer Function

As was mentioned earlier, the PTF provides the gain from the mouse velocity V_m to the cursor one V_c. Every operating system has look-up tables with standard gains, and every mouse velocity input is interpolated accordingly. The set of the final gains constitutes a nonlinear function. The authors of [Casiez and Roussel, 2011] created a useful library called Libpointing, which captures raw mouse data and allows one to create and use one's own PTF.

In this chapter, we assume that the shape of the PTF is unknown to develop a platform-independent approach. Therefore, it has to be reconstructed from the measured data, and our idea is that a polynomial of the mouse velocity can approximate the PTF function in (2.1):

$$\mathrm{PTF}(V_m(t)) = V_c(t) = \sum_{i=0}^{q} c_i V_m^i(t),\ \forall t \geq 0$$

where the nonlinear gain is a polynomial of order q with unknown coefficients $c_0, \ldots c_q$. Taking into account the discrete-time nature of the measurements, we have:

$$V_c^k = \sum_{i=0}^{q} c_i V_m^i(k),$$

where $V_c^k = V_c(t_k)$ and $V_m(k) = V_m(t_k)$. The cursor velocity can be approximated by a simple Euler formula

$$\widehat{V}_c^k = \frac{d^k - d^{k-1}}{h^{k-1}},$$

where $d^k = \sqrt{x_k^2 + y_k^2}$ is the distance on the screen from the origin corner, or by applying the homogeneous differentiator in [Perruquetti, Floquet, and Moulay, 2008] to d^k.

2.4.2 Ballistic Phase

In this phase, we assume that the whole movement is realized *intuitively* or *automatically* in the motor space based on the averaged PTF gain sensed by the user (*i.e.*, it is an open-loop deterministic motion), and the mouse position follows the curve:

$$x_m(t) = \frac{T_x}{2c}\left(1 - \cos(\eta t)\right), \ \forall t \geq 0,$$

where $\eta > 0$ is a user-dependent parameter, which regulates the velocity of displacement, and the movement amplitude is proportional to the goal position T_x divided by an averaged PTF gain $c > 0$. This coefficient represents the ratio between the motor and operational spaces, and for the user, it is expected that

$$x(t) = c x_m(t).$$

In such a case $x_m\left(\frac{\pi}{\eta}\right) = \frac{T_x}{c}$ and $x\left(\frac{\pi}{\eta}\right) = T_x$. Note that this gain c can be easily estimated if the PTF function is known (if it has been already identified as explained above):

$$c = V_{\max}^{-1} \int_0^{V_{\max}} \mathrm{PTF}(s) ds,$$

where $V_{\max}$ is the maximal admissible computer mouse velocity for the user (can be extracted from the data). Nevertheless, as we demonstrate below, we do not need this parameter to estimate the endpoint. Thus, if the ballistic movement is well-realized, and the human approximation of the PTF gain c is adequate, then the cursor has to fall into a vicinity of the desired position T_x. Simple calculations show that

$$\dot{x}_m(t) = V_{mx}(t) = \frac{T_x \eta}{2c}\sin(\eta t), \ \dot{V}_{mx}(t) = a_{mx}(t) = \frac{T_x \eta^2}{2c}\cos(\eta t),$$

hence,

$$\dot{V}_{mx}(t) = -\eta^2\left(x_m(t) - \frac{T_x}{2c}\right) = -\frac{\eta^2}{c}\left(x(t) - \frac{T_x}{2}\right),$$

and the obtained model can be related to the one proposed in the next subsection for the correction phase by imposing $F_{\mathrm{fr}} \equiv 0$ and $F_{\mathrm{input}} = b_2\left(x - \frac{T_x}{2}\right)$ with $b_2 = \frac{\eta^2}{c}$. Consequently, in the ballistic phase, it is assumed that the friction force can be neglected during such a fast transient and the goal position for the ballistic phase is just half away from the desired set-point T_x (this is an interpretation in terms of visual user feedback).

2.4.3 Corrective Phase

In (2.1), we choose the input force as a simple linear feedback

$$F_{\mathrm{input}} = b_2(x - T_x),$$

with a parameter $b_2 > 0$, which is unknown and can be different for each trial (such a choice is often assumed in the so-called Equilibrium-point hypothesis [Feldman, 1986]). We can select the dynamic friction force in a usual form

$$F_{\mathrm{fr}} = -b_1 V_{mx},$$

where $b_1 > 0$ is the friction coefficient, which is also unknown and trial-sensitive. Usually, $b_1 > 0$ is dependent on the mouse and the surface mouse operated on, but it also depends on the users' hand position, which influences the mass and makes this coefficient not constant, despite operating the same surfaces. If the parameters b_1 and b_2 are non-negative, then the resulting dynamics is stable, which corresponds to our intuition about the

pointing process. Thus, we obtain the model:

$$\dot{V}_{mx}(t) = -b_1 V_{mx}(t) - b_2(x(t) - T_x),\ \forall t \geq 0.$$

2.5 Identification

2.5.1 Pointing Transfer Function

For the coefficients of a polynomial PTF, a simple linear regression estimation technique [Ljung, 1999] can be used to estimate the parameters $c_0, \ldots, c_q$:

$$\begin{bmatrix}\widehat{c}_0 & \ldots & \widehat{c}_q\end{bmatrix}^\top = A_k^{-1}\psi^k$$

provided that the matrix A_k is not singular, where

$$A_k = \delta A_{k-1} + \omega_k \omega_k^\top,\ \psi^k = \delta\psi^{k-1} + \omega_k \widehat{V}_c^k,$$
$$\omega_k = \begin{bmatrix}V_m^0(k) & \ldots & V_m^q(k)\end{bmatrix}^\top$$

with the regression vector ω_k; ψ^k and A^k are auxiliary matrix variables, and $\delta \in (0, 1]$ is a forgetting factor.

After some trials, we obtained the polynomial function of the current PTF, which can be used for modeling and prediction. The higher the polynomial order, the more accurately the final coefficient set will represent the current PTF in future trials. So, it can be helpful to utilize the model with continuous functions, avoiding the usage of look-up tables.

2.5.2 Ballistic Phase

To estimate the goal position T_x using ballistic model, let us observe that if for some $t' \geq 0$, we have $a_{mx}(t') = 0$ then $x(t') = \frac{T_x}{2}$. So, a basic estimation algorithm during ballistic phase is:

$$\widehat{T}_x(t) = \begin{cases}2x(t), & \text{if } a_{mx}(t) \cdot V_{mx}(t) \geq 0 \\ \widehat{T}_x(t^-), & \text{otherwise}\end{cases},\ \forall t \geq 0,$$

where $\widehat{T}_x(t^-)$ stands for the estimated value of T_x at the previous instant of time.

The idea of doubling the position until the velocity peak for endpoint estimation is not new. In [Oirschot and Houtsma, 2001], observing the experimental data, the authors concluded that it could be an option to obtain the users' goal during the movement. We derived this conclusion here from the equations presented for the ballistic phase of the switched model (thus suggesting a mathematical explanation for [Oirschot and Houtsma, 2001]).

2.5.3 Dynamic Regressor Extension and Mixing (DREM)

Consider the linear regression equation:

$$y(t) \quad = \quad \phi(t)^\top \theta,\ \forall t \geq 0,$$

where $y(t) \in \mathbb{R}$ is the measured output signal, $\phi(t) \in \mathbb{R}^n$ is the regressor, and $\theta \in \mathbb{R}^n$ is the vector of unknown constant parameters. The DREM technique, introduced in [Aranovskiy et al., 2016], consists of two steps.

The first step is the *dynamic regressor extension*, where we introduce linear BIBO (bounded-input bounded-output) stable dynamic operators H_i for $1 \leq i \leq n$ and define the vector $Y : \mathbb{R}_+ \to \mathbb{R}^n$ and the matrix $\Phi : \mathbb{R}_+ \to \mathbb{R}^{n\times n}$ by applying the operators on the scalar output y and on the regression vector ϕ:

$$Y = [Y_1 \ldots Y_n]^\top,\ \Phi = [\Phi^1 \ldots \Phi^n]^\top;$$
$$Y_i = H_i(y),\ \Phi^i = H_i(\phi),\ 1 \leq i \leq n.$$

Due to the linearity of the operators H_i and BIBO stability, these signals satisfy the equation:

$$Y = \Phi\theta$$

subject to transient asymptotically converging errors. One of the options of the extension is a *delay operator*

$$H_i(\cdot)(t) := \cdot(t - \tau_i)$$

for some $\tau_i > 0$, $\tau_i \neq \tau_j$ for $1 \leq i \neq j \leq n$.

The second step is *mixing*, whose objective is to derive a set of n scalar equations to separate the estimation of each parameter θ_i. Denoting $\widetilde{Y} = \Phi^* Y$ and $\varphi = \det(\Phi)$, where Φ^* is the adjugate matrix of Φ, we obtain:

$$\widetilde{Y}_i(t) = \varphi(t)\theta_i$$

for all $1 \leq i \leq n$. For this set of scalar equations, the gradient parameter estimation algorithm is applicable to obtain $\widehat{\theta}$ the estimate of θ:

$$\dot{\widehat{\theta}}_i = \gamma_i \varphi(\widetilde{Y}_i - \varphi\widehat{\theta}_i)$$

for $1 \leq i \leq n$, where $\gamma_i > 0$ is a tuning parameter.

2.5.4 Corrective Phase

In order to apply estimation techniques to the model:

$$\dot{V}_{mx}(t) = -b_1 V_{mx}(t) - b_2(x(t) - T_x),\ \forall t \geq 0$$

we need to divide it by b_2 to decouple the main parameter we want to estimate here, T_x. Thus, we can present this equation in a suitable form for the linear regression:

$$x(t) = -\frac{1}{b_2}\dot{V}_{mx}(t) - \frac{b_1}{b_2}V_{mx}(t) + T_x = \omega^\top(t)\theta,$$

where $\omega(t) = \begin{bmatrix} -a_{mx}(t) & -V_{mx}(t) & 1 \end{bmatrix}^\top$ is the regression vector, which contains measured signals, and $\theta = \begin{bmatrix} \frac{1}{b_2} & \frac{b_1}{b_2} & T_x \end{bmatrix}^\top$ is the vector of unknown constant parameters to estimate. Next, a linear estimation technique (as for PTF previously) can be applied. However, the PE condition [Bitmead, 1984] needs to be satisfied for the convergence of the parameter estimation error, which is not confirmed in our setting (the system is stable, and the external input is constant; therefore, V_x and a_{mx} approach zero asymptotically, while $x(t)$ goes to the constant T_x as t goes to infinity). Since we mainly need to estimate only one parameter, *i.e.*, the desired position T_x, a strong excitation providing the PE property for all three parameters in θ is not needed. It is useful to separate the estimation variables for better identification. An efficient and recently introduced DREM procedure [Aranovskiy et al., 2016; Korotina et al., 2020] (see Section 2.5.3) allows the coefficients in θ to be evaluated separately. This procedure can also provide a finite-time convergent estimation even without the satisfaction of the PE condition [Wang, Efimov, and Bobtsov, 2019] (interval excitation, presented in pointing tasks, is enough). In this chapter, we selected the auxiliary filters as delays: $H_i(s) = e^{i\tau s}$ for $i = 0, 1, 2$ for some basic delay $\tau > 0$, then using the steps described in subsection 2.5.3, we can get three scalar equations with separated parameters:

$$\widetilde{Y}_i(t) = \varphi(t)\theta_i + v(t),\ \forall t \geq 0 \tag{2.3}$$

where v is the error variable related to the measurement and differentiation noise, and φ is the new scalar regressor, which leads to the adaptation algorithm

$$\dot{\widehat{T}}_x(t) = -\gamma_3\varphi(t)(\varphi(t)\widehat{T}_x(t) - \widetilde{Y}_3(t)),$$

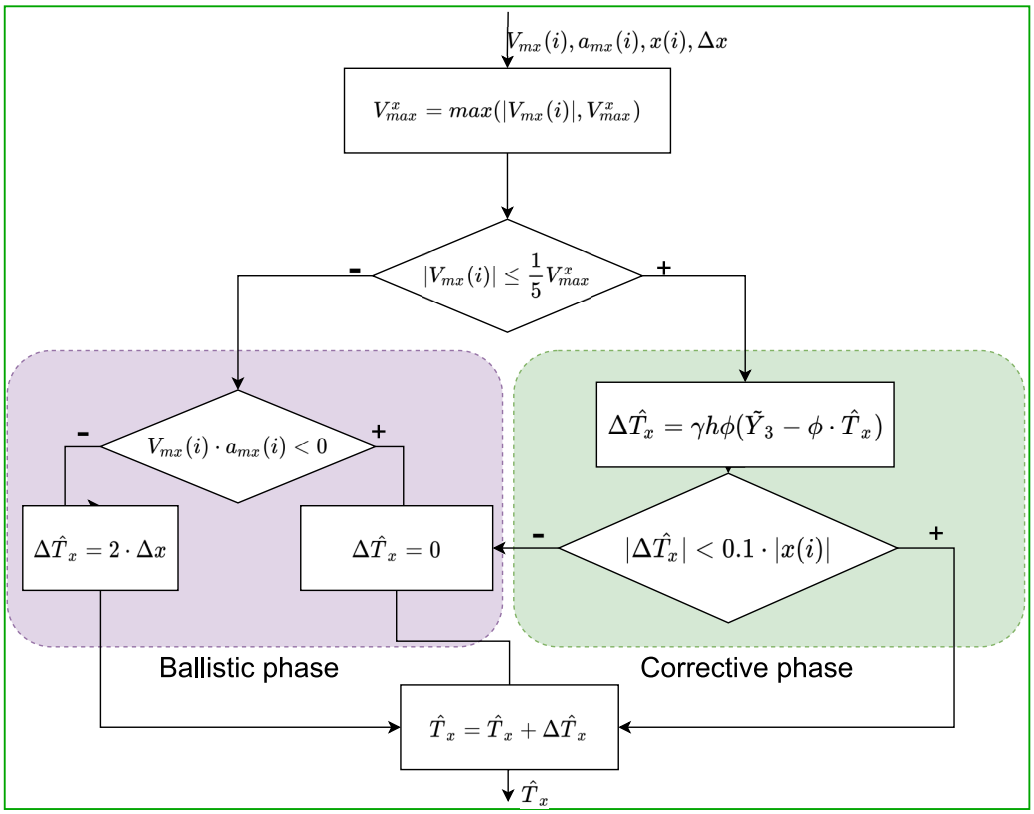

FIGURE 2.4: Switched Model Diagram

with $\gamma_3 > 0$ a tuning parameter and $\widehat{T}_x$ the estimate of T_x.

The noise is unknown, but we can detect when its influence is too strong and cut the prediction in corresponding regions.

A simple way to do it would be to introduce an additional condition on the estimate $\widehat{T}_x$. To reduce the significant influence of the noise, we can bound $\widehat{T}_x$ under the assumption that it is supposed to be close to the endpoint after the ballistic phase. Although the screen resolution naturally bounds the endpoint position, we want to avoid using the introduced model's setup-dependent data. We can restrict our prediction estimation using only the cursor position data obtained from the current trial. Because the correction phase serves for the final navigation of the pointer to the goal, it should ideally operate around the current position value. Choosing the approximate evaluation (bound) as $\frac{1}{10}$ of the distance already traveled, we can introduce the condition as follows:

$$\left|\widehat{T}_x(t) - \widehat{T}_x(t^-)\right| < 0.1 \ |x(t)|$$

where $\widehat{T}_x(t^-)$ denotes the estimate of T_x at the previous instant of time. If it is satisfied, we update $\widehat{T}_x$. Otherwise, we keep the previous value, cutting out the noisy region affecting the estimation and producing numerical instability.

2.5.5 Switched prediction algorithm

The procedure for updating the endpoint estimation $\widehat{T}_x$ using the proposed simplified switched model is divided into three modes:

a) Ballistic phase before velocity peak (before a_{mx} reaches zero). We look for the velocity V_{mx} peak during this part of the ballistic phase by comparing the current absolute value to the previous maximum. While V_{mx} grows, $\widehat{T}_x$ can be found as:

$$\widehat{T}_x(t) = 2x(t).$$

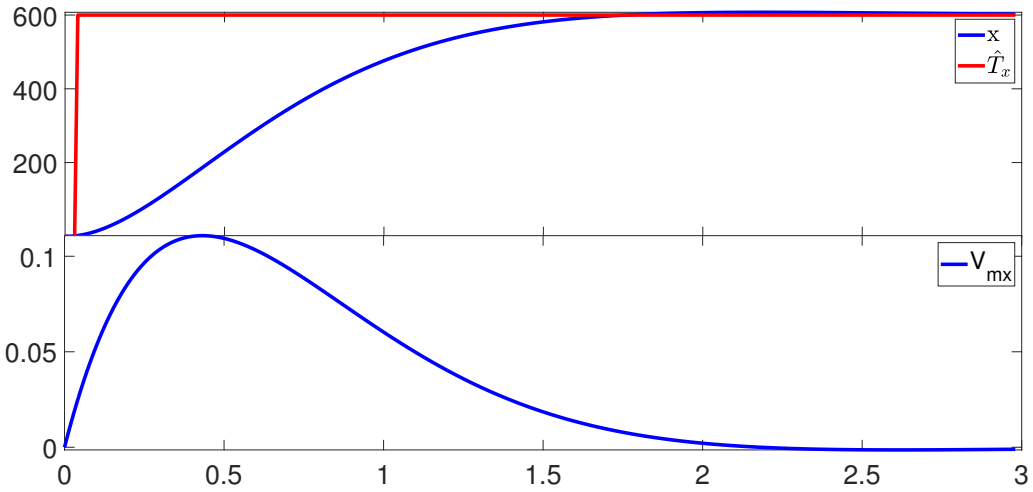

FIGURE 2.5: Simulation of corrective phase model: top sub-figure t [s] vs x and $\widehat{T}_x$ [pxl]; bottom sub-figure t [s] vs V_{mx}[m/s]

b) Ballistic phase after velocity peak. If the current velocity V_{mx} is lower than its maximum, then $\widehat{T}_x$ is constant and defined by its previous value at the peak.

c) The correction phase. Here, we use the DREM estimation procedure as described before.

Moreover, we can generalize such an approach to the situation when the user's estimation of PTF is not adequate.

2.5.6 Endpoint Prediction algorithm with submovements

Sometimes during the trial, the user cannot reach the goal on the first try. It is a well-known problem in the pointing task. The additional ballistic phases, which appear before the goal is reached (it is easy to recognize them in the velocity profile shown in Fig. 2.3), are called sub-movements and make the endpoint prediction task much more complicated. The switching model presented in this chapter allows us to change the mode at any time. Therefore, we can generalize the prediction algorithm presented above by considering possible sub-movements.

The generalized idea for updating the endpoint prediction is presented in Fig. 2.4. Basically, we check $\Delta\widehat{T}_x$ at each time step, depending on the conditions of the current value of the velocity $V_{mx}(i)$ and acceleration $a_{mx}(i)$.

First, we search for the maximum mouse velocity magnitude by comparing it to the current value. Second, we determine in which phase of motion we currently are. Below $\frac{1}{5}$ of the maximum velocity, we use the estimation from the model for the correction phase; otherwise, we use the ballistic prediction. If we are in the ballistic phase, we have the following condition to verify: whether the velocity is increasing with regard to the direction of the motion or decreasing (it means that we require current acceleration and velocity have the same sign to adjust the prediction by $2\Delta x$). Through this modified condition from the previous section, we also consider overshooting: when the target has already passed and the user moves the mouse in the opposite direction, $\Delta\widehat{T}_x$ is negative and our prediction is decreasing in the same way as with undershoot, the sign is considered. Simultaneously, we have the corrective phase condition to bound the prediction when the data is the noisiest. Since the noise is unknown, we cannot compensate for its influence, but we can restrict the estimation to those moments when the estimation is leaving the predefined boundaries. It usually signifies exactly when the measurement data is the noisiest. When it is satisfied, we update the $\widehat{T}_x$; otherwise, we keep the prediction to avoid possible numerical instabilities and make the algorithm more robust to the disturbances.

Remark 2.5.1. *We have the same diagram for $\hat{T}_y$ in parallel at each timestep. It is possible that according to the V_{mx} velocity profile, we are still in the ballistic phase, while according to V_{my}, we are in the corrective*

phase and vice versa*. We assume that this situation is possible, based on the observation of the 2-D cursor trajectories from the experimental data.*

The generalized algorithm cannot estimate the final desired value in the case of sub-movements after the first velocity peak. However, we can estimate the sub-movement final value earlier by accumulating new estimates with the first peak value.

Let us demonstrate the efficiency of the proposed model and the estimation approach using real data and simulations.

2.6 Results and Simulations

2.6.1 Pointing Transfer Function

Regarding PTF estimation, a fifth-order polynomial was chosen to represent the gain, $q = 5$ (the parameter tuning has been performed via the error and trial method). Several trials were used to identify the coefficients (12×4 trials in Fig. 2.6), and the position of the next trial (x, y) was built using only the velocity V_m set with the model (2.1). In Fig. 2.6, it is shown that the used approach reconstructs the PTF pretty accurately. The more trials used to build the polynomial – the more accurate the approximation is. In the experiments recorded in [Antoine, Malacria, and Casiez, 2018], two different PTFs were used for the pointing task: a) the sigmoid function that mimics the default macOS transfer function provided by `libpointing`, configured with the following parameters: ($gmin = 1$ $gmax = 15$ $v1 = 0.05$ m/s $v2 = 0.6$ m/s), and b) the custom one, created with *Libpointing* which mimics constant gain of 4. The resulting gain curve,

$$\texttt{gain}(V_m) = \frac{TF(V_m)}{V_m},$$

of full trials for one user (in the range 0.0127-0.3 [m/s] of mouse inputted velocity) is represented in Fig. 2.7. One can see from these plots that in the lower range (0.0127-0.2 [m/s]), the curves tend to align more with the real gain curve because there were more points presented with these velocity values in the trials during the identification process, while in the range 0.2-0.3 [m/s] the values were rarer, so the deviation is bigger and the gain is less accurate.

These results confirm that the presented methodology provides an accurate way to reconstruct the PTF by an analytical function, which can help in future analysis and position estimation.

2.6.2 Model Validation

First, the chosen model in the correction phase was evaluated in the simulation, where the model parameters were assigned artificially: $b_1 = 4$, $b_2 = 7$, $T_x = 600$ pxl and PTF= arctan (it can be any bounded function according to [Aranovskiy et al., 2020]). The model identification results are presented in Fig. 2.5, the final position and other coefficients are estimated almost simultaneously with the constant time step $h = 0.01$ [s], meaning that the proposed estimation method works for the designed model. Real data from experiments in [Antoine, Malacria, and Casiez, 2018] were used for the switched model validation.

We try to avoid the division into two phases and represent the movement via the correction phase model. However, the estimation results given in Fig. 2.8 show that the process's high-velocity part (the ballistic phase) does not fully correspond to the chosen model with the experimental data, and it is hard to estimate the value of T_x early enough. An explanation for this phenomenon is that there might be some nonlinear terms missed in the model (2.1) for the forces F_{fr} and F_{input}, which leads to high modeling error and inaccurate identification during the ballistic phase. Investigating such a missed term can be a task for future model improvements. Still, as one can see in Fig. 2.8, the model represents the process in the corrective phase well.

After analyzing the performance of the reduced model, we would like to return to the classic division in two phases, where we use the complete designed model with separate equations for the ballistic phase until the motion is close to the correction phase. Such a model demonstrates a better overall performance (check Fig.

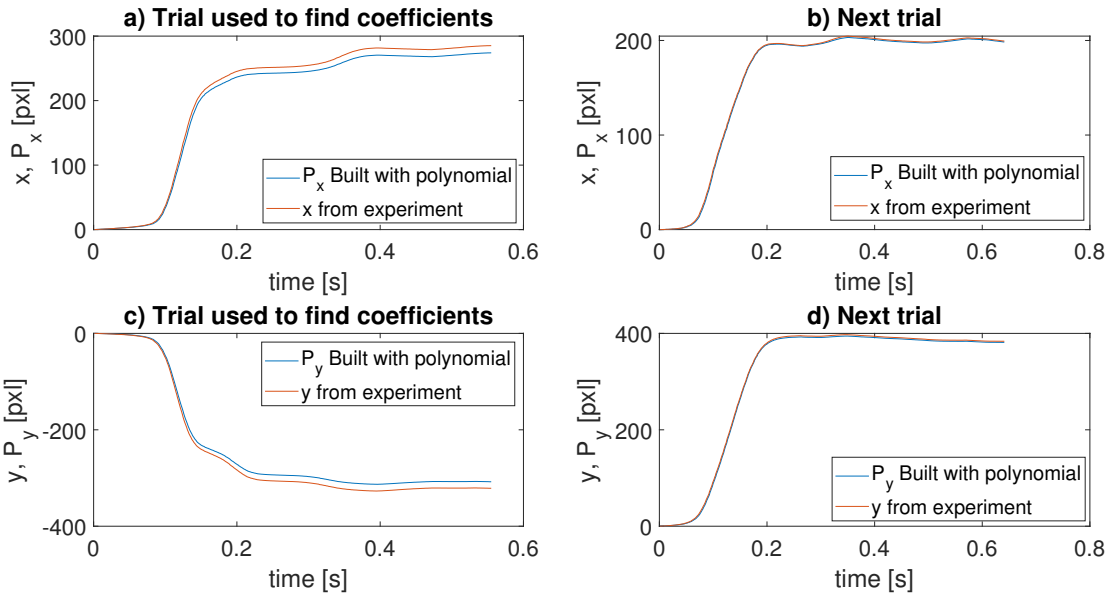

FIGURE 2.6: Transfer functions: x, y [pxl] vs time

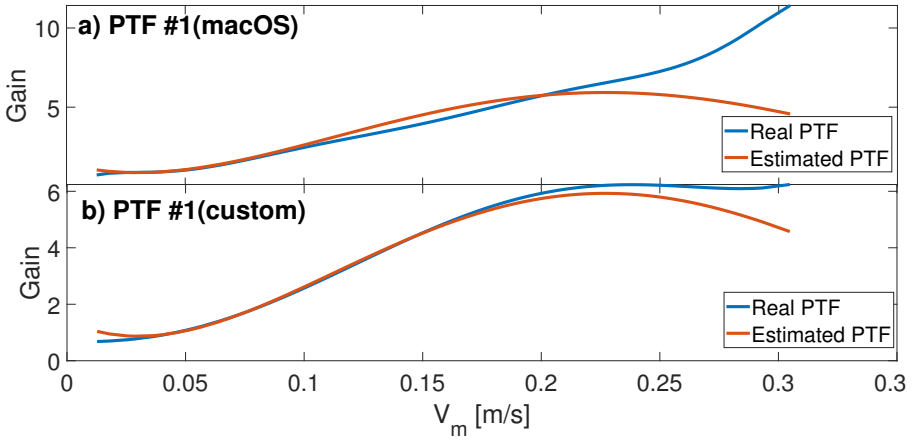

FIGURE 2.7: Gains comparison: V_m [m/s] vs gain

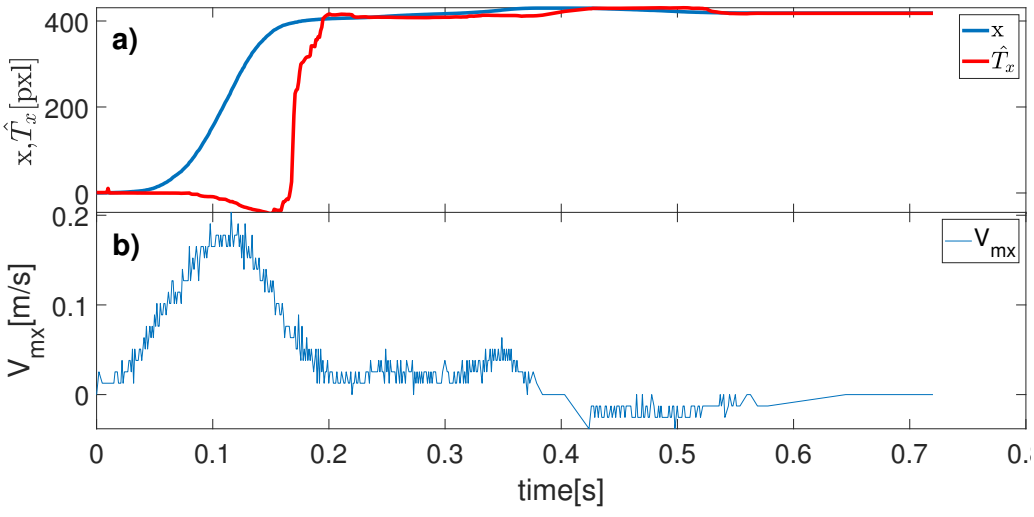

FIGURE 2.8: Correction phase model estimation: a) t[s] vs x and $\widehat{T}_x$ [pxl]; b) t [s] vs V_{mx} [m/s]

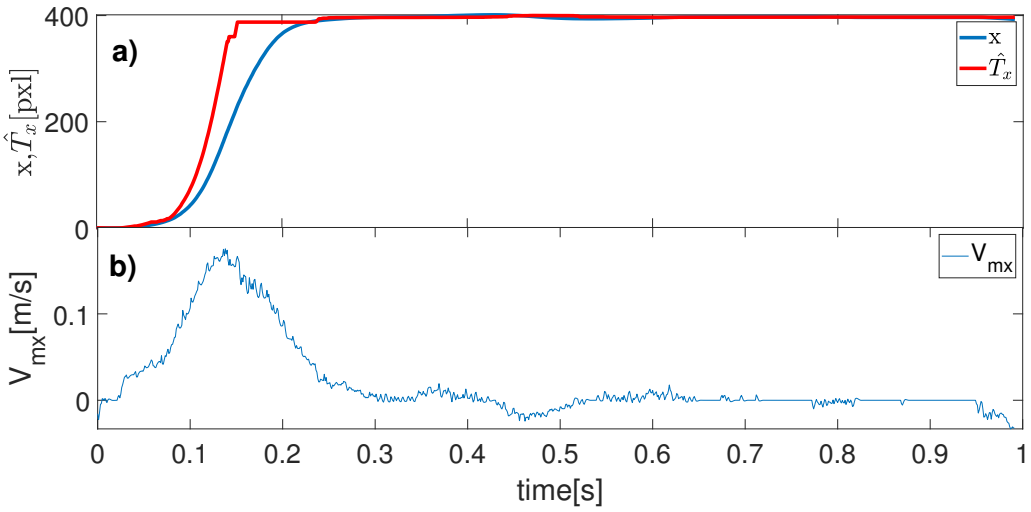

FIGURE 2.9: Switched model estimation for one trial: a) t [s] vs x and $\widehat{T}_x$ [pxl]; b) t [s] vs V_{mx} [m/s]

2.9), and it guesses the destination point on the peak of the velocity profile rather accurately, but only when the user has enough experience. When the sub-movements appear, the algorithm recognizes them as explained in Section 5.4 and gives a fair prediction reacting to them in the same way as to the main peak (check Fig. 2.10). However, to validate the model performance more concretely, let us compare it with another algorithm.

2.6.3 Comparison with existing algorithms

As mentioned in the introduction, prediction algorithms can be divided into two groups (with or without prior knowledge). Both groups have their pros and cons. For instance, algorithms with foreknowledge can be more precise on average but require the user to complete the range of motion, usually taking some time and memory. Moreover, the result can be unpredictable under unknown circumstances. Concurrently, algorithms without memory can produce immediate results, which may be less accurate but more stable in any setup and unpredictable situation.

The problem is then to find the trade-off between the final accuracy and robustness of the prediction. The work [Pasqual and Wobbrock, 2014] shows that the algorithm with foreknowledge does not improve the estimation significantly, even when theoretically, this should be a significant advantage.

This chapter introduces an algorithm belonging to the second group and fits the theoretical and mechanical models presented above. For this reason, in this section, we make a comparison with the KEP algorithm to show our model's performance using the same data. It is worth mentioning that the KEP algorithm was improved later in [Ruiz and Lank, 2009], the newer version became more stable in terms of estimation (the stability check was added), and the prediction started in 85% of the movement, which improved the accuracy of the final prediction but removed information about early prediction. Later, the single-point prediction, based on the KEP algorithm was introduced in [Ruiz and Lank, 2010], but since we are interested in the early prediction - a single point and the improved model were not considered in the comparison, only the stability condition from the improved model was applied. Apart from this, we reconstructed the KEP algorithm from the original paper of [Lank, Cheng, and Ruiz, 2007], applying it to every motion step.

Interestingly, the ballistic phase prediction also satisfies the Hogan Minimal Jerk model [Hogan, 1984] theoretical data, used as a basis for the KEP algorithm. It is easy to verify that the amplitude of the velocity in the equation is precisely the doubled position at the time of the maximum velocity ($x(1) = 2x(\frac{1}{2})$, $t \in [0, 1]$ in Eqn. 8 of [Lank, Cheng, and Ruiz, 2007]). Therefore, if we apply our ballistic algorithm to the Hogan equations, we obtain the earlier exact prediction halfway on the velocity peak (Fig. 2.11). It is another reason why we think that our algorithm should outperform the KEP.

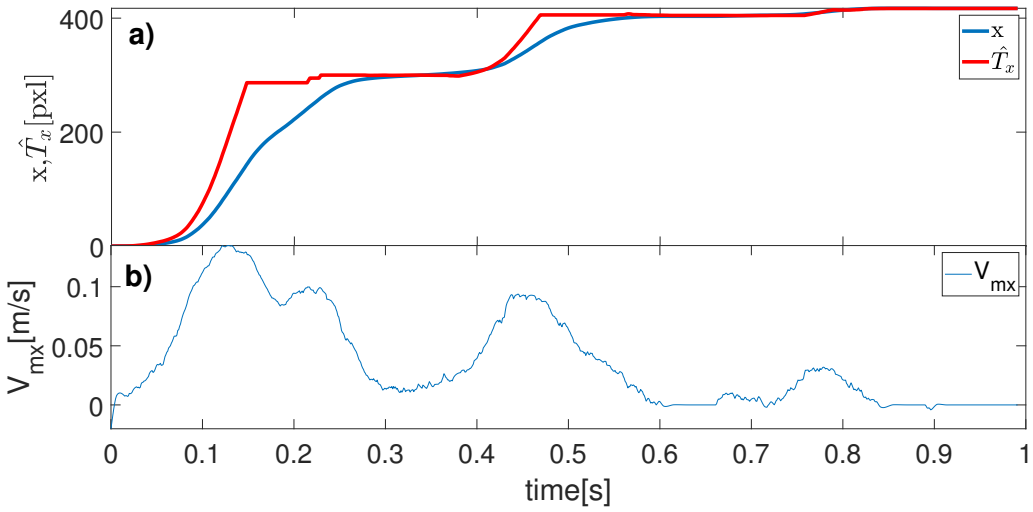

FIGURE 2.10: Switched model estimation for one trial: a) t [s] vs x and $\widehat{T}_x$ [pxl]; b) t [s] vs V_{mx} [m/s]

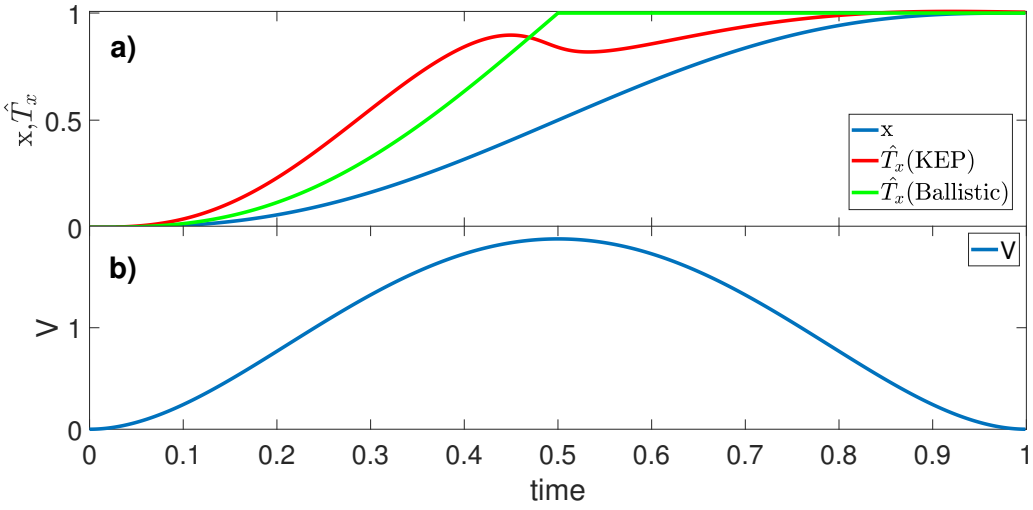

FIGURE 2.11: Hogan's law theoretical model (unitless): a) t vs x and $\widehat{T}_x$; b) t vs V

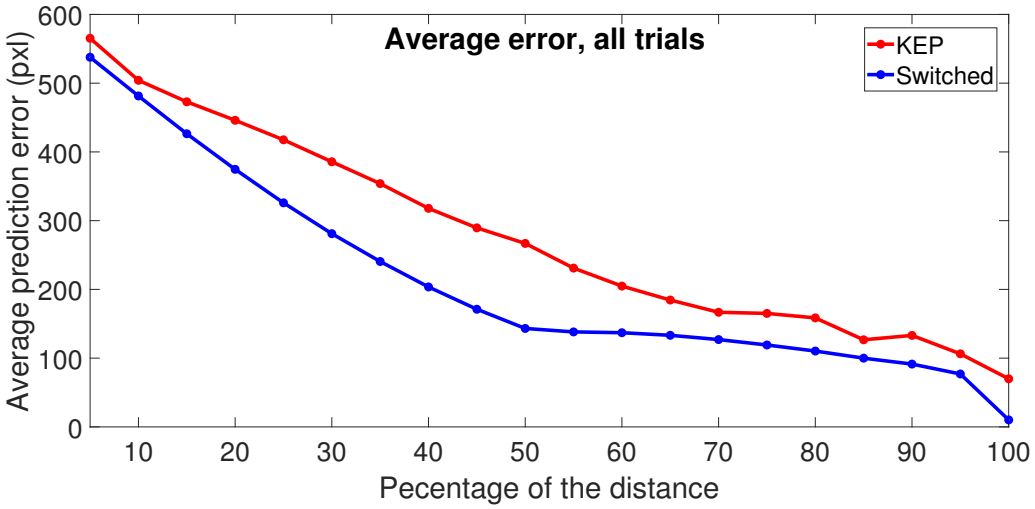

FIGURE 2.12: Comparison: percentage of the path vs error [pxl]. All trials

Since users were not used to the setup, most of the trials in the experiments of [Antoine, Malacria, and Casiez, 2018] had sub-movements. It is important to mention that by trials without sub-movements, we mean the ones where the highest peak of the velocity is at least 5 times higher than all the others, and peaks below this threshold are not considered as sub-movements due to the low impact on the prediction, the example can be found in Fig. 2.3. Since our prediction algorithm considers trials with sub-movements in Fig. 2.12, we then chose all the experiment trials (960).

The way of evaluating the model was as follows: we had 960 trials from users performing pointing tasks in 2-D space, but since the estimation in our model is separate for $\widehat{T}_x$ and $\widehat{T}_y$, we took one set of data from each trial, the vertical or the horizontal (x, y), depending on which distance (T_x or T_y) was longer. This choice was made to obtain a suitable range, for comparison with KEP (in [Ruiz and Lank, 2009], the target range was $200-600$ pxl). The range of target in the chosen data was $265-800$ pxl.

The MAE (Mean Absolute Error) comparison at the different percentages of the way shows that, on average, we have a better estimate at all trajectories (see Fig. 2.12). In our switched model, we have faster error convergence to the 50 % of the way, where the velocity peak is supposed to be situated and after the rate decreases to 95 %, and finally, it converges to the endpoint value with an average error of 9.6 pxl. In contrast, KEP shows convergence close to linear with the final average error of 69.9 pxl.

However, a more detailed analysis in the box-whisker plot in Fig. 2.13 shows that our reconstructed KEP algorithms mean error is affected by the larger amount of the outlier points and their wider distribution. By outlier, we mean a value bigger than 1.5 times the interquartile (box range). This could mean that the stability check applied from [Ruiz and Lank, 2009] might not be enough to provide bounded prediction using the curve fitting process in all real-world cases.

For the more solid comparison, the statistical test on the prediction error data for all 10 users, considering different model (KEP, Switched), different target width, distance, PTF was provided. Repeated measures ANOVA showed a significant effect of model on the error (from 0.1 to 0.75 of the distance $p < 0.001$), with the most significant in 0.5 - $F(1,9) = 38.81$, $p < 0.001$, $\eta_p^2 = 0.81$. In the range from 0.75 to 1, the test showed no significant difference in the model performance. Also, the effect of the distance was significant in all cases (for instance, $F(1,9) = 214.35$, $p < 0.001$, $\eta_p^2 = 0.96$ for 0.5) target width in some cases ($F(1,9) = 11.34$, $p < 0.008$, $\eta_p^2 = 0.56$ for 0.5), pair model*distance ($F(1,9) = 16.61$, $p < .003$, $\eta_p^2 = 0.65$ for 0.5) and there was no effect of the PTF.

Another test was conducted using the error data without outliers in Fig. 2.13 (for all outliers (red-crossed points), the quartile bound was assigned (0.25 or 0.75 percentile)). Repeated measures ANOVA still showed a significant effect of the model in the range from 0.15 to 0.6 of the distance ($p < 0.01$) with the highest in 0.5 with $F(1,9) = 15.70$, $p < 0.003$, $\eta_p^2 = 0.64$, and no significant effect after. This means that even considering the instability of KEP early prediction, the Switched model introduced in this chapter still outperforms KEP in the

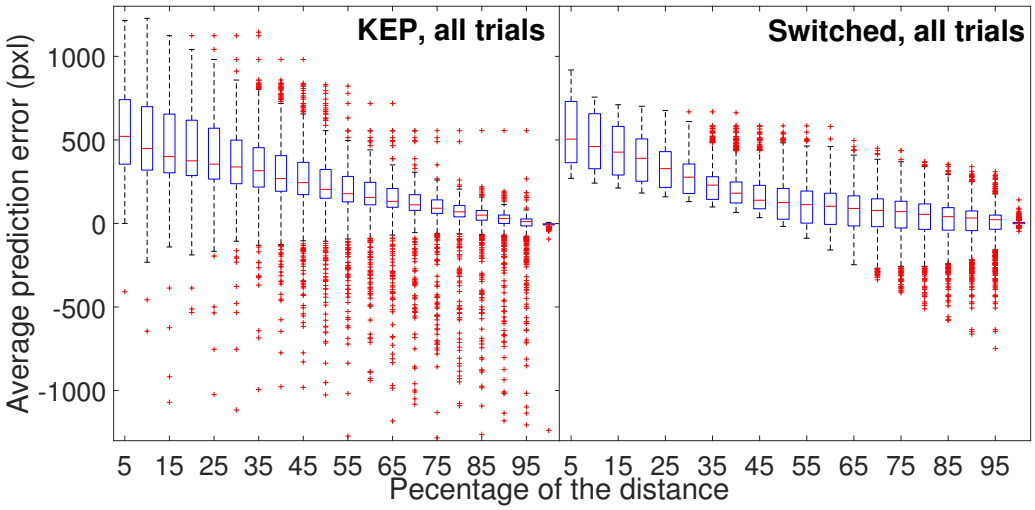

FIGURE 2.13: Box-whisker plot comparison: percentage of the path vs error distribution [pxl]

early and mid-distance prediction. Another advantage is that after removing the outliers for both models, the average final prediction is still closer with the Switched (5.2 pxl to 6.4 in KEP).

The comparison results are not surprising because the disadvantage of the KEP model is that the estimation is unstable in the early stage. This is why the KEP model authors claim to obtain a good estimation starting only from 80 % of the total path, which is not the case in the model introduced in this chapter. To conclude the section, we can state that the average error analysis showed that the presented switched algorithm outperforms the most known algorithm in the group of algorithms without memory (KEP), especially at the early phase (trajectory path 85 %) and converges to almost exact value at the end due to the separated correction phase estimation algorithm.

Part II

Estimation and control of nonlinear systems using steady-state response

Chapter 3

Design of reduced-order observers and regulators using linear steady-state mapping

3.1 Introduction

Moving to the second problem of the thesis, formulated in Chapter 1, we consider an interconnection of two dynamical systems, Σ_1 and Σ_2, as presented in Fig. 3.1. We assume that there exists a mapping π, connecting two steady-states of the system. The goal of this chapter is to investigate the case where this mapping is linear, consider different variations of the connection illustrated in Fig. 1.2-1.6, and provide a solution of relevant estimation and control problems, exploiting linearity of the steady-state response.

For a general class of nonlinear systems, it is difficult to establish the linear map π since it has to be a solution of PDE (1.9). However, it appears that in cases of some classes of nonlinear systems, under certain assumptions, the steady-state can become a linear map. This happens due to a so-called "weakness" of nonlinearity and a "strong" linear part. Examples of such systems are Lur'e systems or Persidskii systems, where the dynamics of the system Σ_1 is characterized as a sum of a linear part and a nonlinear one, and the system Σ_2 has similar dynamics, with a similar nonlinearity. Then, the nonlinearity of the first system can cancel the nonlinearity of the second one under the linear substitution (in the PDE (1.9) with π).

This form of the considered system, called Persidskii (or forced Lur'e-like), is common in theoretical analysis and practical applications. They can be found in many fields, such as in neural networks [Forgione and Piga, 2021], [Kambhampati, Garces, and Warwick, 2000], mechanical and robotic systems [Rajamani and Cho, 1998, Spong, 1987], electrical circuits [Chua, 1994], genetic networks [Li et al., 2006], or in the description of a bioreactor [Bernard et al., 2001]. Such systems attracted the attention of researchers in control theory, starting from Aizerman's and Kalman's conjectures and Persidskii or Lur'e systems [Persidskii, 1969]. Roughly speaking, it is an asymptotically stable linear system under the presence of a *weak* nonlinearity, which makes a system suitable for quasi-linear approaches and greatly simplifies the analysis.

Many applications usually consider multi-plant scenarios (networks, multi-agent tasks, multi-circuits, *etc.*), which makes an interconnection to be justified for the analysis. Moreover, as shown in this part of the thesis, an advantage of the models describing these systems is that a global steady-state solution can be derived analytically (without applying numeric interpolation tools) under mild conditions.

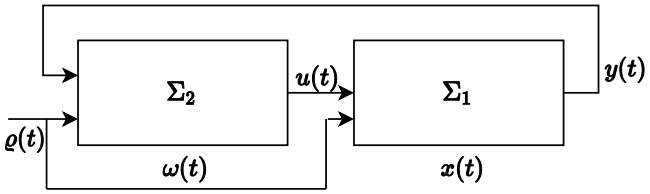

$$t \to \infty, x(t) \to \pi(\omega(t))$$

FIGURE 3.1: Interconnected systems with a reference signal

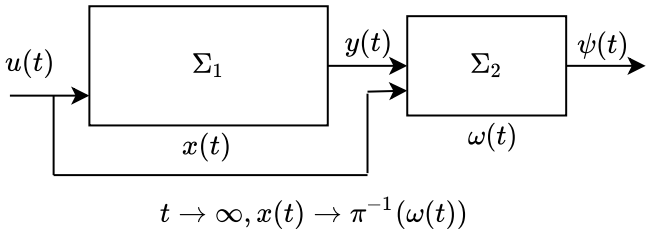

FIGURE 3.2: Interconnected systems with a reference signal

In Section 3.2, we consider the connection of such systems Σ_1 and Σ_2 as presented in Fig. 1.4 or 3.1, where we begin by applying the tools of nonlinear model reduction by moment matching theory to the mentioned class of nonlinear systems. In [Astolfi, 2010], only a cascade of a signal generator and a plant is studied. In this work, we analyze a complete feedback interconnection. By interconnection, we mean a set of two systems with the same nonlinearity [Arcak and Kokotovic, 2001], where the first system's input is the second's output and *vice versa* (see Fig. 3.1). Such a generalization allows us to apply the presented result to a broader class of problems for a given particular class of systems.

Later, in Section 3.2, two of the many possible applications of the invariant solutions are presented. First, they help to design a reduced-order observer for the cascade scenario. Another possibility is to design a dynamic trajectory tracking controller or an observer for a non-uniformly observable system, *i.e.*, under properly selected inputs only. It is a case that is rarely studied in the literature. Generally, the observer's design for models showing observability for any input (the so-called *uniform observability*) is more straightforward; it only focuses on the observer structure, skipping the input selection problem. In the non-uniform case, an input signal (generator) should be incorporated into the observer synthesis procedure. The effects of measurement noises and disturbances are taken into account.

In Section 3.3 of this thesis, we consider a setting where the connection is reversed, as it is described in Fig. 1.6 and the connection is not reciprocal anymore since we assume that we cannot or do not need to alter system Σ_1. This idea presented in Section 3.3 follows the so-called invariant manifold approach proposed in [Karagiannis and Astolfi, 2005, Karagiannis, Carnevale, and Astolfi, 2008], where it was specifically applied to reduced-order observers for a general class of nonlinear time-varying systems. It provides conditions for the existence of a solution, described by a nonlinear invertible function (chosen as a solution of the corresponding PDE), embedded into an invariant manifold containing both the observer and system dynamics. Later, this idea continued in the immersion and invariance approach [Astolfi and Ortega, 2003] where it was used primarily in adaptive control and estimation. The application of the invariant manifold method is non-trivial. It might lead to some difficulties (related to the requirement of the existence of an invertible solution of a PDE), which complicates its implementation (the choice of a solution is case-dependent).

The chosen system class is of particular interest regarding the invariant manifold approach because a set of LMEs can replace the conventional PDE of the invariant manifold method and a set of LMIs can provide the conditions of system stability. As we show later in the section, this procedure for the considered class of systems is more constructive in practice and easy to implement. We also demonstrate that our result can be applied to the reduced-order state observation problem and fits a conventional linear regression solution and, in some instances, a nonlinear one, displaying a broader field of implementation and problem-solving for a class of Persidskii systems.

Section 3.2 consists of the problem statement, the main results, including the analytic steady-state expressions for particular forms of interconnected nonlinear systems, building the observer, and the tracking control design (the state estimation in the absence of uniform observability), arranged in subsections. The conditions of all theorems and proofs use linear matrix inequalities (LMIs) and the Lyapunov function approach to analyze the error dynamics stability. In subsection 3.2.4, we show the efficiency of the proposed observers through numerical examples, with applications to a bioreactor model, a one-link robotic arm model, and a Chua circuit.

Section 3.3 is outlined as follows. The main result on the observer existence and convergence conditions is

provided in continuous- and discrete- time. Some applications, including reduced-order observers and parameter estimation in regression analysis (both in linear and nonlinear settings), are given as well as a discrete-time reduced-order observer. Two nonlinear examples in subsection 3.3.6 demonstrate the efficiency of the presented work.

3.2 Problem statement I. Interconnection

The class of systems of interest is composed of Persidskii systems [Persidskii, 1969, Efimov and Aleksandrov, 2019, Efimov and Aleksandrov, 2021] with only one nonlinearity satisfying the following sector condition

$$sf(s) > 0, \forall s \in \mathbb{R} \setminus \{0\}.$$

These systems are also often addressed in literature as Lur'e system [Yalçin, Suykens, and Vandewalle, 2001] (or forced Lur'e-like [Arcak and Kokotovic, 2001; Yakubovich, 2002; Liberzon, 2006]). Therefore, consider an interconnection of two such nonlinear systems:

$$\begin{cases} \dot{x}(t) = A_0 x(t) + A_1 f(Hx(t)) + Bu(t) + Q\varrho(t) + d(t), \\ y(t) = C_0 x(t) + C_1 f(Hx(t)), \end{cases} \tag{3.1}$$

$$\begin{cases} \dot{\omega}(t) = S_0 \omega(t) + S_1 f(J\omega(t)) + Gy(t) + E\varrho(t) + w(t), \\ u(t) = L_0 \omega(t) + L_1 f(J\omega(t)), \end{cases} \tag{3.2}$$

where $x : \mathbb{R}_+ \to \mathbb{R}^n$ is the state function and $y : \mathbb{R}_+ \to \mathbb{R}^p$ is the output function of (3.1); $\omega : \mathbb{R}_+ \to \mathbb{R}^q$ is the state function and $u : \mathbb{R}_+ \to \mathbb{R}^m$ is the output function of (3.2); $\varrho \in \mathcal{L}_\infty^z$ is the known common input to both systems; $f : \mathbb{R}^r \to \mathbb{R}^k$ is a nonlinear continuous function, $A_0 \in \mathbb{R}^{n\times n}$, $A_1 \in \mathbb{R}^{n\times k}$, $H \in \mathbb{R}^{r\times n}$, $B \in \mathbb{R}^{n\times m}$, $C_0 \in \mathbb{R}^{p\times n}$, $C_1 \in \mathbb{R}^{p\times k}$, $S_0 \in \mathbb{R}^{q\times q}$, $S_1 \in \mathbb{R}^{q\times k}$, $J \in \mathbb{R}^{r\times q}$, $G \in \mathbb{R}^{q\times p}$, $L_0 \in \mathbb{R}^{m\times q}$, $L_1 \in \mathbb{R}^{m\times k}$, $Q \in \mathbb{R}^{n\times z}$ and $E \in \mathbb{R}^{q\times z}$ are known constant matrices; $d \in \mathcal{L}_\infty^n$ and $w \in \mathcal{L}_\infty^q$ are unknown essentially bounded disturbances. We assume that the nonlinearity f allows the forward existence and uniqueness of solutions of systems (3.1), (3.2).

Remark 3.2.1. *Note that for $G = 0$, $E = 0$, the dynamics of* (3.2) *is an example of* (1.7)*, so it becomes a signal generator for* (3.1)*. In such a case, we have a nonlinear system as in* (1.1) *and* (1.7)*, eligible under Assumption 1.3.1, for applying the nonlinear moment theory [Scarciotti and Astolfi, 2017b] with $d = 0$, $w = 0$.*

First, this section, aims to find analytically an invariant/steady-state solution of the interconnection of systems (3.1), (3.2) for the case $d = 0, w = 0$. Second, for the case of noisy measurements, a reduced-order observer is designed using these steady responses, where stability conditions of the estimation error are formulated using LMIs. Third, an additional attention will be paid to relaxing the uniformity constraint for the observability of the system (3.1). The existence conditions for a signal generator will be proposed, allowing estimating the state x, or designing the trajectory tracking control.

3.2.1 Steady-state solutions in noise-free case

Using tools from the nonlinear model reduction by moment matching theory, we can formulate the conditions for the existence of a steady-state/invariant solution for (3.1), (3.2) with $d = 0$ $w = 0$:

Proposition 3.2.1. *Assume that there exists $\Pi \in \mathbb{R}^{n\times q}$ such that $J = H\Pi$ and*

$$\begin{aligned} (A_0 - \Pi G C_0)\Pi - \Pi S_0 + BL_0 = 0, \\ A_1 + BL_1 - \Pi(S_1 + GC_1) = 0,\ Q - \Pi E = 0, \end{aligned} \tag{3.3}$$

then

$$x(t) = \Pi\omega(t),\ \forall t \in \mathbb{R}_+$$

is a solution of the system (3.1), (3.2), *for any* $\omega(0) \in \mathbb{R}^q$, $x(0) = \Pi\omega(0)$ *and* $\varrho \in \mathcal{L}^z_\infty$.

In addition, if for some $\omega(0) \in \mathbb{R}^q$, $x(0) \in \mathbb{R}^n$ *and* $\varrho \equiv 0$ *the functions* ω *and* $g = f(J\omega)$ *are linearly independent, and for all* $t \in \mathbb{R}_+$, $x(t) = \Pi\omega(t)$ *is a solution of the system* (3.1), (3.2), *with* $J = H\Pi$, *then the equalities* (3.3) *are necessarily verified.*

Proof. Let us check that $x(t) = \Pi\omega(t)$, $\forall t \in \mathbb{R}_+$, is a solution of the system (3.1), (3.2). Taking derivatives and using the equations describing the system dynamics gives the equality:

$$\begin{aligned} &A_0x(t) + A_1 f(Hx(t)) + B\left(L_0\omega(t) + L_1 f(J\omega(t))\right) + Q\varrho(t) \\ &= \Pi\left(S_0\omega(t) + S_1 f(J\omega(t)) + G\left(C_0x(t) + C_1 f(Hx(t))\right) + E\varrho(t)\right). \end{aligned}$$

Substituting $J = H\Pi$ and $g = f(J\omega)$ leads to the relation

$$\begin{aligned} &\left((A_0 - \Pi GC_0)\Pi - \Pi S_0 + BL_0\right)\omega(t) + (Q - \Pi E)\varrho(t) \\ &\qquad = -\left(A_1 + BL_1 - \Pi(S_1 + GC_1)\right)g(t), \end{aligned}$$

which is satisfied thanks to (3.3).

Conversely, let $x(t) = \Pi\omega(t)$, $\forall t \in \mathbb{R}_+$, be a solution of (3.1), (3.2) for $\varrho \equiv 0$. Transposing and differentiating this relation, then multiplying it by ω, and taking integrals on $[0,t]$ yield:

$$\begin{aligned} &\int_0^t \omega(s)\omega^\top(s)ds\left((A_0 - \Pi GC_0)\Pi - \Pi S_0 + BL_0\right)^\top \\ &= -\int_0^t \omega(s)g^\top(s)ds\left(A_1 + BL_1 - \Pi(S_1 + GC_1)\right)^\top. \end{aligned}$$

For all $t \geq T$, $\int_0^t \omega(s)\omega^\top(s)ds$ is a non-singular matrix and $\left(\int_0^t \omega(s)\omega^\top(s)ds\right)^{-1}\int_0^t \omega(s)g^\top(s)ds$ is not constant (see Definition 1.3.13), which confirms at least the first equality in (3.3). The second claim of the proposition can be justified by the multiplication of transposed and differentiated expression $x(t) = \Pi\omega(t)$ by the function g and taking integrals on the same interval $[0,t]$:

$$\begin{aligned} &\int_0^t g(s)\omega^\top(s)ds\left((A_0 - \Pi GC_0)\Pi - \Pi S_0 + BL_0\right)^\top \\ &= -\int_0^t g(s)g^\top(s)ds\left(A_1 + BL_1 - \Pi(S_1 + GC_1)\right)^\top. \end{aligned}$$

For all $t \geq T$, $\int_0^t g(s)g^\top(s)ds$ is a nonsingular matrix and $\left(\int_0^t g(s)g(s)^\top(s)ds\right)^{-1}\int_0^t g(s)\omega(s)^\top(s)ds$ is not constant (Definition 1.3.13). The equation $Q - \Pi E = 0$ can be proven in a similar way. □

The advantage of considering the chosen class of forced nonlinear dynamics and its input generator, as in (3.1) and (3.2), is that the found solution π is global in $\omega \in \mathbb{R}^q$ and analytically obtained. Since both systems, (3.1) and (3.2), have the same form of nonlinearity (a conventional hypothesis for Persidskii systems), under suitable relations between the matrices given in Proposition 3.2.1, the obtained function is linear, which simplifies the complexity of further analysis and design for this interconnection greatly.

In Proposition 3.2.1, only the existence of an invariant solution $x(t) = \Pi\omega(t)$ is established, $\forall t \in \mathbb{R}_+$. If the solution $x = \Pi\omega$ is also (locally) attracting in (3.1), (3.2) (see [Khalil, 2002] or Definition 1.3.6), then $\pi(\omega) = \Pi\omega$ represents the steady-state response of the system (3.1) with the input generator (3.2) (for $G = 0$).

Corollary 3.2.1. *Assume that there exists* $\Pi \in \mathbb{R}^{n\times q}$ *such that*

$$(A_0 - \Pi G C_0)\Pi - \Pi S_0 + B L_0 = 0,$$
$$A_1 - \Pi G C_1 = 0,\ B L_1 - \Pi S_1 = 0,\ Q - \Pi E = 0,$$

then $x(t) = \Pi\omega(t)$, $\forall t \in \mathbb{R}_+$, *is a solution of* (3.1), (3.2).

Proof. Differentiating $x(t) = \Pi\omega(t)$, $\forall t \in \mathbb{R}_+$, and using (3.1), (3.2), we obtain:

$$0 = ((A_0 - \Pi G C_0)\Pi - \Pi S_0 + B L_0)\,\omega(t) + (Q - \Pi E)\varrho(t)$$
$$+ (A_1 - \Pi G C_1)\, f(H\Pi\omega(t)) + (B L_1 - \Pi S_1)\, f(J\omega(t)),$$

which is satisfied under the introduced restrictions. □

We remark that this corollary skips the requirement $J = H\Pi$.

3.2.2 Reduced-order observer design

Let us assume that the output of the system (3.1) is available for measurement with a noise signal $v \in \mathcal{L}_\infty^p$:

$$Y(t) = y(t) + v(t),\ \forall t \in \mathbb{R}_+, \tag{3.4}$$

and that the input signal u of (3.1) is not measured (it is the output of (3.2), so it can be interpreted as an internal signal for (3.1), (3.2)). For brevity of exposition, in this section, we assume that f is a globally Lipschitz continuous function, *i.e.*, $\|f(\xi_1) - f(\xi_2)\| \le \lambda\|\xi_1 - \xi_2\|$, for some $\lambda > 0$ and all $\xi_1, \xi_2 \in \mathbb{R}^r$. Our goal is to estimate the state of the interconnected system (3.1), (3.2). To this end, we need the following hypotheses:

Assumption 3.2.1. *There exists a matrix* $\Pi \in \mathbb{R}^{n\times q}$ *such that the equalities* (3.3) *and* $J = H\Pi$ *are satisfied for* (3.1), (3.2).

According to Proposition 3.2.1, it implies that $x = \Pi\omega$ is an invariant solution of the system with $d = 0$, $w = 0$, which may be not unique. To streamline our presentation, we exclude such a situation by supposing that:

Assumption 3.2.2. *The systems* (3.1) *and* (3.2) *are incrementally input-to-state stable by considering* $Q\varrho d$ *and* $E\varrho w$ *as inputs.*

In the last hypothesis, the incremental input-to-state stability is assumed to be global, *i.e.*, for any initial conditions $x(0) \in \mathbb{R}^n$, the corresponding trajectories of (3.1) converge to a region of size $\|d\|_\infty + \|w\|_\infty$ around the trajectory entrained by the signal generator (3.2) and the input ϱ for a given $\omega(0) \in \mathbb{R}^q$. There is no requirement on the boundedness of ω (so, of x). Similar results can be obtained for the local convergence considering the attraction domain (see the following section and examples).

Remark 3.2.2. *Note that under Assumption 3.2.2, the system* (3.1), (3.2) *admits an observer:*

$$\begin{aligned}
\dot{\hat{x}}(t) &= A_0\hat{x}(t) + A_1 f(H\hat{x}(t)) + B\hat{u}(t) + Q\varrho(t) + L_x(Y(t) - \hat{y}(t)),\\
\dot{\hat{\omega}}(t) &= S_0\hat{\omega}(t) + S_1 f(J\hat{\omega}(t)) + GY(t) + E\varrho(t) + L_\omega(Y(t) - \hat{y}(t)),\\
\hat{y}(t) &= C_0\hat{x}(t) + C_1 f(H\hat{x}(t)),\\
\hat{u}(t) &= L_0\hat{\omega}(t) + L_1 f(J\hat{\omega}(t)), \forall t \in \mathbb{R}_+
\end{aligned}$$

where $L_x \in \mathbb{R}^{n\times p}$ *and* $L_\omega \in \mathbb{R}^{q\times p}$ *are gain matrices to be tuned. Even for* $L_x = 0$, $L_\omega = 0$ *we have that* $\hat{x}(t) \to x(t)$, $\hat{\omega}(t) \to \omega(t)$ *when* $t \to +\infty$ *due to the convergence property (provided that* $\|d\|_\infty = \|w\|_\infty = 0$*). The gains* L_x, L_ω *can accelerate the convergence taking into account the attenuation of the noise influence* v*. Moreover, assumptions 3.2.1 and 3.2.2 do not imply observability of* (3.1), (3.2) *(the latter hypothesis implies detectability [Sontag and Wang, 1997] of the system).*

Then Assumption 3.2.1 may help reduce the observer's dimension: since the relation $x = \Pi\omega$ corresponds to the system (3.1) response to the particular input produced by the generator (3.2), its utilization allows designing the observer for the latter dynamics only. Indeed, assumptions 3.2.1 and 3.2.2 have a consequence:

$$Y(t) = \psi(t) + \tilde{v}(t),\ \psi(t) = C_0\Pi\omega(t) + C_1 f(J\omega(t)),$$

where $\tilde{v}(t) = v(t) + \epsilon(t)$ is a new bounded measurement noise for the output system (3.2) and

$$\epsilon(t) = C_0\left(x(t) - \Pi\omega(t)\right) + C_1\left(f(Hx(t)) - f(H\Pi\omega(t))\right),$$

Proposition 3.2.2. *Assume that Assumption 3.2.2 is satisfied. Then, the system* (3.1)*,* (3.2) *is input-to-output stable with the output ϵ and inputs d, w.*

Proof. Let us denote by x_0 and ω_0 the solutions of the system (3.1), (3.2) obtained for some initial conditions and $\|d\|_\infty = \|w\|_\infty = 0$. Since this system is δISS (Assumption 3.2.2), then there exists $\beta \in \mathcal{KL}$ such that for all $t \geq 0$,

$$\|x_0(t) - \Pi\omega_0(t)\| \leq \beta(\|x_0(0) - \Pi\omega_0(0)\|, t),$$

for any initial conditions $x_0(0) \in \mathbb{R}^n$ and $\omega_0(0) \in \mathbb{R}^q$ with $\|d\|_\infty = \|w\|_\infty = 0$ (existence of the solution $x(t) = \Pi\omega(t)$ for all $t \geq 0$ follows from Assumption 3.2.1). By the same reasoning, for any initial conditions $x(0) \in \mathbb{R}^n$ and $\omega(0) \in \mathbb{R}^q$:

$$\begin{aligned}\|x(t) - x_0(t)\| &\leq \beta(\|x(0) - x_0(0)\|, t) + \gamma(\|d\|_\infty + \|w\|_\infty),\\ \|\omega(t) - \omega_0(t)\| &\leq \beta(\|\omega(0) - \omega_0(0)\|, t) + \gamma(\|d\|_\infty + \|w\|_\infty)\end{aligned}$$

for all $t \geq 0$ and some $\gamma \in \mathcal{K}$. Assuming without loosing generality that $x_0(0) = x(0)$, $\omega_0(0) = \omega(0)$, and combining these estimates we obtain:

$$\begin{aligned}\|x(t) - \Pi\omega(t)\| &\leq \|x(t) - x_0(t)\| + \|\Pi\|\|\omega(t) - \omega_0(t)\| + \|x_0(t) - \Pi\omega_0(t)\|\\ &\leq \beta(\|x(0) - \Pi\omega(0)\|, t) + (1 + \|\Pi\|)\gamma(\|d\|_\infty + \|w\|_\infty)\end{aligned}$$

for all $t \geq 0$ with any $x(0) \in \mathbb{R}^n$ and $\omega(0) \in \mathbb{R}^q$. Therefore,

$$\begin{aligned}\|\epsilon(t)\| &\leq \|C_0\|\|x(t) - \Pi\omega(t)\| + \|C_1\|\|f(Hx(t)) - f(H\Pi\omega(t))\|\\ &\leq (\|C_0\| + \lambda\|C_1\|\|H\|)\|x(t) - \Pi\omega(t)\|\end{aligned}$$

for any $t \geq 0$, which justifies boundedness and convergence of the error ϵ. □

Then, the following observer can be designed for (3.2):

$$\begin{aligned}\dot{\hat{\omega}} &= S_0\hat{\omega} + S_1 f(J\hat{\omega}) + GY + E\varrho + M(Y - \hat{\psi}),\\ \hat{\psi} &= C_0\Pi\hat{\omega} + C_1 f(J\hat{\omega}),\end{aligned} \tag{3.5}$$

where $\hat{\omega} \in \mathbb{R}^q$ is the estimate of ω, and $M \in \mathbb{R}^{q\times p}$ is the gain to be selected. The dynamics of the estimation error $e := \omega - \hat{\omega}$ can be written as follows:

$$\dot{e} = (S_0 - MC_0\Pi)\,e - (Gv + M\tilde{v}) + w + (S_1 - MC_1)\left(f(Je + J\hat{\omega}) - f(J\hat{\omega})\right). \tag{3.6}$$

where $Gv + M\tilde{v}$ represents an accumulated measurement perturbation. Various approaches can be used to prove robust stability or boundedness of the estimation error e, which depend on the form and the role of the nonlinearities. For example, the techniques for Lur'e [Arcak and Kokotovic, 2001] or Persidskii [Mei, Efimov, and Ushirobira, 2020] systems can be applied. In this work, we will use the approach based on introduced Lipschitzness of f:

Theorem 3.2.1. *Let assumptions 3.2.1 and 3.2.2 be satisfied. Assume that there exist* $F \in \mathbb{R}^{q\times k}$ *and* $W = W^\top \in \mathbb{R}^{q\times q}$ *such that*

$$e^\top F\left(f(Je+J\hat{\omega})-f(J\hat{\omega})\right) \le e^\top We$$

for all e, $\hat{\omega} \in \mathbb{R}^q$, *and there exist* $P = P^\top \in \mathbb{R}^{q\times q}$, $\Theta = \Theta^\top \in \mathbb{R}^{q\times q}$, $\Gamma = \Gamma^\top \in \mathbb{R}^{p\times p}$, $\Xi = \Xi^\top \in \mathbb{R}^{q\times q}$ *and* $U \in \mathbb{R}^{q\times p}$ *such that the LMIs*

$$P>0,\ \Theta>0,\ \Gamma>0,\ \Xi>0,$$
$$\begin{pmatrix} \Upsilon & -PG & -U & P \\ -G^\top P & -\Gamma & 0 & 0 \\ -U^\top & 0 & -\Gamma & 0 \\ P & 0 & 0 & -\Xi \end{pmatrix} \le 0,$$
$$\Upsilon = S_0^\top P + PS_0 - \Pi^\top C_0^\top U^\top - UC_0\Pi + 2W + \Theta$$

together with the linear matrix equality (LME) $PS_1 - UC_1 = F$, *have a solution. Then for* $M = P^{-1}U$ *in* (3.1), (3.2), (3.4), (3.5)*:*

$$\|e(t)\| \le \sqrt{\frac{\lambda_{\max}(P)}{\lambda_{\min}(P)}}\left[e^{-0.5\frac{\lambda_{\min}(\Theta)}{\lambda_{\max}(P)}t}\|e(0)\|\right.$$
$$\left.+\sqrt{\frac{\lambda_{\max}(\Gamma)}{\lambda_{\min}(\Theta)}}\left(\|v\|_\infty+\|\tilde{v}\|_\infty\right)+\sqrt{\frac{\lambda_{\max}(\Xi)}{\lambda_{\min}(\Theta)}}\|w\|_\infty\right]$$

for all $t \ge 0$.

Proof. Assumption 3.2.1 ensures the existence of the solution $x = \Pi\omega$, while Assumption 3.2.2 provides boundedness of ϵ. To analyze the behavior of e, we select a quadratic Lyapunov function $V(e) = e^\top Pe$, with P given in the conditions of the theorem. Then, its derivative for (3.6) takes the form:

$$\dot{V} = \begin{pmatrix} e \\ v \\ \tilde{v} \\ w \end{pmatrix}^\top \begin{pmatrix} \Upsilon' & -PG & -PM & P \\ -G^\top P & 0 & 0 & 0 \\ -M^\top P & 0 & 0 & 0 \\ P & 0 & 0 & 0 \end{pmatrix} \begin{pmatrix} e \\ v \\ \tilde{v} \\ w \end{pmatrix}$$
$$+2e^\top P\left(S_1 - MC_1\right)\left(f(Je+J\hat{\omega})-f(J\hat{\omega})\right)$$

$$\le \begin{pmatrix} e \\ v \\ \tilde{v} \\ w \end{pmatrix}^\top \begin{pmatrix} \Upsilon'+2W+\Theta & -PG & -PM & P \\ -G^\top P & -\Gamma & 0 & 0 \\ -M^\top P & 0 & -\Gamma & 0 \\ P & 0 & 0 & -\Xi \end{pmatrix} \begin{pmatrix} e \\ v \\ \tilde{v} \\ w \end{pmatrix} - e^\top\Theta e$$
$$+v^\top\Gamma v + \tilde{v}^\top\Gamma\tilde{v} + w^\top\Xi w,$$

where $\Upsilon' = \left(S_0 - MC_0\Pi\right)^\top P + P\left(S_0 - MC_0\Pi\right)$, while Θ, W, Γ and Ξ are given in the formulation of the theorem, and we imposed $P\left(S_1 - MC_1\right) = F$. It is easy to see that for $PM = U$ this relation is true, and the above matrix is non-positive, then we obtain:

$$\dot{V} \le -e^\top\Theta e + v^\top\Gamma v + \tilde{v}^\top\Gamma\tilde{v} + w^\top\Xi w,$$

which implies input-to-state stability of the error dynamics (3.6) (state-independent input-to-output stability of (3.2), (3.6) for the output e) with respect to the inputs w, v and $\tilde{v}$ [Sontag and Wang, 1995, Sontag and Wang, 2000]. The estimate on the behavior of e given in the theorem statement can be obtained by a straightforward computation. □

Remark 3.2.3. *The LMIs presented in Theorem 3.2.1 are conventionally used for controlling or estimating a*

Lipschitz continuous system. These LMIs are feasible if the linear part given by the matrix S_0 is detectable for the output matrix $C_0\Pi$ and the Lipschitz constant of f reflected by the matrix W is sufficiently small.

According to Theorem 3.2.1 (the respective assumptions are satisfied), the variable $\hat{\omega}$ asymptotically approaches ω in the noise-free case (or stays in a neighborhood of the ideal value with error proportional to the amplitude of the perturbations v and disturbances w), and we can select

$$\hat{x} = \Pi\hat{\omega} \tag{3.7}$$

as an asymptotic estimate for the state of the system (3.1).

Finally, conclude that (3.5) with (3.7) is a reduced-order robust observer for the system (3.1), (3.2) (if $q < n$).

3.2.3 Tracking control

Consider the design problem for trajectory tracking control for (3.1), and assume that the output (3.4) is available for measurements in (3.1) with noise v. In this case, a part of the external input ϱ can be interpreted as a reference signal, which must be processed by a given desired dynamics and followed by x. It is common to assume that the desired dynamics has a form similar to (3.1) [Isidori and Byrnes, 1990; Khalil, 2002]. Then, a feedback u must be designed based on the discrepancy of the state x and the filtered reference.

Since only a part of the state x is measured by (3.4), an observer has to be designed as (3.1) with an output injection term. Due to the closeness of the desired and the observer dynamics to the system (3.1), in many practical cases, these systems can be presented in a combined form of a dynamical regulator, which becomes similar to the input generator (3.2) that uses available measurements instead of y:

$$\begin{aligned} \dot{\omega}(t) &= S_0\omega(t) + S_1 f(J\omega(t)) + GY(t) + E\varrho(t) + w(t), \\ u(t) &= L_0\omega(t) + L_1 f(J\omega(t)), \end{aligned} \tag{3.8}$$

where all matrices are chosen such that Assumption 3.2.1 is valid, and the relation $x = \Pi\omega$ corresponds to a solution of the posed tracking/estimation problem.

Remark 3.2.4. *We wish to use a more relaxed constraint here than Assumption 3.2.2 that may imply a local and non-uniform observability/controllability of (3.1), as expressed in Assumption 1.3.2 This is frequently met in adaptive estimation and identification, where it is related to persistent excitation [Narendra and Annaswamy, 2005], [Efimov, Barabanov, and Ortega, 2019].*

Hence, by Proposition 3.2.1, the interconnection (3.1), (3.4), (3.8) has a solution $x = \Pi\omega$ in the noise-free setting, *i.e.*, more precisely, for any $\omega(0) \in \mathbb{R}^q$ if $x(0) = \Pi\omega(0)$ and $\|v\|_\infty = \|d\|_\infty = \|w\|_\infty = 0$, then $x(t) = \Pi\omega(t)$ for all $t \geq 0$. In other words, Assumption 3.2.1 in this setting guarantees the tracking/observation problem solution for (3.1) by the selected input u only under the constraint $x(0) = \Pi\omega(0)$ (if this equality is not satisfied, then x may converge to other solution than $\Pi\omega$, or even diverge). Since we cannot check the property $x(0) = \Pi\omega(0)$, we will formulate the checking conditions to ensure local robust stability of the hyperplan $x = \Pi\omega$.

However, to replace Assumption 3.2.2 with a local, more relaxed requirement, we need to find robust stability conditions for the input generator (3.8) regarding the measurement noise and disturbances. To do that, we need to introduce several hypotheses, and for brevity, we will assume in this section that $r = k$.

The conditions given in this section are rather sophisticated due to the use of non-quadratic Lyapunov functions [Arcak and Kokotovic, 2001, Yakubovich, 2002], with the idea of enlarging the applicability domain. To this end, we need several assumptions.

First, we should verify the properties of the ISS-Lyapunov function for ω-dynamics by formulating them in terms of LMIs.

Assumption 3.2.3. *There exist* $0 < P = P^\top \in \mathbb{R}^{q\times q}$, $0 < \Gamma = \Gamma^\top \in \mathbb{R}^{q\times q}$, $0 \le \Xi = \Xi^\top \in \mathbb{R}^{q\times q}$, *diagonal* $0 \le \Omega \in \mathbb{R}^{r\times r}$ *and* $0 \le \Lambda = \operatorname{diag}(\Lambda_j)_{j=1}^r \in \mathbb{R}^{r\times r}$ *such that the LMIs are verified:*

$$\Phi = \begin{pmatrix} S^\top P + PS + \Xi & P\tilde{S} + S^\top J^\top \Lambda + J^\top \Omega & P & P \\ \tilde{S}^\top P + \Lambda J S + \Omega J & \tilde{S}^\top J^\top \Lambda + \Lambda J \tilde{S} & \Lambda J & \Lambda J \\ P & J^\top \Lambda & -\Gamma & 0 \\ P & J^\top \Lambda & 0 & -\Gamma \end{pmatrix} \le 0$$

where $S = S_0 + GC_0\Pi$, $\tilde{S} = S_1 + GC_1$.

Next, auxiliary quadratic constraints should be introduced as in the theory of absolute stability [Yakubovich, 2002].

Assumption 3.2.4. *The following inequalities hold for sufficiently small* $\omega \in \mathbb{R}^q$ *and* $z \in \mathbb{R}^n$*:*

$$\begin{aligned} f(Hz)^\top f(Hz) &\le z^\top \Sigma_1 z + 2z^\top H^\top \Sigma_2 f(Hz) + 2z^\top H^\top \Sigma_3 \Delta f(z,\omega) + 2\Delta f(z,\omega)^\top \Sigma_4 f(Hz) \\ \Delta f(z,\omega)^\top \Delta f(z,\omega) &\le z^\top \Psi_1 z + 2z^\top H^\top \Psi_2 f(Hz) \end{aligned}$$

where $z = x - \Pi\omega$, $\Delta f(z,\omega) = f(J\omega + Hz) - f(J\omega)$, $\Sigma_1^\top = \Sigma_1 \ge 0, \Psi_1^\top = \Psi_1 \ge 0$ *and* Σ_2, Σ_3, Σ_4, $\Psi_2 \ge 0$ *are diagonal matrices.*

We need to impose conditions on the lower bounds for f, where its local sector shape and incremental passivity are assumed:

Assumption 3.2.5. *The function* f *satisfies the following sector conditions for all* $j = 1, \dots, k$ *and all sufficiently small* $s \in \mathbb{R}$, $\omega \in \mathbb{R}^q$, $z \in \mathbb{R}^n$*:*

a) $s f_j(s) > 0$ *if* $s \ne 0$*;*

b) $\Delta f(z,\omega) Hz > 0$ *if* $Hz \ne 0$.

Using the assumptions above, we formulate the conditions of boundedness of solutions for the system (3.8):

Theorem 3.2.2. *Let assumptions 3.2.1, 3.2.3, 3.2.4, and 3.2.5 be satisfied. There exists* $\rho > 0$ *such that for* $\|\omega(0)\|$, $\|z\|_\infty$, $\|w\|_\infty$, $\|v\|_\infty < \rho$, *the system (3.8), (3.4) is locally ISS [Sontag and Wang, 1995] with respect to z, w, v, provided that*

$$\Xi + \mu J^\top \Omega J > 0$$

for some $\mu \in \mathbb{R}$.

Proof. Define the error due to noise and disturbances as $\tilde{\delta} = Gv + w$ and the convergence error $\delta_z = GC_0 z + GC_1 \Delta f(z,\omega)$. Then the generator dynamics takes the form:

$$\dot{\omega} = S\omega + \tilde{S} f(J\omega) + \delta_z + \tilde{\delta}.$$

Set a Lyapunov function V, where J_j denotes the j^{th} row of the matrix J, $j = 1, \dots, k$

$$V(\omega) = \omega^\top P \omega + 2\sum_{j=1}^{k} \left(\Lambda_j \int_0^{J_j \omega} f_j(s)\, ds \right),$$

which is positive definite and radially unbounded due to assumptions 3.2.3 and 3.2.5. Using the notation from Assumption 3.2.3, the derivative of V can be rewritten as follows:

$$\dot{V} = \begin{pmatrix} \omega \\ f(J\omega) \\ \delta_z \\ \tilde{\delta} \end{pmatrix}^\top \Phi \begin{pmatrix} \omega \\ f(J\omega) \\ \delta_z \\ \tilde{\delta} \end{pmatrix} + \tilde{\delta}^\top \Gamma \tilde{\delta} + \delta_z^\top \Gamma \delta_z - \omega^\top \Xi \omega - 2\omega^\top J^\top \Omega f(J\omega)$$

where the matrices Φ, Ξ, Γ, Ω come from Assumption 3.2.3. The matrix Φ is non-positive, then:

$$\dot{V} \leq \tilde{\delta}^\top \Gamma \tilde{\delta} + \delta_z^\top \Gamma \delta_z - \omega^\top \Xi \omega - 2\omega^\top J^\top \Omega f(J\omega).$$

Due to Assumption 3.2.4, the norm of the perturbation δ_z is upper bounded by a function of z. Using the condition a) of Assumption 3.2.5, we can show that $2\omega^\top J^\top \Omega f(J\omega) \geq 0$, while condition b) implies that f is strictly increasing, then this term is unbounded in $J\omega$. Using Finsler's lemma [Finsler, 1936/37], we obtain that if there is $\mu \in \mathbb{R}$ such that

$$\Xi + \mu J^\top \Omega J > 0,$$

so the dynamics of ω is ISS [Sontag and Wang, 1995], which proves the claim of the theorem. □

Having local robust stability of ω, we can impose assumptions to formulate a similar result for the dynamics of z (*i.e.*, that by the choice of the dynamic regulator, or signal generator, (3.8), the invariant solution $\Pi\omega$ is locally attracting for the system (3.1)). Analogous to Assumption 3.2.3, the LMIs for z-dynamics can be introduced as follows.

Assumption 3.2.6. *There exist* $\gamma_1,\ \gamma_2 > 0$, $0 < \tilde{P} = \tilde{P}^\top \in \mathbb{R}^{n\times n}$, $0 < \tilde{\Gamma} = \tilde{\Gamma}^\top \in \mathbb{R}^{n\times n}$, $0 \leq \tilde{\Xi} = \tilde{\Xi}^\top \in \mathbb{R}^{n\times n}$ *such that the LMIs are verified:*

$$\tilde{\Phi} = \begin{pmatrix} \tilde{A}_0^\top \tilde{P} + \tilde{P}\tilde{A}_0 + \tilde{\Xi} & \tilde{A}_0^\top H^\top \Lambda + H^\top \Omega_1 & \tilde{P}\tilde{A}_1 + H^\top \Omega_2 & \tilde{P} \\ \Lambda H \tilde{A}_0 + \Omega_1 H & -\gamma_1 I & \Lambda H \tilde{A}_1 + \Upsilon & \Lambda H \\ \tilde{A}_1^\top \tilde{P} + \Omega_2 H & \tilde{A}_1^\top H^\top \Lambda + \Upsilon & -\gamma_2 I & 0 \\ \tilde{P} & H^\top \Lambda & 0 & -\tilde{\Gamma} \end{pmatrix} \leq 0$$

where $0 \leq \Lambda = \operatorname{diag}(\Lambda_j)_{j=1}^r$, Ω_1, Ω_2, $\Upsilon \in \mathbb{R}^{r\times r}$ *are diagonal, and* $\tilde{A}_0 = A_0 - \Pi G C_0$, $\tilde{A}_1 = A_1 - \Pi G C_1$.

The linear matrix inequalities given in assumptions 3.2.3 and 3.2.6 have similar form due to the same property of the dynamics in (3.1) and (3.8), respectively.

Theorem 3.2.3. *Let assumptions 3.2.1, 3.2.4, 3.2.5 and 3.2.6 be satisfied and*

$$\begin{aligned} R_1 &= \tilde{\Xi} - \gamma_1 \Sigma_1 - \gamma_2 \Psi_1 \geq 0, \\ R_2 &= \Omega_1 - \gamma_1 \Sigma_2 - \gamma_2 \Psi_2 \geq 0, \\ R_3 &= \Omega_2 - \gamma_1 \Sigma_3 \geq 0, \\ R_4 &= \Upsilon - \gamma_1 \Sigma_4 \geq 0. \end{aligned}$$

There exists $\rho > 0$ *such that for all* $\|z(0)\|$, $\|d\|_\infty$, $\|w\|_\infty$, $\|v\|_\infty < \rho$, *the dynamics of* z *is locally ISS with respect to* d, w, v *provided that*

$$R_1 + \mu H^\top (R_2 + R_3) H > 0$$

for some $\mu \in \mathbb{R}$.

Proof. Define the error due to disturbances $\delta = d - \Pi w + \Pi G v$. Following Assumption 3.2.1, the error dynamics takes the form:

$$\dot{z}(t) = \tilde{A}_0 z(t) + \tilde{A}_1 \Delta f(z, \omega) + \delta.$$

Set a Lyapunov function V, where H_j denotes the j^{th} row of the matrix H, $j = 1, \ldots, k$

$$V(z) = z^\top \tilde{P} z + 2 \sum_{j=1}^{k} \left(\Lambda_j \int_0^{H_j z} f_j(s)\, ds \right),$$

which is positive definite and radially unbounded due to assumptions 3.2.5 and 3.2.6. The time derivative of the Lyapunov function with the bounds in Assumption 3.2.4 can be rewritten as follows:

$$\dot{V} \leq \begin{pmatrix} z \\ f(Hz) \\ \Delta f(z,\omega) \\ \delta \end{pmatrix}^{\top} \tilde{\Phi} \begin{pmatrix} z \\ f(Hz) \\ \Delta f(z,\omega) \\ \delta \end{pmatrix} + \delta^{\top}\tilde{\Gamma}\delta - z^{\top}R_1 z - 2z^{\top}H^{\top}R_2 f(Hz) - 2z^{\top}H^{\top}R_3\Delta f(z,\omega)$$
$$-2\Delta f(z,\omega)^{\top}R_4 f(Hz).$$

where the matrices $\tilde{\Xi}$, $\tilde{\Gamma}$, Υ, Ω_1 and Ω_2 come from Assumption 3.2.6. According to Assumption 3.2.6 the matrix $\tilde{\Phi}$ is non-positive, so:

$$\dot{V} \leq \delta^{\top}\tilde{\Gamma}\delta - z^{\top}R_1 z - 2z^{\top}H^{\top}R_2 f(Hz) - 2z^{\top}H^{\top}R_3\Delta f(z,\omega) - 2\Delta f(z,\omega)^{\top}R_4 f(Hz).$$

Recall that $\tilde{\Gamma} > 0$ and $R_i \geq 0$ for $i = 1,\ldots,4$. Using conditions a) and b) of Assumption 3.2.5 we can show that $2z^{\top}H^{\top}R_2 f(Hz) + 2z^{\top}H^{\top}R_3\Delta f(z,\omega) + 2\Delta f(z,\omega)^{\top}R_4 f(Hz) \geq 0$ (note also that only the last term may be a bounded function of z). Applying Finsler's lemma [Finsler, 1936/37] to

$$R_1 + \mu H^{\top}(R_2 + R_3)H > 0,\ \mu \in \mathbb{R}$$

we obtain that the right-hand side of the estimate for $\dot{V}$ is a radially unbounded function of z, hence, the dynamics of z is ISS [Sontag and Wang, 1995], which proves the claim of the theorem. □

Combining theorems 3.2.2 and 3.2.3 provides a local version of the property given previously in Assumption 3.2.2:

Corollary 3.2.2. *Let assumptions 3.2.1, 3.2.3, 3.2.4, 3.2.5, 3.2.6 be satisfied. There exists $\rho > 0$ such that for all $\|\omega(0)\|$, $\|x(0)\|$, $\|w\|_\infty$, $\|d\|_\infty$, $\|v\|_\infty < \rho$, the interconnection (3.1), (3.4), (3.8) is locally input-to-output stable [Sontag and Wang, 2000] with respect to the output z and the inputs v, w, d.*

Proof. Since under the imposed assumptions, ISS of both dynamics, ω and z, was proven in theorems 3.2.2 and 3.2.3, we can consider them as a serial connection of two systems (ω depends on signal z, and z does not depend on ω), which is also ISS due to [Jiang, Teel, and Praly, 1994] and the state of such common system is bounded (with bounded input). For the system (3.1), (3.4), (3.8), this leads to the required input-to-output stability property. □

Note that Corollary 3.2.2 implies that x is locally asymptotically observable by $\Pi\omega$, then this claim can also be interpreted as the existence of a robust local asymptotic observer for x (of reduced-order if $q < n$) in the form

$$\hat{x} = \Pi\omega,$$

and the *uniform observability* of original system is not required, it is relaxed to a local *detectability* [Sontag and Wang, 1997] of the system under properly selected input generated by (3.8).

Concluding both theorems and the subsection, in comparison to subsection 3.2.2, the ISS property of the interconnected system (3.1),(3.2) was proven locally rather than globally. For nonlinear systems, it is difficult to check the conservativeness and feasibility of LMIs. In the linear case, the feasibility can be investigated by relating the proposed LMIs with stabilizability/detectability conditions. However, in the nonlinear case, these conditions are also nonlinear. It is straightforward to check the necessary conditions for the feasibility of LMIs given in assumptions 3.2.3, 3.2.6: the matrices on the main diagonal of Φ and $\tilde{\Phi}$ should be negative definite, which can be connected with the stability of corresponding matrices in the dynamics of the systems.

3.2.4 Examples

First, an academic example is given to illustrate the studied problem. Next, the approach is applied to three models: a bioreactor, a robotic arm, and two Chua circuits.

Example 1. *(Section 3.2.2) Consider systems* (3.1), (3.2) *with* $G = 0$, $q = m = 2$, $k = r = p = 1$ *and* $n = 3$*:*

$$A_0 = \begin{pmatrix} 0 & 1 & 0 \\ 0 & 0 & 0 \\ -1 & -2 & -1 \end{pmatrix}, \quad A_1 = \begin{pmatrix} 0 \\ 1 \\ 0 \end{pmatrix}, \quad B = \begin{pmatrix} 0 & 0 \\ 1 & 0 \\ 0 & 1 \end{pmatrix}, \quad f(Hx) = \sin(Hx), \quad f(J\omega) = \sin(J\omega),$$

$$L_1 = \begin{pmatrix} -1 \\ 0 \end{pmatrix}, \quad C_0 = \begin{pmatrix} 1 & 0 & 0 \end{pmatrix}, \quad H = \begin{pmatrix} 0 & 0 & 1 \end{pmatrix}, \quad C_1 = 0,$$

$$S_0 = \begin{pmatrix} 0 & 1 \\ -2 & 0 \end{pmatrix}, \quad S_1 = \begin{pmatrix} 0 \\ 0 \end{pmatrix}, \quad J = \begin{pmatrix} \frac{3}{2} & \frac{1}{2} \end{pmatrix}, \quad L_0 = \begin{pmatrix} 1 & 0 \\ 0 & 1 \end{pmatrix}.$$

with additive disturbances $d : t \mapsto 0.2\sin(10t)$, $w : t \mapsto 0.1\cos(10t)$ *and a bounded stochastic measurement noise* v.

For this choice of matrices, the equalities (3.3) *and* $J = H\Pi$ *are satisfied for*

$$\Pi = \begin{pmatrix} -\frac{1}{2} & 0 \\ 0 & -\frac{1}{2} \\ \frac{3}{2} & \frac{1}{2} \end{pmatrix}.$$

Thus, Assumption 3.2.1 is verified, and it is possible to show that Assumption 3.2.2 is also valid in a neighborhood of the origin (the system (3.1) *can be linearized having a canonical form with a Hurwitz matrix). One of the solutions of the LMIs given in Theorem 3.2.1 is*

$$P = \begin{pmatrix} 1.129 & 0.332 \\ 0.332 & 0.611 \end{pmatrix}, \quad Q = \begin{pmatrix} 0.388 & 0.024 \\ 0.024 & 0.175 \end{pmatrix}, \quad \Gamma = 6.764, \Xi = \begin{pmatrix} 5 & 0.457 \\ 0.457 & 3.65 \end{pmatrix}, \quad U = \begin{pmatrix} -2.837 \\ -0.03 \end{pmatrix}.$$

Then, the observer (3.5), (3.7) *can be applied with gain matrix*

$$M = P^{-1}U = \begin{pmatrix} -2.973 \\ 1.565 \end{pmatrix}.$$

In Fig. 3.3, we can see that the observer output $\hat{\psi} = C_0\Pi\hat{\omega} + C_1 f(J\hat{\omega})$ *converges to the are of disturbances of the virtual output* $\psi(t) = C_0\Pi\omega + C_1 f(J\omega)$*, as well as to the measured output* $Y = C_0 x + C_1 f(Hx) + v$*. That means that* $\hat{\omega}$ *converges to a neighborhood of the state* ω *and* $x = \Pi\omega$ *is indeed the steady-state solution of the system* (3.1)*, which corresponds to the results of Theorem 3.2.1. As we can also see, the noise and disturbances do not impact the stability of the system.*

Example 2. *(Section 3.2.2) Let us consider a bioreactor model based on Example 4.1 in Moreno and Besancon, 2021, rewritten as follows:*

$$\begin{cases} \dot{x}_1 = -Dx_1 + \frac{\mu_1 x_1 x_2}{K_{s1} + x_2} \\ \dot{x}_2 = D(S_{in1} - x_2) - k_1 \frac{\mu_1 x_1 x_2}{K_{s1} + x_2} \end{cases} \qquad \begin{cases} \dot{\omega}_1 = -D\omega_1 + \frac{\mu_2 \omega_1 \omega_2}{K_{s2} + \omega_2 + \frac{\omega_2^2}{K_{I2}}} \\ \dot{\omega}_2 = D(S_{in2} - \omega_2) + k_3 \frac{\mu_1 x_1 x_2}{K_{s1} + x_2} - k_2 \frac{\mu_2 \omega_1 \omega_2}{K_{s2} + \omega_2 + \frac{\omega_2^2}{K_{I2}}} \end{cases}$$

where all the coefficients are identified as in Bernard et al., 2001:

$$D = 0.35, \quad K_{s1} = 7.1, \quad K_{s2} = 9.28, \quad K_{I2} = 256,$$
$$\mu_1 = 1.2, \quad \mu_2 = 0.74, \quad k_1 = 42.14, \quad k_2 = 116.5, \quad k_3 = 268.$$

The model represents a two-stage anaerobic digestion process. In the the first step, one bacteria population, with a concentration x_1*, consumes the substrate with concentration* x_2 *and produces acids, with concentration* ω_2*. In contrast, the population of other bacteria of concentration* ω_1 *consumes acids as substrate for growth,*

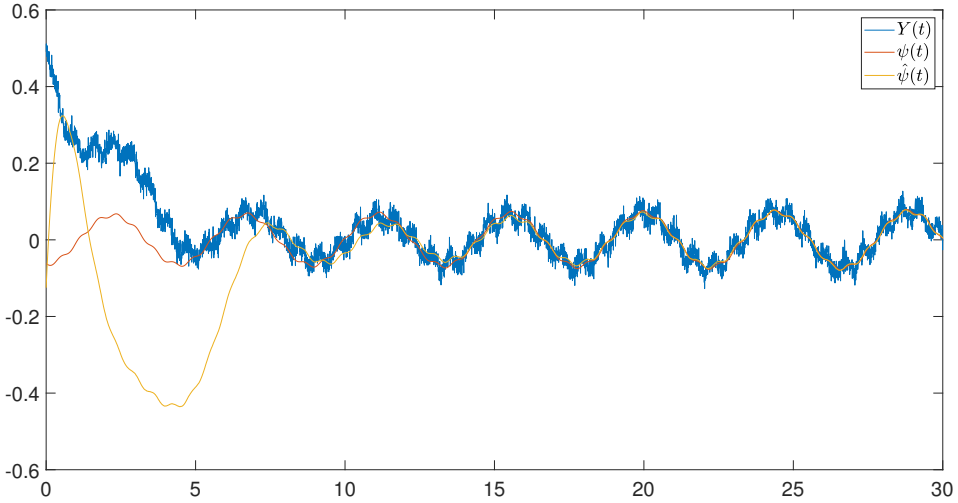

FIGURE 3.3: Simulation results for Example 1. Initial conditions: $\omega(0) = (\frac{1}{8} \quad 0)^\top$, $x(0) = (\frac{1}{2} \quad -\frac{1}{2} \quad \frac{1}{2})^\top$, $\hat{\omega}(0) = (\frac{1}{4} \quad 0)^\top$.

and S_{in1} and S_{in2} are the concentrations of the substrates in the input flow. Since the stages are linked through the nonlinear sector terms, the theory introduced in this chapter can be applied to this model.

More precisely, we have two nonlinearities: $f_1(x) = \frac{\mu_1 x_1 x_2}{K_{s1}+x_2}$ and $f_2(\omega) = \frac{\mu_2 \omega_1 \omega_2}{K_{s2}+\omega_2+\frac{\omega_2^2}{K_{I2}}}$. Also, we can present concentration levels S_{in1}, S_{in2} as third (quasi) constant states in dynamics (x_3, ω_3 correspondingly). Then, the cascade system takes the required form (1.1)-(1.7)*, where*

$$A_0 = S_0 = \begin{pmatrix} -D & 0 & 0 \\ 0 & -D & D \\ 0 & 0 & 0 \end{pmatrix}, \quad A_1 = \begin{pmatrix} 1 \\ -k_1 \\ 0 \end{pmatrix}, \quad B = \begin{pmatrix} 0 \\ 0 \\ 0 \end{pmatrix}, \quad C_0 = \begin{pmatrix} 0 \\ 0 \\ 0 \end{pmatrix}^\top,$$

$$S_1 = \begin{pmatrix} 1 & -k_2 & 0 \end{pmatrix}^\top, \; G = \begin{pmatrix} 0 & 1 & 0 \end{pmatrix}^\top, \; L_0 = \begin{pmatrix} 0 & 0 & 0 \end{pmatrix}, \; L_1 = 0, \; C_1 = k_3.$$

Since inputs S_{in1} and S_{in2} serve to excite both dynamics, let us assume that we can determine them. We can select them, for instance, as a square wave, the amplitude of which varies from 12.7 *to* 7.5*. Proposition 3.2.1 is not applicable since the nonlinearities are slightly different, and it is impossible to separate the arguments in f_1 and f_2 to determine the matrices J and H. However, we can still apply the relaxed version of the result presented in Corollary 3.2.1 to skip the requirement $J = \Pi H$. Then, we can find Π from:*

$$\begin{aligned} A_0\Pi - \Pi S_0 &= 0, \\ A_1 - \Pi G C_1 &= 0, \\ \Pi S_1 &= 0. \end{aligned}$$

This system consists of 15 equations (some of them are trivial or automatically satisfied due to zero dynamics states), from which we can deduce all the coefficients of matrix Π:

$$\Pi = \frac{1}{k_3} \begin{pmatrix} k_2 & 1 & -1 \\ -k_1 k_2 & -k_1 & k_3 + k_1 \\ 0 & 0 & k_3 \end{pmatrix}.$$

The states x converge to their steady-state response $\Pi\omega$ (see Fig. 3.4), so the asymptotic observer for the system can be designed as $\hat{x} = \Pi\omega$. It means that it is enough to observe the states of ω to have an observer for x. Regardless of the relation $J = H\Pi$, Assumption 3.2.1 is satisfied in this example and Theorem 3.2.1 still can be

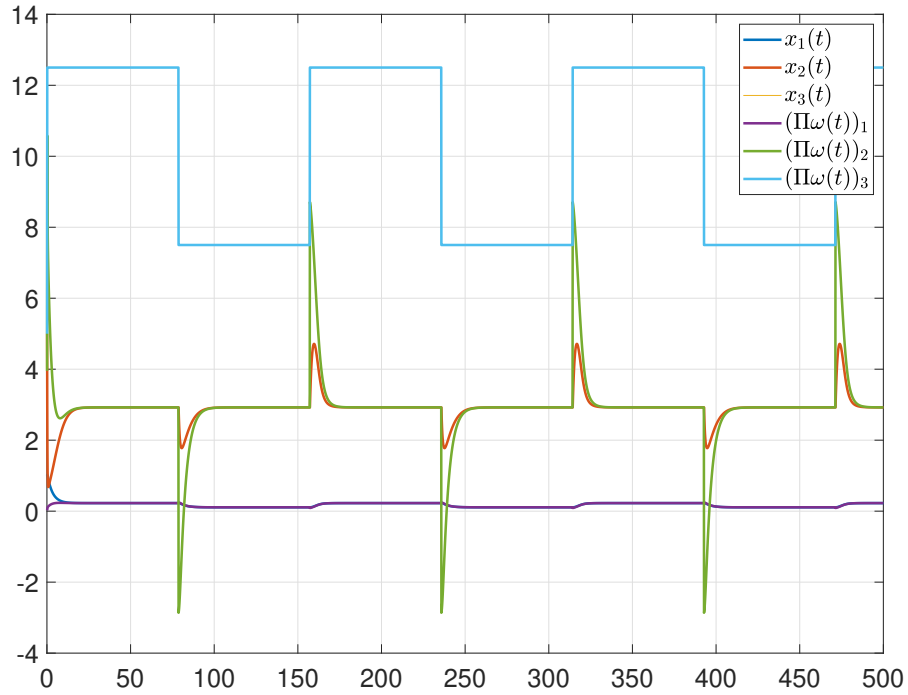

FIGURE 3.4: Linear mapping between x and ω

used.

Let us assume that we measure the output $y = C_0 x + C_1 f_1(x) = k_3 \frac{\mu_1 x_1 x_2}{K S_1 + x_2}$ *(the link between two systems), and the inflow concentrations* $\omega_3 = x_3$ *are known. Let us rewrite the dynamics of* ω *in the initial 2-dimensional form with* $S_{in2} = \omega_3 = \varrho(t)$ *given. Consider an observer for* ω *in the following form:*

$$\begin{cases} \dot{\hat{\omega}}_1 = -D\hat{\omega}_1 + f_2(\hat{\omega}) + m_1 (y - k_3 f_1(\Pi\hat{\omega})) \\ \dot{\hat{\omega}}_2 = D(\omega_3 - \hat{\omega}_2) - k_2 f_2(\hat{\omega}) + k_3 y + m_2 (y - k_3 f_1(\Pi\hat{\omega})) \end{cases}$$

where $M = (m_1 \quad m_2)^\top$ *is matrix of gains to be designed.*

The error dynamics for $e = \omega - \hat{\omega}$ *will be as follows:*

$$\dot{e} = \tilde{S}_0 e + \tilde{S}_1 (f_2(\omega) - f_2(\omega)) - M C_1 (f_1(\Pi\omega) - f_1(\Pi\hat{\omega})) - M\epsilon \tag{3.9}$$

where $\tilde{S}_0$ *and* $\tilde{S}_1$ *are matrices without the third rows and columns,* ϵ *is from Proposition 3.2.1. The nonlinearities* f_1 *and* f_2 *are similar in behavior, but have different arguments, so we have to consider two Lipschitz conditions from Theorem 3.2.1 instead of one:*

$$e^\top F_1 (f_2(\omega) - f_2(\hat{\omega})) \le e^\top W_1 e, \tag{3.10}$$

$$e^\top \tilde{\Pi}^\top F_2 (f_1(\Pi\omega) - f_1(\Pi\hat{\omega})) \le e^\top \tilde{\Pi}^\top W_2 \tilde{\Pi} e, \tag{3.11}$$

where $\tilde{\Pi} \in \mathbb{R}^{2\times 2}$ *is a matrix* Π *without 3rd row and column. Recall that* ω_i *are strictly positive, then for the estimation we can consider only positive projections* $\hat{\omega}_i$*, as well as for* $\tilde{\Pi}\omega_i$ *and* $\tilde{\Pi}\hat{\omega}_i$*. Performing straightforward calculations with* $F_1 = \begin{pmatrix} f^1 & f^2 \end{pmatrix}^\top$ *and* $\phi_1(\omega_2) = K_{s2} + \omega_2 + \frac{\omega_2^2}{K_{I2}}$ *in (3.10) we obtain:*

$$f^1 \frac{\omega_2}{\phi_1(\omega_2)} e_1^2 + f^1 e_1 \hat{\omega}_1 \left(\frac{\omega_2}{\phi_1(\omega_2)} - \frac{\hat{\omega}_2}{\phi_1(\hat{\omega}_2)} \right) + f^2 e_1 e_2 \frac{\omega_2}{\phi_1(\omega_2)} + f^2 e_2 \hat{\omega}_1 \left(\frac{\omega_2}{\phi_1(\omega_2)} - \frac{\hat{\omega}_2}{\phi_1(\hat{\omega}_2)} \right) \le e^\top W_1 e.$$

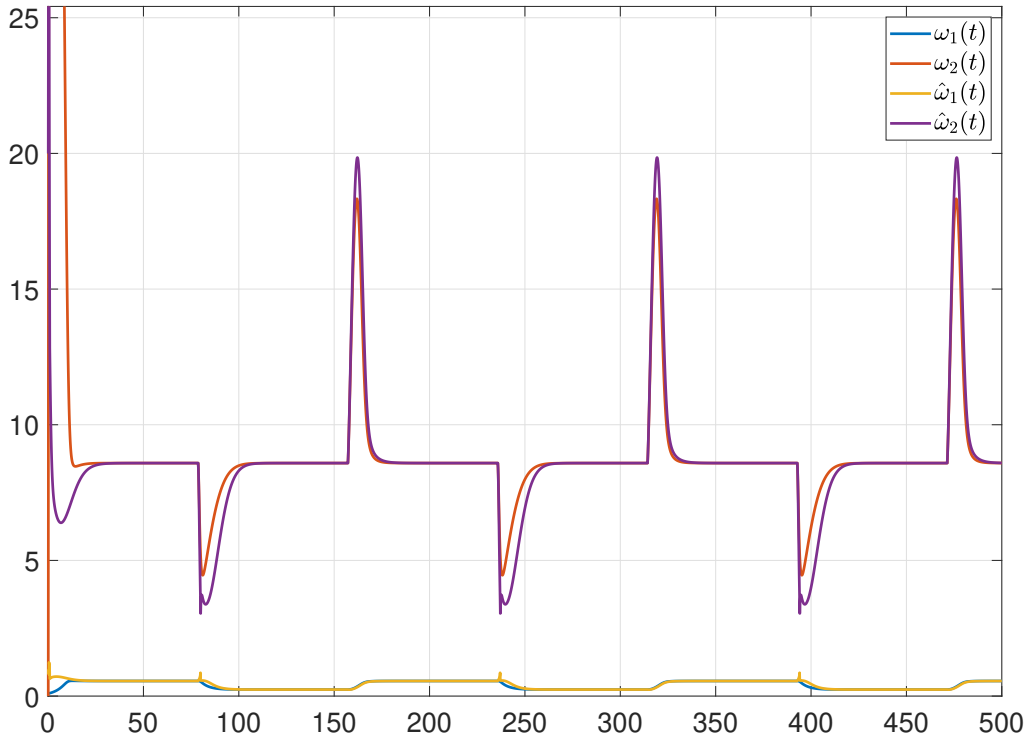

FIGURE 3.5: Observer for ω. Initial conditions: $z(0) = (1 \quad 20)^\top$, $x(0) = (1 \quad 5)^\top$, $\omega(0) = (0.1 \quad 0)^\top$

Then, we can bound

$$\frac{\omega_2}{\phi_1(\omega_2)} \le \eta_1, \quad e_1\left(\frac{\omega_2}{\phi_1(\omega_2)} - \frac{\hat{\omega}_2}{\phi_1(\hat{\omega}_2)}\right) \le |e_1||e_2|l, \quad \hat{\omega}_1 \le \eta_2, \quad e_2\left(\frac{\omega_2}{\phi_1(\omega_2)} - \frac{\hat{\omega}_2}{\phi_1(\hat{\omega}_2)}\right) \le \sigma e_2^2,$$

where $\eta_1, \eta_2, l, \sigma$ are the constants to be defined from model behavior. Performing similar calculations for (3.11), but with F_2, $(\tilde{\Pi}e)_i$ and $\phi_2((\Pi\omega)_2) = K_{s1} + (\Pi\omega)_2$, $\tilde{\eta}_1, \tilde{\eta}_2, l, \sigma$ we obtain W_2. Final LMI and LME from Theorem 3.2.1 take the form:

$$P > 0,\ \Theta > 0,\ \Gamma > 0,\ P\tilde{S}_1 = F_1,\ UC_1 = \tilde{\Pi}^\top F_2$$
$$\begin{pmatrix} \Upsilon & -U \\ -U^\top & -\Gamma \end{pmatrix} \le 0,$$
$$\Upsilon = \tilde{S}_0^\top P + P\tilde{S}_0 + 2W_1 + 2\tilde{\Pi}^\top W_2 \tilde{\Pi} + \Theta.$$

For $F_1 = \begin{pmatrix} 0.1 & -2 \end{pmatrix}^\top$, $F_2 = \begin{pmatrix} 0.2 & -2 \end{pmatrix}^\top$ and constants $\eta_1 = 0.7, \eta_2 = 0.8, \tilde{\eta}_1 = 0.35, \tilde{\eta}_2 = 10.25, l = 0.1, \sigma = 0.1$ solver finds LMIs feasible as follows

$$P = \begin{pmatrix} 71.546 & 0.613 \\ 0.613 & 0.022 \end{pmatrix}, \quad \Theta = \begin{pmatrix} 10.905 & 0.093 \\ 0.093 & 0.003 \end{pmatrix}, \quad \Gamma = 68.147,$$

and the gains are found as $M = \begin{pmatrix} 1.914\text{e}{-3} & 9.572\text{e}{-5} \end{pmatrix}$. Fig. 3.5 shows the convergence of the observer to the states ω, resulting in the convergence to x of the estimate $\hat{x} = \Pi\hat{\omega}$. (see Fig. 3.5).

Example 3. *(Section 3.2.3) The following example concerns the theory presented for tracking control. Consider a commonly studied simplified benchmark model of a one-link flexible robotic arm Rajamani and Cho, 1998:*

$$A_0 = \begin{pmatrix} 0 & 1 & 0 & 0 \\ -48.6 & -1.25 & 48.6 & 0 \\ 0 & 0 & 0 & 1 \\ 19.5 & 0 & -19.5 & 0 \end{pmatrix}, \quad A_1 = \begin{pmatrix} 0 \\ 0 \\ 0 \\ -3.33 \end{pmatrix}, \quad B = \begin{pmatrix} 0 \\ 21.6 \\ 0 \\ 0 \end{pmatrix},$$

$$f(\cdot) = \sin(\cdot), \quad C_1 = \begin{pmatrix} 0 \end{pmatrix}, \quad H = \begin{pmatrix} 0 & 0 & 1 & 0 \end{pmatrix}, \quad C_0 = \begin{pmatrix} 1 & 0 & 0 & 0 \end{pmatrix}.$$

where the first two states are the motor position (angle) and velocity, and last two are the link position (angle) and velocity. The model is in a form similar to (3.1),(3.4)*, which allows us to consider the tracking control problem:*

$$\begin{cases} \dot{x}(t) = A_0 x(t) + A_1 f(Hx(t)) + Bu(t) + d(t), \\ Y(t) = C_0 x(t) + C_1 f(Hx(t)) + v, \end{cases}$$

where u is an input to be chosen, Y is a measurable output, d is a disturbance due to modeling error or uncertainties, and v is a white measurement noise. Let us assume that there exists a feedback-control input of the following form:

$$\tilde{u}(t) = L_0 x(t) + L_1 f(Hx(t)) + \tilde{Q}\varrho(t),$$

that forces the system state x or the output Y to track the desired trajectory predefined by the signal ϱ. Then we obtained a closed-loop system

$$\dot{x}(t) \quad = \quad (A_0 + BL_0)x(t) + (A_1 + BL_1) f(Hx(t)) + B\tilde{Q}\varrho(t) + d(t), \tag{3.12}$$

driven by the external input ϱ, which in our case is an excitation signal, commanded by the DC motor.

However, such feedback control cannot be designed directly since only part of the state is assumed to be measured (the angle position of the motor). Then an observer for the reference plant is required. Consider an observer of the same dimension ($q = n$) in a form:

$$\dot{\omega}(t) = S_0\omega(t) + S_1 f(J\omega(t)) + GY(t) + BE\varrho(t). \tag{3.13}$$

We then have our problem statement as introduced in the tracking control subsection. Therefore, our observer design ensures that our input u will converge to $\tilde{u}$ and the dynamics plant will follow the reference dynamics (3.12)*.*

Let us consider, for simplicity, $\Pi = I_n$. Then $H = J$ and the matrices S_0, S_1 can be found from Proposition 3.2.1 (with $d = 0$) as follows:

$$S_0 = A_0 + BL_0 - GC_0, \quad S_1 = A_1 + BL_1 - GC_1.$$

Let us introduce the error between states as $z = x - \omega$, the dynamics of which will be as follows:

$$\dot{z}(t) = (A_0 - GC_0)z(t) + (A_1 - GC_1)\left(f(Jx(t)) - f(J\omega(t))\right) + d(t) - Gv(t). \tag{3.14}$$

With the error z converging to some region of bounded disturbance, the output of the observer

$$u(t) = L_0\omega(t) + L_1 f(J\omega(t)) + E\varrho(t), \tag{3.15}$$

will converge to the input $\tilde{u}$ of the system with state-feedback (3.12)*. Let us choose the observer gain matrix as:*

$$G = \begin{pmatrix} 21.6 & 21.6 & 0 & 0 \end{pmatrix}^\top, \quad \tilde{Q} = 1$$

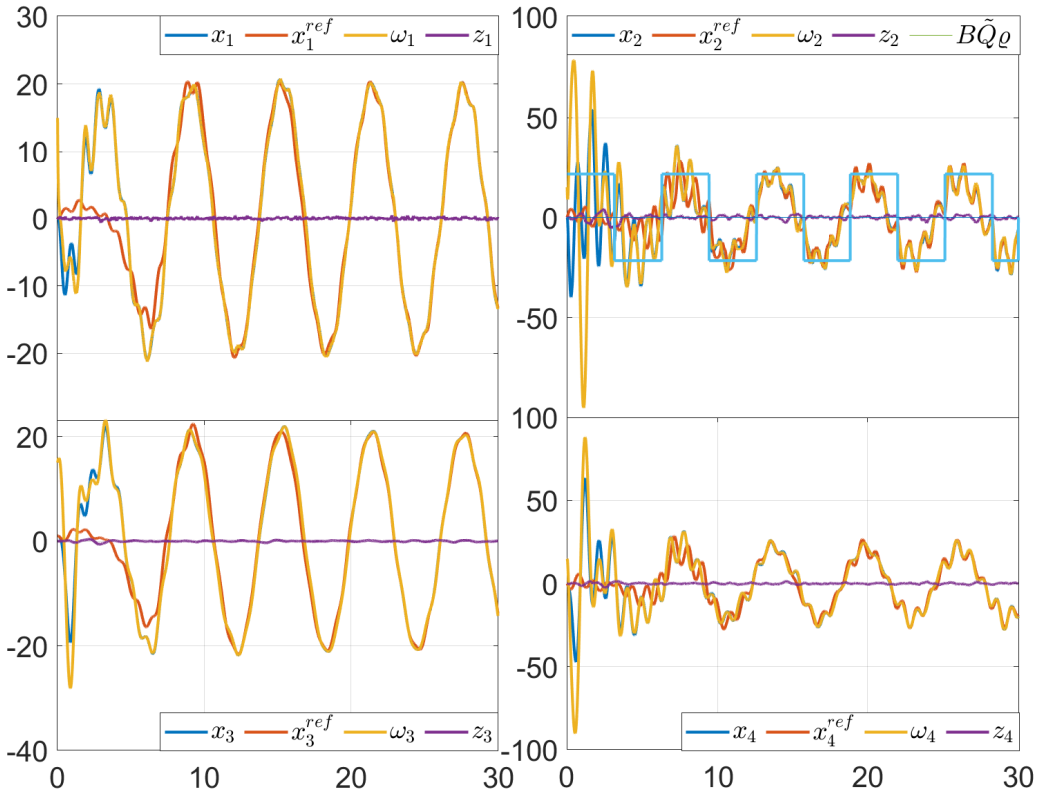

FIGURE 3.6: Observer for Example 3. Initial conditions: $z(0) = (0 \quad 0 \quad 0 \quad 0)^\top$, $\omega(0) = (15 \quad 15 \quad 15 \quad 15)^\top$, $x(0) = x^{rev}(0) = (0 \quad 0 \quad 1 \quad 0)$

and a signal ϱ as a square wave of fixed unit frequency and amplitude, to excite the plant. For the LMIs in Assumption 3.2.3 to be feasible, the matrices L_0 and L_1 of the reference model must be chosen in such a way that S, $J\tilde{S} < 0$. For instance:

$$L_0 = \begin{pmatrix} 1 & 0 & -\frac{24.3}{21.6} & 0 \end{pmatrix} \quad L_1 = -1.$$

however, since we have an under actuated system (we can control only the motor), that is not possible due to the form of B. It does not necessarily mean that the system becomes unstable, but to apply Theorem 3.2.2, let us add and subtract the matrix $W = \begin{pmatrix} 0 & 0 & 21.6 & 0 \end{pmatrix}^\top$. Then we have:

$$\dot{x}(t) = A_0 x(t) + A_1 f(Hx(t)) + (\tilde{B} - W)u(t) + d(t),$$

where $\tilde{B} = \begin{pmatrix} 0 & 21.6 & 21.6 & 0 \end{pmatrix}^\top$ is a new input matrix and the term Wu can be considered as a part of the disturbance d.

With the modified dynamics, Assumption 3.2.3 is satisfied, and the solver gives us a feasible solution with P, Ξ, Ω, Γ, $\Lambda > 0$, the values of which are omitted. Assumptions 3.2.4 and 3.2.5 are satisfied since f is the sine function, for sufficiently small initial conditions $z(0)$, $\omega(0)$ (for example, with Σ_2, Σ_3, Σ_4, $\Phi_2 = 0$ and Σ_1, $\Phi_1 = I_q$). Next, there exists μ (for instance, $\mu = 0.934$) satisfying conditions of Theorem 3.2.2, and the system (3.12), (3.15) is ISS with respect to z and disturbances.

Now, it is only left to prove that z converges. The LMIs in Assumption 3.2.6 were found feasible by a solver, the values for $\tilde{P}$, $\tilde{\Gamma}$, $\tilde{\Xi}$, γ_1, γ_2, are omitted. Conditions for Theorem 3.2.3 are satisfied. For example, for $\mu = 19$, we have ($R_i \geq 0$) and local ISS of z.

Fig. 3.6 shows that in simulation with $d = \begin{pmatrix} 0 & \frac{1}{2}\sin(5t) & 0 & 0 \end{pmatrix}^\top$, the system is ISS and the observer converges to the reference dynamics, validating another application of the result presented in this chapter.

Example 4. *(Section 3.2.2) One of the possible applications of our approach can be the synchronization and observer design for a pair of Chua circuits with a cubic nonlinearity in the resistor, introduced in [Zhong, 1994].*

Consider one of them to be autonomous and oscillating due to the choice of coefficients ($k_1 = 10, k_2 = \frac{100}{7}$)*:*

$$\begin{aligned}\dot{\omega}_1(t) &= k_1\left(\omega_2(t) - \frac{1}{7}(2\omega_1^3(t) - \omega_1(t))\right),\\ \dot{\omega}_2(t) &= \omega_1(t) - \omega_2(t) + \omega_3(t),\\ \dot{\omega}_3(t) &= -k_2\omega_2(t).\end{aligned}$$

Such a circuit was a popular research subject for many years, since its introduction by Leon Chua [Chua, 1994]. It had many applications in chaos theory, dynamical systems (it appeared as an example for observer design [Howell and Hedrick, 2002]), and other fields.

Consider that the second system is affected by a control input $U \in \mathbb{R}^3$ *that has to synchronize the two circuits. For a non-trivial case, let us select two non-identical circuits, due to, for example, a different resistance in a circuit or a different capacitance with* $k_3 = 10, k_4 = 16$ *and* $k_5 = -2.857$*:*

$$\begin{aligned}\dot{x}_1(t) &= k_3\left(x_2(t) - x_1^3(t) + k_5 x_1(t)\right) + U(t),\\ \dot{x}_2(t) &= x_1(t) - x_2(t) + x_3(t) + U(t),\\ \dot{x}_3(t) &= -k_4 x_2(t) + U(t).\end{aligned}$$

A similar setup with two or more Chua circuits can be frequently found in synchronization problems [Yassen, 2003], with the aim of implementation in data encryption.

Problem 2a). Even though the main problem presented in this section is not synchronization, it can still be investigated using the same approach [Nijmeijer and Mareels, 1997]. We can view our setup as a typical leader-follower system, where the signal x *has to follow the dynamics of* ω*, which in our case is oscillating.*

It is easy to notice that both systems are in required form (3.1), (3.2) *with* $G = 0$*:*

$$A_0 = \begin{pmatrix}-28.57 & 10 & 0\\ 1 & -1 & 1\\ 0 & -16 & 0\end{pmatrix},\quad A_1 = \begin{pmatrix}-10\\ 0\\ 0\end{pmatrix},\quad f(x) = x^3,\quad C_0 = \begin{pmatrix}0 & 0 & 1\end{pmatrix},\quad H = \begin{pmatrix}1 & 0 & 0\end{pmatrix},\quad C_1 = 1,$$

$$S_0 = \begin{pmatrix}\frac{10}{7} & 10 & 0\\ 1 & -1 & 1\\ 0 & -\frac{100}{7} & 0\end{pmatrix},\quad S_1 = \begin{pmatrix}-\frac{20}{7}\\ 0\\ 0\end{pmatrix},\quad J = \begin{pmatrix}1 & 0 & 0\end{pmatrix}.$$

Let us consider Π *as the identity matrix (the needed relation for synchronization of these two systems). Then we can design* BL_0 *and* BL_1 *such that the signal* $U = u - L_0 x - L_1 f(Hx)$*, where* $u = L_0\omega - L_1 f(J\omega)$ *as before, will synchronize both dynamics using Proposition 3.2.1. In our case, the matrices will be, for example:*

$$BL_0 = S_0 - A_0 = \begin{pmatrix}1 & 1 & 0\\ 0 & 0 & 0\\ 0 & 0 & 1\end{pmatrix}\begin{pmatrix}31.43 & 0 & 0\\ -1.43 & 0 & 0\\ 0 & 1.7143 & 0\end{pmatrix},\qquad BL_1 = S_1 - A_1 = \begin{pmatrix}1 & 1 & 0\\ 0 & 0 & 0\\ 0 & 0 & 1\end{pmatrix}\begin{pmatrix}2.857\\ 10\\ 0\end{pmatrix}.$$

After this regularization we can state that the dynamics of $x(t)$ *become convergent and Assumption 3.2.2 is satisfied at least locally. Therefore, systems* (3.1) *and* (3.2) *will converge to a common steady-state (see Fig. 3.7).*

Problem 2b). As it was assumed before, we measure only $Y = C_0 x + C_1 f(Hx) + v$ *and the signal* u *is not measured as well as the states* ω *and* x*. Task 2b then would be to build an observer to estimate the state of both systems, using Proposition 3.2.1 and Theorem 3.2.1.*

Proposition 3.2.1 is satisfied by the choice of matrices for the input (B, L_0, L_1) *for* $\Pi = I_q$ *from problem 2a. Since* Π *is the identity matrix, Assumption 3.2.1 is also verified.*

Since the first system is oscillating and the second one is asymptotically stable, Assumption 1.3.1 is satisfied. It is also possible to show that Assumption 3.2.2 is verified in a vicinity of the origin. By choosing corresponding

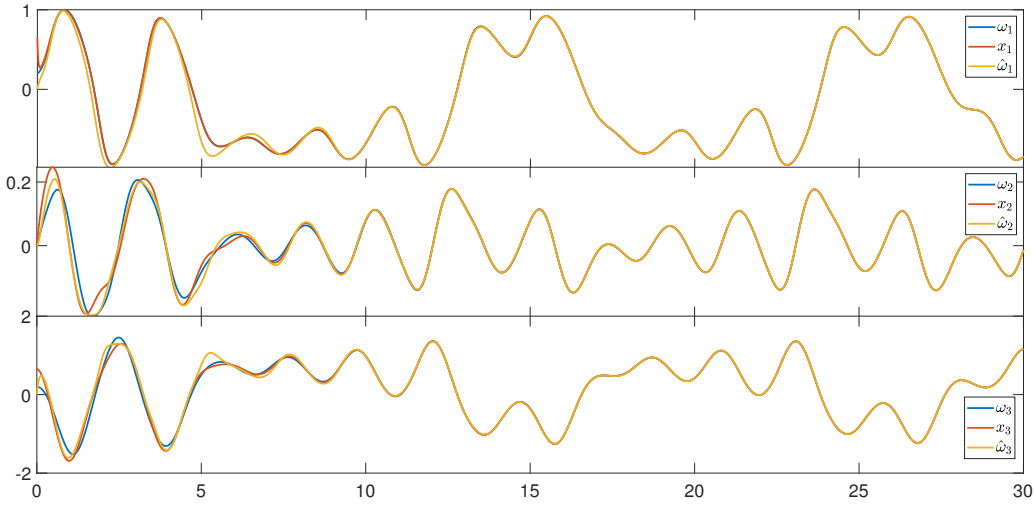

FIGURE 3.7: Simulation results for example 4 (2a,2b). Initial conditions: $\omega(0) = (0.2 \quad 0 \quad 0.2)^\top$, $x(0) = (0.65 \quad 0 \quad \frac{1}{2})^\top$, $\hat{\omega}(0) = (0 \quad 0 \quad 0)^\top$.

matrices F, W, we can check LMIs of Theorem 3.2.1 to determine an observer gain. Consider matrices

$$F = \begin{pmatrix} 0.5 \\ -5 \\ 0.2 \end{pmatrix}, \quad W = \begin{pmatrix} 0.25 & -2.5 & 0.1 \\ -2.5 & 0 & 0 \\ 0.1 & 0 & 0 \end{pmatrix}.$$

A solution of LMIs was found as follows.

$$P = \begin{pmatrix} 0.223 & -1.160 & 0.087 \\ -1.160 & 8.398 & -0.589 \\ 0.087 & -0.589 & 0.066 \end{pmatrix}, \quad Q = \begin{pmatrix} 0.460 & -1.073 & 0.093 \\ -1.073 & 5.489 & 0.077 \\ 0.093 & 0.077 & 0.118 \end{pmatrix}, \quad \Xi = \begin{pmatrix} 6.5664 & -0.7234 & 0.0832 \\ -0.7234 & 12.4347 & -0.4819 \\ 0.0832 & -0.4819 & 6.4706 \end{pmatrix},$$

$$\Gamma = 10.933.$$

And the resulting matrix of gains is:

$$M = \begin{pmatrix} -0.34 \\ 1.32 \\ 5.35 \end{pmatrix}.$$

Fig. 3.7 shows the convergence of all three signals $(x, \omega, \hat{\omega})$, which illustrates well one of possible applications of the presented approach.

3.3 Problem Statement II. Reversed connection

In this section, we consider the case analogous to the previous section, but where the connection of the systems is reversed (Fig. 1.6). Moreover, To broaden our result's applicability, here we consider the dynamics time-variant and both a discrete-time setting and a continuous one.

Continuous-time

Consider a time-varying nonlinear system in the Persidskii form:

$$\begin{cases} \dot{x}(t) = A_0(t)x(t) + A_1(t)f\left(H(t)x(t)\right) + Q(t)u(t) + d(t), \\ y(t) = D_0(t)x(t) + D_1(t)f\left(H(t)x(t)\right) + v(t), \end{cases} \tag{3.16}$$

where $x : \mathbb{R}_+ \to \mathbb{R}^n$ is the state function and $y : \mathbb{R}_+ \to \mathbb{R}^p$ is the output function; $u : \mathbb{R}_+ \to \mathbb{R}^m$ is an essentially bounded external input function; $f : \mathbb{R}^r \to \mathbb{R}^\ell$ is a nonlinear continuous function, $A_0(t) \in \mathbb{R}^{n\times n}$, $A_1(t) \in \mathbb{R}^{n\times \ell}$, $H(t) \in \mathbb{R}^{r\times n}$, $Q(t) \in \mathbb{R}^{n\times m}$, $D_0(t) \in \mathbb{R}^{p\times n}$, $D_1(t) \in \mathbb{R}^{p\times \ell}$ are known time-varying matrices; $d \in \mathcal{L}_\infty^n$ and $v \in \mathcal{L}_\infty^q$ are unknown essentially bounded disturbances. We assume that the function f allows the forward existence and uniqueness of a solution of the system (3.16).

Let us build an observer for system (3.16) of the form:

$$\dot{\omega}(t) = S_0(t)\omega(t) + S_1(t) f\left(J(t)\omega(t)\right) + B(t)y(t) + O(t)u(t), \tag{3.17}$$

where $\omega : \mathbb{R}_+ \to \mathbb{R}^q$ is the state function and $S_0(t) \in \mathbb{R}^{q\times q}$, $S_1(t) \in \mathbb{R}^{q\times \ell}$, $J(t) \in \mathbb{R}^{r\times q}$, $B(t) \in \mathbb{R}^{q\times p}$, $O(t) \in \mathbb{R}^{q\times p}$ are time-varying matrices to be chosen.

Discrete-time

Now consider a time-varying nonlinear discrete-time system in the same form:

$$\begin{cases} x_{k+1} = A_{0,k}x_k + A_{1,k} f(H_k x_k) + Q_k u_k + d_k, \\ y_k = D_{0,k}x_k + D_{1,k} f(H_k x_k) + v_k, \end{cases} \tag{3.18}$$

where $x_k \in \mathbb{R}^n$, $u_k \in \mathbb{R}^m$, $y_k \in \mathbb{R}^p$ are the state, bounded external input and the output vector at time instant $k \in \mathbb{N}$, respectively; $f : \mathbb{R}^r \to \mathbb{R}^\ell$ is a nonlinear function as before, $A_{0,k} \in \mathbb{R}^{n\times n}$, $A_{1,k} \in \mathbb{R}^{n\times \ell}$, $H_k \in \mathbb{R}^{r\times n}$, $Q_k \in \mathbb{R}^{n\times m}$, $D_{0,k} \in \mathbb{R}^{p\times n}$, $D_{1,k} \in \mathbb{R}^{p\times \ell}$ are known time-varying matrices at time instant k; $d \in L_\infty^n$ and $v \in L_\infty^q$ are unknown bounded disturbances.

Let us build an observer for (3.3):

$$\omega_{k+1} = S_{0,k}\omega_k + S_{1,k} f\left(J_k\omega_k\right) + B_k y_k + O_k u_k, \tag{3.19}$$

where $\omega_k \in \mathbb{R}^q$ is the state-vector and $S_{0,k} \in \mathbb{R}^{q\times q}$, $S_{1,k} \in \mathbb{R}^{q\times \ell}$, $J_k \in \mathbb{R}^{r\times q}$, $B_k \in \mathbb{R}^{q\times p}$, $O_k \in \mathbb{R}^{q\times p}$ are time-varying matrices to be chosen.

This section aims to establish conditions for using (3.17) and (3.19) as (reduced-order) observers for (3.16) and (3.3). Conditions for the existence of a static relationship between solutions of (3.16), (3.3), and (3.17), (3.19) have to be established (an analog of (1.17)), and also convergence conditions must be set. Next, the goal is to apply the proposed observer to different estimation problems: reduced-order state observer design and parameter estimation in linear and nonlinear settings.

First, the conditions for the existence of a static relationship between solutions of the systems (3.16), (3.17), and systems (3.3), (3.19) should be established. To this end, the invariant manifold method [Karagiannis, Carnevale, and Astolfi, 2008] will be adapted to the present problem to obtain a simple linear interconnection between the solutions of (3.16), (3.17), and (3.3), (3.19).

3.3.1 Steady-state estimation

Continuous-time

We can state the proposition analogous to Proposition 3.2.1 for the considered case as follows.

Proposition 3.3.1. *Assume that there exist time-varying matrices $\Pi(t) \in \mathbb{R}^{q\times n}$ and $\Upsilon(t) \in \mathbb{R}^{q\times q}$ such that $\Upsilon(t)D_1(t) = 0$, and also matrices $S_0(t)$, $S_1(t)$, $B(t)$, $O(t)$, $\forall t \in \mathbb{R}_+$, that satisfy the following linear equalities:*

$$J\left(\Pi + \Upsilon D_0\right) = H, \tag{3.20}$$

and

$$\begin{aligned} &S_0\left(\Pi+\Upsilon D_0\right)+\left(B-\dot{\Upsilon}\right)D_0-\left(\Pi+\Upsilon D_0\right)A_0-\dot{\Pi}-\Upsilon\dot{D}_0=0,\\ &BD_1-\left(\Pi+\Upsilon D_0\right)A_1+S_1=0,\\ &\left(\Pi+\Upsilon D_0\right)Q=O. \end{aligned} \tag{3.21}$$

Then, for $d=0$ *and* $v=0$*:*

$$\omega(t)=\Pi(t)x(t)+\Upsilon(t)y(t),\ t\in\mathbb{R}_+ \tag{3.22}$$

is a solution of the system (3.16)*,* (3.17)*, for any* $x(0)\in\mathbb{R}^q$ *and* $\omega(0)=\Pi(0)x(0)+\Upsilon(0)y(0)$*.*

Proof. Taking the derivative of (3.22) and using equations (3.16), (3.17), since $\Upsilon D_1=0$, we have:

$$\begin{aligned} S_0(\Pi+\Upsilon D_0)x+S_1f\left(J(\Pi x+\Upsilon y)\right)+B\left(D_0x+D_1f\left(Hx\right)\right)+Ou\\ =\left(\Pi+\Upsilon D_0\right)\left(A_0x+A_1f(Hx)+Qu\right)+\dot{\Pi}x+\dot{\Upsilon}y+\Upsilon\left(\dot{D}_0x+\dot{D}_1f(Hx)\right). \end{aligned}$$

Also $\dot{\Upsilon}D_1=-\Upsilon\dot{D}_1$, so substituting (3.20) leads to the relation

$$\begin{aligned} &\left(S_0(\Pi+\Upsilon D_0)+(B-\dot{\Upsilon})D_0-(\Pi+\Upsilon D_0)A_0-\dot{\Pi}-\Upsilon\dot{D}_0\right)x\\ &=\left(-BD_1+(\Pi+\Upsilon D_0)A_1-S_1\right)f(Hx)+\left((\Pi+\Upsilon D_0)Q-O\right)u, \end{aligned}$$

which is satisfied thanks to (3.21) in a disturbance-free setting. □

Discrete-time

A similar proposition can be also stated for a discrete-time case.

Proposition 3.3.2. *Assume that for each* $k\in\mathbb{N}$ *there exist* $\Pi_k\in\mathbb{R}^{q\times n}$ *and* $\Upsilon_k\in\mathbb{R}^{q\times q}$ *such that* $\Upsilon_kD_{1,k}=0$*, and also matrices* $S_{0,k}$*,* $S_{1,k}$*,* B_k*,* O_k*, satisfying:*

$$J_k\left(\Pi_k+\Upsilon_kD_{0,k}\right)=H_k, \tag{3.23}$$

and

$$S_{0,k}\left(\Pi_k+\Upsilon_kD_{0,k}\right)+B_kD_{0,k}-\left(\Pi_{k+1}+\Upsilon_{k+1}D_{0,k+1}\right)A_{0,k}=0,$$

$$\begin{aligned} &B_kD_{1,k}-\left(\Pi_{k+1}+\Upsilon_{k+1}D_{0,k+1}\right)A_{1,k}+S_{1,k}=0,\\ &\left(\Pi_{k+1}+\Upsilon_{k+1}D_{0,k+1}\right)Q_k=O_k. \end{aligned} \tag{3.24}$$

Then, for $d=0$ *and* $v=0$*:*

$$\omega_k=\Pi_kx_k+\Upsilon_ky_k,\ k\in\mathbb{N} \tag{3.25}$$

is a solution of the system (3.3)*,* (3.19)*, for any* $x_0\in\mathbb{R}^q$ *and* $\omega_0=\Pi_0x_0+\Upsilon_0y_0$*.*

Proof. Taking the next time instant for (3.25)

$$\omega_{k+1}=\Pi_{k+1}x_{k+1}+\Upsilon_{k+1}y_{k+1}=\left(\Pi_{k+1}+\Upsilon_{k+1}D_{0,k+1}\right)x_{k+1},$$

and using equations (3.3), (3.19), since $\Upsilon_kD_{1,k}=0$, we have the following equality:

$$\begin{aligned} S_{0,k}(\Pi_k+\Upsilon_kD_{0,k})x_k+S_{1,k}f\left(J_k(\Pi_k+\Upsilon_kD_{0,k})x_k\right)+B_k\left(D_{0,k}x_k+D_{1,k}f\left(H_kx_k\right)\right)+O_ku_k\\ =\left(\Pi_{k+1}+\Upsilon_{k+1}D_{0,k+1}\right)\left(A_{0,k}x_k+A_{1,k}f(H_kx_k)+Q_ku_k\right). \end{aligned}$$

which leads to the relation

$$\begin{aligned}\left(S_{0,k}(\Pi_k+\Upsilon_k D_{0,k})+B_k D_{0,k}-(\Pi_{k+1}+\Upsilon_{k+1}D_{0,k+1})A_{0,k}\right)x_k &= (S_{1,k}+B_k D_{1,k}\\ &\quad-(\Pi_{k+1}+\Upsilon_{k+1}D_{0,k+1})A_{1,k})f(H_k x_k)+\left((\Pi_{k+1}+\Upsilon_{k+1}D_{0,k+1})Q_k-O_k\right)u_k,\end{aligned}$$

which is satisfied thanks to (3.24) in a disturbance-free setting. □

Since the observers (3.17), (3.19) of the systems (3.16), (3.3) have the same shape of nonlinearity, under suitable interconnections among the matrices given in Propositions 3.3.1 and 3.3.2, the obtained relation between solutions is linear, reducing the complexity of analysis significantly and opening space for many applications.

3.3.2 Convergence to the invariant solution

In Propositions 3.3.1 and 3.3.2, only the existence of relations (3.22), (3.25) is proven. Whether this relation is attracting for (3.16), (3.3) and (3.17), (3.19) or not, it should be established in further analysis.

Continuous-time

Assume that the conditions of the Proposition 3.3.1 are verified:

Assumption 3.3.1. *There exist* Π *and* Υ *such that* $\Upsilon D_1 = 0$ *and the equalities* (3.20) *and* (3.21) *are satisfied for* (3.16)*,* (3.17)*.*

Next, consider the following dynamical system with a copy dynamics of (3.17):

$$\dot{z}(t) = S_0(t)z(t)+S_1(t)f(J(t)z(t))+B(t)y(t)+O(t)u(t)+\delta(t),$$

where $\delta \in \mathcal{L}_\infty^q$ represents an exogenous perturbation (the influence of d and v). Let us introduce the error $e := \omega - z$ between two solutions of (3.17), initiated for different initial conditions, with the same inputs (y and u). Then we have the following dynamics:

$$\dot{e}(t) = S_0(t)e(t)+S_1(t)\left(f\left(J(t)\omega(t)\right)-f\left(J(t)z(t)\right)\right)-\delta(t). \tag{3.26}$$

Now we can state a theorem about the convergence and robust stability of the observer.

Theorem 3.3.1. *Let Assumption 3.3.1 be satisfied. Assume there exist* $F(t) \in \mathbb{R}^{q\times k}$ *and* $W(t) = W(t)^\top \in \mathbb{R}^{q\times q}$ *such that*

$$e^\top F\left(f\left(J\omega\right)-f\left(Jz\right)\right) \le e^\top W e,$$

for all $\omega(t)$, $z(t) \in \mathbb{R}^q$*, and that there exist* $P(t) = P(t)^\top \in \mathbb{R}^{q\times q}$, $\Xi(t) = \Xi(t)^\top \in \mathbb{R}^{q\times q}$ *such that the inequalities*

$$\begin{gathered}\alpha_1 I_n \le P,\Xi \quad P \le \alpha_2 I_n, \quad PS_1 = F,\\ \dot{P}+S_0^\top P+PS_0+2W+\Xi+\gamma P<0\end{gathered}$$

have a solution for some $0<\alpha_1<\alpha_2<+\infty$ *and* $\gamma>0$*. Then, the system* (3.26) *is ISS and* (3.17) *is globally convergent.*

Proof. Assumption 3.3.1 ensures the existence of an estimate, so let us select a Lyapunov function $V(e) = e^\top P e$, with P given by the conditions of the theorem (this Lyapunov function is positive definite and radially unbounded in e due to the introduced restriction). Its derivative for (3.26) takes the form:

$$\begin{aligned}\dot{V} &= e^\top(S_0^\top P+PS_0+\dot{P})e+2e^\top PS_1\left(f(J\omega)-f(Jz)\right)-2e^\top P\delta\\ &\le e^\top\left(S_0^\top P+PS_0+\dot{P}+2W+\Xi+\gamma P\right)e-e^\top\Xi e+\gamma^{-1}\delta^\top P\delta,\end{aligned}$$

where $F = PS_1$ and W, γ are given in the formulation of the theorem. According to the imposed conditions, the above expression is non-positive and:

$$\|e(t)\| \leq \sqrt{\frac{\lambda_{\max}(P)}{\lambda_{\min}(P)}} \left(e^{-0.5 \frac{\lambda_{\min}(\Xi)}{\lambda_{\max}(P)} t} \|e(0)\| + \gamma^{-0.5} \|\delta\| \right)$$

for all $t \geq 0$. □

The conditions presented in Theorem 3.3.1 are given for an illustration, and any other conditions for convergence to zero and robust stability of e in (3.26) can be used.

Discrete-time

Assume that the conditions of the Proposition 3.3.2 are verified:

Assumption 3.3.2. *There exist* Π_k *and* Υ_k *such that* $\Upsilon_k D_{1,k} = 0$ *and the equalities* (3.23) *and* (3.24) *are satisfied for* (3.3)*,* (3.19)*.*

Next, consider the following dynamical system with a copy dynamics of (3.19):

$$z_{k+1} \quad = \quad S_{0,k} z_k + S_{1,k} f(J_k z_k) + B_k y_k + O_k u_k + \delta_k,$$

where $\delta \in L_\infty^q$ is an auxiliary bounded disturbance as before. Let us introduce the error $e_k := \omega_k - z_k$ between two solutions of (3.19), initiated for different initial conditions, with the same inputs (y_k and u_k). Then we have the following system:

$$e_{k+1} = S_{0,k} e_k + S_{1,k} \left(f\left(J_k \omega_k\right) - f\left(J_k z_k\right) \right) - \delta_k. \tag{3.27}$$

Now we can state a theorem about the convergence and robust stability of the observer.

Theorem 3.3.2. *Let Assumption 3.3.2 be satisfied. Assume there exists* $\gamma > 0$ *such that*

$$|f(J_k \omega_k) - f(J_k z_k)| \leq \gamma |e_k|$$

for all ω_k*,* $z_k \in \mathbb{R}^q$*, and that there exist* $P_k = P_k^\top \in \mathbb{R}^{q \times q}$*,* $\Xi = \Xi^\top \in \mathbb{R}^{q \times q}$ *and* $\Gamma = \Gamma^\top \in \mathbb{R}^q$ *such that the inequalities*

$$\begin{pmatrix} \Sigma_k & S_{0,k}^\top P_{k+1} S_{1,k} & -S_{0,k}^\top P_{k+1} \\ S_{1,k}^\top P_{k+1} S_{0,k} & S_{1,k}^\top P_{k+1} S_{1,k} - \alpha I & -S_{1,k}^\top P_{k+1} \\ -P_{k+1} S_{0,k} & -P_{k+1} S_{1,k} & P_{k+1} - \Gamma \end{pmatrix} \leq 0$$

where $\Sigma_k = S_{0,k}^\top P_{k+1} S_{0,k} - P_k + \Xi + \alpha \gamma^2 I$*, have a solution for some* $\alpha > 0$*. Then the system* (3.27) *is ISS and* (3.19) *is globally convergent.*

Proof. Assumption 3.3.2 ensures the existence of an estimate, so let us select a Lyapunov function $V_k = e_k^\top P_k e_k$, where P_k is given in the conditions of the theorem. Consider the difference $V_{k+1} - V_k$ and denote $\Delta f_k := f(J_k \omega_k) - f(J_k z_k)$ then using the bound defined in the theorem, we have

$$V_{k+1} - V_k \leq \begin{pmatrix} e_k \\ \Delta f_k \\ \delta_k \end{pmatrix}^\top \begin{pmatrix} \Sigma_k & S_{0,k}^\top P_{k+1} S_{1,k} & -S_{0,k}^\top P_{k+1} \\ S_{1,k}^\top P_{k+1} S_{0,k} & S_{1,k}^\top P_{k+1} S_{1,k} - \alpha I & -S_{1,k}^\top P_{k+1} \\ -P_{k+1} S_{0,k} & -P_{k+1} S_{1,k} & P_{k+1} - \Gamma \end{pmatrix} \begin{pmatrix} e_k \\ \Delta f_k \\ \delta_k \end{pmatrix} - e_k^\top \Xi e_k + \delta_k^\top \Gamma \delta_k.$$

According to the imposed conditions, $\Phi_k \leq 0$ and the error e_k is ISS for the input δ_k. □

3.3.3 Reduced-order observer design

Let us demonstrate how the generic results presented in the previous section can be used to estimate the system's unobserved states, starting with a continuous-time case.

Linear reduced-order observer

The first application of the result presented in the previous section is a reduced-order observer for the linear case, where $S_1 = 0$, $D_1 = 0$, and all other matrices are known and constant in (3.16) (the time-invariance has been imposed to simplify the presentation and comparison). Then we have an ordinary LTI system of the form:

$$\begin{cases} \dot{x}(t) = A_0 x(t) + Qu(t) + d(t),\ t \in \mathbb{R}_+, \\ y(t) = D_0 x(t) + v(t). \end{cases} \tag{3.28}$$

As in the classical problem of reduced-order observer design, we can present our state $x(t) \in \mathbb{R}^n$ with new variables $y(t) \in \mathbb{R}^p$ representing a set of directly measured state variables and $w(t) \in \mathbb{R}^{n-p}$ a set of unmeasured states:

$$\begin{pmatrix} y(t) \\ w(t) \end{pmatrix} = \begin{pmatrix} D_0 \\ \Pi \end{pmatrix} x(t) + \begin{pmatrix} v(t) \\ 0 \end{pmatrix}. \tag{3.29}$$

In practice, v is often considered a bounded measurement noise. The task is to build an observer, which will effectively reduce the dynamic order of (3.17) from n to $n-p$. Therefore, consider the following LTI system (the respective presentation of (3.17)):

$$\dot{\omega}(t) = S_0 \omega(t) + By(t) + Ou(t), \tag{3.30}$$

where $\omega(t) \in \mathbb{R}^{n-p}$ is the observer state, and $S_0 \in \mathbb{R}^{(n-p)\times(n-p)}$, $B \in \mathbb{R}^{(n-p)\times p}$, $O \in \mathbb{R}^{(n-p)\times m}$ are constant matrices to be determined.

Then, Proposition 3.3.1 can be applied for the considered case. If the following matrix equalities are verified:

$$\begin{aligned} &S_0(\Pi + \Upsilon D_0) + BD_0 - (\Pi + \Upsilon D_0) A_0 = 0, \\ &(\Pi + \Upsilon D_0) Q = O, \end{aligned} \tag{3.31}$$

then there exists a solution

$$\omega(t) = \Pi x(t) + \Upsilon y(t),\ \forall t \in \mathbb{R}_+ \tag{3.32}$$

for any $x(0) \in \mathbb{R}^q$ and $\omega(0) = \Pi x(0) + \Upsilon y(0)$, connecting (3.28) and (3.30). Applying Assumption 3.3.1 to (3.32), (3.28), and (3.30), we can use Theorem 3.3.1 (we ask for the existence of a positive definite symmetric matrix $P \in \mathbb{R}^{p\times p}$ such that $S_0^\top P + PS_0 < 0$) to show that (3.30) is globally asymptotically stable (the estimation error is input-to-state stable). Furthermore, it is, in fact, a global asymptotic observer for w, making it a reduced-order observer for (3.28). This classical result is well-known and was first presented in [Luenberger, 1964]. The purpose of considering such a case here is to demonstrate that the traditional result for linear systems can be obtained through the previous idea.

Nonlinear reduced-order observer

Consider (3.16) and (3.17) with constant matrices for simplicity, and let $D_1 = 0$. We have a nonlinear system:

$$\begin{cases} \dot{x}(t) = A_0 x(t) + A_1 f(Hx(t)) + Qu(t) + d(t),\ t \in \mathbb{R}_+, \\ y(t) = D_0 x(t) + v(t), \end{cases} \tag{3.33}$$

where $x(t) \in \mathbb{R}^n$ is the full state, $y(t) \in \mathbb{R}^p$ is the measured part of the state and A_0, A_1, Q, H are matrices of corresponding dimensions, $d \in \mathcal{L}_\infty^n$ is an external disturbance or a modeling error and $v \in \mathcal{L}_\infty^p$ is a measurement noise. Our goal is to design a reduced-order observer for (3.33) of a smaller dimension $q = n - p$:

$$\dot{\omega}(t) = S_0\omega(t) + S_1 f(J\omega(t)) + By(t) + Ou(t), \tag{3.34}$$

where $\omega(t) \in \mathbb{R}^q$, and constant matrices are of corresponding dimensions. All of them have to be defined using the presented method. Proposition 3.3.1 gives us the conditions of existence of a solution in a disturbance-free scenario ($d = 0$, $v = 0$ and the matrix Π is obtained from the representation (3.29)):

$$\omega(t) = \Pi x(t) + \Upsilon y(t) = (\Pi + \Upsilon D_0)x(t) = Zx(t), \tag{3.35}$$

where $Z \in \mathbb{R}^{q\times n}$ is a matrix connecting solutions of the initial system (3.33) and the observer (3.34). Then, (3.20) and (3.21) in this case are as follows:

$$\begin{aligned} &JZ = H, \\ &S_0Z = ZA_0 - BD_0, \\ &S_1 = ZA_1, \\ &O = ZQ. \end{aligned} \tag{3.36}$$

The equations above can be solved with respect to S_0, S_1, B, O and J, knowing Z. Theorem 3.3.1 can be directly applied with a constant matrix P to prove the convergence of the observer (3.34) to a hyperplane given by (3.35). Since the order of (3.34) is lower than the one of (3.33), we can say that (3.34) is an asymptotical reduced-order observer.

Remark 3.3.1. *The same result can be derived for time-varying matrices. The difference will lay only in matrix equations from Proposition 3.3.1 and in the form of $S_0(t)$ and $S_1(t)$.*

Discrete-time reduced-order observer

Consider (3.3) and (3.19) and let $D_{1,k} = 0$, $k \in \mathbb{N}$. We have a nonlinear discrete-time system:

$$\begin{cases} x_{k+1} = A_{0,k}x_k + A_{1,k}f(H_kx_k) + Q_ku_k + d_k,\ k \in \mathbb{N}, \\ y_k = D_{0,k}x_k + v_k, \end{cases} \tag{3.37}$$

where $x_k \in \mathbb{R}^n$ is the full state, $y_k \in \mathbb{R}^p$ is the measured part of the state and $A_{0,k}$, $A_{1,k}$, Q_k, H_k are matrices of corresponding dimensions at time instant k, d_k is an external disturbance and v_k is a measurement noise as before. Then we build an observer again:

$$\omega_{k+1} = S_{0,k}\omega_k + S_{1,k}f(J_k\omega_k) + B_ky_k + O_ku_k, \tag{3.38}$$

where $\omega_k \in \mathbb{R}^q$, and all matrices are of corresponding dimensions. Proposition 3.3.2 gives us the existence conditions for a solution in a disturbance-free scenario and the matrices Π_k are as follows:

$$\omega_k = \Pi_k x_k + \Upsilon_k y_k = (\Pi_k + \Upsilon_k D_{0,k})x_k = G_k x_k, \tag{3.39}$$

where $G_k \in \mathbb{R}^{q\times n}$ is a matrix at time instant k, connecting solutions of the initial system (3.37) and the observer (3.38). Then, (3.23) and (3.24) are as follows:

$$\begin{aligned} &S_{0,k}G_k + B_k D_{0,k} - G_{k+1}A_{0,k} = 0,\\ &B_k D_{1,k} - G_{k+1}A_{1,k} + S_{1,k} = 0,\\ &G_{k+1}Q_k = O_k,\\ &J_k G_k = H_k. \end{aligned} \tag{3.40}$$

The equations above can be solved to determine $S_{0,k}$, $S_{1,k}$, B_k, O_k, and J_k, knowing G_k. Theorem 3.3.2 can be directly applied with a matrix P_k to prove the convergence of the observer (3.38).

The results on reduced-order observer design for nonlinear systems given in [Sundarapandian, 2006b] and [Sundarapandian, 2006a] are local and based on linearization analysis, while the general results presented in [Karagiannis, Carnevale, and Astolfi, 2008] cover the considered case, but they are less constructive due to the requirement of the existence of a solution for the PDE.

3.3.4 Regression

Let us consider another possible application of the result presented above.

Linear regression

A well-known and commonly method used in practical estimation problems is the linear parameter regression. The application of our result is less intuitive in this setting than previously. However, it fits the problem statement rather well. To demonstrate it, let us consider a simple linear regression equation:

$$\dot{x}(t) = d(t),\ t \in \mathbb{R}_+ \tag{3.41}$$

$$y(t) = D_0(t)x(t) + v(t), \tag{3.42}$$

where $y(t) \in \mathbb{R}^p$ is a measured output, $D_0(t) \in \mathbb{R}^{p\times n}$ is a regression matrix, $x(t) \in \mathbb{R}^n$ is the vector of unknown parameters to be estimated, which in our case is the state-vector and $d(t) \in \mathbb{R}^n$ is a bounded disturbance signal. Having nonzero disturbance means that the parameter vector x may not be necessarily constant but can be affected by external factors and vary in time in a certain region. In the case of linear regression, the disturbance v can represent an unmodeled observational or experimental error. Usually, this error is assumed to be independent and normally distributed with zero mean and unknown variance[Gallant, 1975]. To apply Proposition 3.3.1, we consider $A_0 \equiv A_1 \equiv D_1 \equiv Q \equiv 0$ in (3.16), and we represent the parameter observer in the required form (3.17) with $S_1 \equiv O \equiv 0$:

$$\dot{\omega}(t) = S_0(t)\omega(t) + B(t)y(t), \tag{3.43}$$

Then, we can choose $\Pi \equiv I_n$ as the constant identity matrix, $\Upsilon \equiv 0$, leading to:

$$\omega(t) = x(t), \tag{3.44}$$

meaning that (3.43) is an observer for x. Applying Proposition 3.3.1, we have the equality:

$$S_0 = -BD_0. \tag{3.45}$$

Since we need to choose the matrices S_0 and B, let us assign $B = \Gamma D_0^\top$, where Γ is a nonsingular matrix, and can substantiate $S_0 = -\Gamma D_0^\top D_0$. Substituting in (3.43), it results in a conventional gradient estimator:

$$\dot{\omega}(t) = \Gamma D_0^\top(t)\left(y(t) - D_0(t)\omega(t)\right). \tag{3.46}$$

For the asymptotic convergence of this observer, we need a standard additional assumption[Bitmead, 1984]:

Assumption 3.3.3. *The matrix $D_0(t)$ is PE, for $\forall t \in \mathbb{R}_+$.*

Remark 3.3.2. *There exist some techniques to relax the PE condition using preprocessing algorithms, such as the Dynamic Regressor Extension and Mixing (DREM) method (see, for example, [Aranovskiy et al., 2016], briefly described in Section 2.5.3. However, to demonstrate our approach in this chapter, we prefer to keep Assumption 3.3.3 for a sake of generality.*

If Assumption 3.3.3 is satisfied, then applying Theorem 3.3.1 to (3.44), (3.42), and (3.43), we obtain the convergence of the estimator to the state x (under Assumption 3.3.1, it is well known that there is a matrix P satisfying the conditions of the theorem). This result is well-known for parameter estimation in linear regression (see, for instance, [Ljung, 1999]). Despite the result not being novel, this application demonstrates the broad applicability of the presented approach to estimation problems.

Nonlinear regression

Similarly to the linear equation (3.42), we can consider the following form of the system (3.16), where $A_0 \equiv A_1 \equiv Q \equiv 0$:

$$\dot{x}(t) = d(t),\ t \in \mathbb{R}_+ \tag{3.47}$$
$$y(t) = D_0(t)x + D_1(t)f(H(t)x) + v(t), \tag{3.48}$$

where $y(t) \in \mathbb{R}^p$ is measured output vector, $D_0(t) \in \mathbb{R}^{p\times n}$ is a regression matrix in the linear part and $D_1(t) \in \mathbb{R}^{p\times \ell}$, $H(t) \in \mathbb{R}^{r\times n}$ are regression matrices in the nonlinear part, $x(t) \in \mathbb{R}^n$ is a vector of unknown parameters and $d(t) \in \mathbb{R}^n$ is a bounded disturbance signal. As in the linear case we have the corresponding observer:

$$\dot{\omega}(t) = S_0(t)\omega(t) + S_1(t)f(J(t)\omega(t)) + B(t)y(t), \tag{3.49}$$

and we set $\Pi \equiv I_n$ and $\Upsilon \equiv 0$, so we are looking for a solution in the form:

$$\omega(t) = x(t).$$

Using Proposition 3.3.1, we obtain the following equalities:

$$\begin{aligned} &J = H,\\ &S_0 + BD_0 = 0,\\ &S_1 + BD_1 = 0. \end{aligned}$$

Substituting it in (3.49), we have:

$$\dot{\omega}(t) = -B(t)D_0(t)\omega(t) - B(t)D_1(t)f(J(t)\omega(t)) + B(t)y(t).$$

However, the estimation problem for nonlinear regression appears to be more complex and might require some additional conditions to guarantee the observer's convergence. Therefore, let us consider a particular case of (3.48):

$$y(t) = (1 - D_1(t))J(t)x(t) + D_1(t)f(J(t)x(t)), \tag{3.50}$$

where $D_0(t) = (1 - D_1(t))J(t)$ and $0 \le D_1(t) \le 1$, for all $t \ge 0$.

Such a form of regression equation might be found in models where the output is a fusion of data from multiple sensors (i.e., linear and nonlinear parameters) of different nature, is used to improve the estimation [Sandy et al., 2019]. For instance, the possible failure [Chair and Varshney, 1986] or missing data [Housfater, Zhang, and Zhou, 2006] from some sensors is often considered. In any case, D_1 is considered to be a signal that dynamically weights the data from linear and nonlinear sensors.

Let $B = \gamma J^\top$ for some $\gamma > 0$ and consider a copy dynamics of (3.49):

$$\dot{z}(t) = -\gamma(1 - D_1(t))J(t)^\top z(t) - \gamma D_1(t)J(t)^\top f(J(t)z(t)) + B(t)y(t) + \delta(t),$$

then we have error dynamics for $e(t) = \omega(t) - z(t)$:

$$\dot{e}(t) = -\gamma(1 - D_1(t))J(t)^\top J(t)e(t) - \gamma D_1(t)J(t)^\top \left(f(J(t)\omega) - f(J(t)z(t))\right) - \delta(t). \tag{3.51}$$

Remark 3.3.3. *Set $D_1(t) = 0, \forall t \in \mathbb{R}_+$. Then* (3.50) *takes the form of linear regression equation* (3.42)*, where $J \equiv D_0$.*

Theorem 3.3.1 can be used for stability analysis of (3.51), but to get more efficient stability conditions, let us consider its modification. For this purpose, we need an auxiliary hypothesis:

Assumption 3.3.4. *The function J is PE.*

Under this condition, consider a time-dependent matrix

$$P(t) = \int_t^\infty \Phi(s,t)^\top \Phi(s,t) ds,$$

where

$$\dot{\Phi}(t,t_0) = -\gamma J^\top(t)J(t)\Phi(t,t_0) \quad \Phi(t_0,t_0) = I.$$

then the following equality is satisfied

$$\dot{P}(t) - \gamma P(t)J(t)^\top J(t) - \gamma J^\top(t)J(t)P(t) = -I_n. \tag{3.52}$$

Theorem 3.3.3. *Let Assumptions 3.3.4 and 3.3.1 be satisfied. Assume that*

$$-\gamma D_1 e^\top P J^\top \left(f(J\omega) - f(Jz) - Je\right) < \frac{e^\top e}{2},$$

for all ω, $z \in \mathbb{R}^q$ and $e = \omega - z$, with P defined as above. Then, the system (3.51) *is ISS and* (3.49) *is globally convergent.*

Proof. Assumption 3.3.1 ensures the existence of an invariant solution, so select a Lyapunov function candidate $V(e) = e^\top P e$. Then the derivative of V along the trajectories of (3.51) takes the form:

$$\begin{aligned}\dot{V} = {} & e^\top \dot{P} e + \left(-\gamma J^\top J e - \gamma D_1 J^\top \left(f(J\omega) - f(Jz) - Je\right)\right)^\top P(t) e \\ & + e^\top P \left(-\gamma J^\top J(t) e - \gamma D_1 J^\top \left(f(J\omega) - f(Jz) - Je\right)\right).\end{aligned}$$

Substituting the expression of the derivative of P we have:

$$\dot{V} = -e^\top e - 2\gamma D_1(t) e^\top P J^\top \left(f(J\omega) - f(Jz) - Je\right),$$

Using the inequality of the theorem, we obtain $\dot{V} < 0$ and asymptotic stability of the error e. □

3.3.5 Discrete-time regression

Let us extend the linear regression application from the paper to the discrete-time case. Since regression analysis is mainly performed for discrete-time data, we can adapt our approach to this scenario. We will need the following definition

Definition 3.3.1. *A bounded signal $\phi_k : \mathbb{N} \to \mathbb{R}^n$ is called (l,μ)-*PE*, if there exist $l \in \mathbb{N}^*$ and $\mu > 0$ such that*

$$\sum_{i=k}^{k+l-1} \phi_i \phi_i^\top \geq \mu I_n, \forall k \in \mathbb{N}.$$

Let us consider the linear regression equation:

$$x_{k+1} = x_k = x, \tag{3.53}$$
$$y_k = D_{0,k}x + v_k, \tag{3.54}$$

where $y_k \in \mathbb{R}^p$ is the measured value, $x \in \mathbb{R}^n$ is an unknown constant parameter and v_k is a measurement noise. To apply Proposition 2, we consider $A_{0,k} = I_n, A_{1,k} = D_{1,k} = Q_k = 0$ and we represent the parameter observer in the form (26) with $S_{1,k} = O_k = 0$.

$$\omega_{k+1} = S_{0,k}\omega_k + B_k y_k, \tag{3.55}$$

We choose $\Pi_k = I_n$ and $\Upsilon_k = 0$ to have:

$$\omega_k = x. \tag{3.56}$$

The matrix equalities from Proposition 2 imply that:

$$S_{0,k} + B_k D_{0,k} = I_n. \tag{3.57}$$

Note that the main difference with the continuous approach is the form of $S_{0,k}$ for the estimator design. Let us assign $B_k = \Gamma_k D_{0,k}^\top$, with Γ_k being a nonsingular matrix, and we have $S_{0,k} = I_n - \Gamma_k D_{0,k}^\top D_{0,k}$ which results in the gradient estimator:

$$\omega_{k+1} = \omega_k + \Gamma D_{0,k}^\top (y_k - D_{0,k}\omega_k). \tag{3.58}$$

As in the continuous-time case, it is necessary to assume that the following is true:

Assumption 3.3.5. *The signal $D_{0,k}$ is PE.*

If this assumption is satisfied, Theorem 3.3.2 can be applied.

The current subsection demonstrates an advantage of the generality of the considered approach, which allows investigating a rather wide range of both linear and nonlinear estimation problems.

3.3.6 Examples

Example 5. *Let us consider a two mass-spring system with nonlinear stiffness affected by the white Gaussian noise v and disturbance d, the dynamics of which can be expressed as follows:*

$$\begin{cases} \dot{x}_1 = x_2, \\ \dot{x}_2 = -k_1(x_1 - x_3) - k_2(x_1 - x_3)^3 - a_1(x_2 - x_4) + 0.2u_1, \\ \dot{x}_3 = x_4, \\ \dot{x}_4 = k_1(x_1 - x_3) + k_2(x_1 - x_3)^3 + a_1(x_2 - x_4) - k_3 x_3 - a_2 x_4 + u, \\ y_1 = x_1 + v, \\ y_2 = x_2 + v \end{cases} \tag{3.59}$$

with $u(t) = \sin(t)$ and $u_1(t) = u(10t)$, $t \in \mathbb{R}_+$. Presenting the system in the form (3.16)*, we have:*

$$A_0 = \begin{pmatrix} 0 & 1 & 0 & 0 \\ -k_1 & -a_1 & k_1 & a_1 \\ 0 & 0 & 0 & 1 \\ k_1 & a_1 & -k_1 - k_3 & a_1 - a_2 \end{pmatrix}, \quad A_1 = \begin{pmatrix} 0 \\ -k_2 \\ 0 \\ k_2 \end{pmatrix}, \quad f(\mu) = \mu^3 \ (\mu \in \mathbb{R}), \quad Q = \begin{pmatrix} 0 & 0 & 0 & 1 \end{pmatrix}^\top,$$

$$D_0 = \begin{pmatrix} 1 & 0 & 0 & 0 \\ 0 & 1 & 0 & 0 \end{pmatrix}, \quad H = \begin{pmatrix} 1 & 0 & -1 & 0 \end{pmatrix}, \quad D_1 = 0,$$

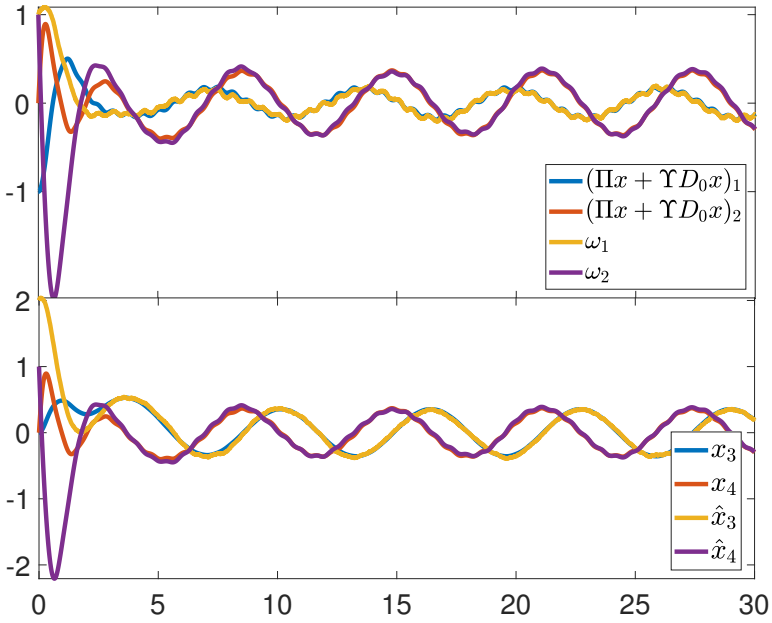

FIGURE 3.8: Example 5. Reduced-order observer for a mass-spring system.

where the states x_1 and x_2 correspond to the position and the velocity of the first mass, assumed to be measured. The states x_3 and x_4 represent the second mass's position and velocity, which we need to estimate. The signal u is the periodic force applied to the second mass to excite the system. The task is to build an observer of the form (3.34) *for the states x_3 and x_4 using Proposition 3.3.1 (or* (3.38) *and Proposition 3.3.2). We have the following LMEs:*

$$\begin{aligned} &J(\Pi + \Upsilon D_0) = H, \\ &S_0(\Pi + \Upsilon D_0) = (\Pi + \Upsilon D_0)A_0 - BD_0, \\ &S_1 = (\Pi + \Upsilon D_0)A_1, \\ &O = (\Pi + \Upsilon D_0)Q. \end{aligned} \tag{3.60}$$

We can assign Π and Υ having full row rank (the matrix Π should have left inverse with respect to the unmeasured state components of (3.59)*, while Υ describes the utilization of the output variables) as, for example:*

$$\Pi = \begin{pmatrix} 0 & 0 & 1 & 0 \\ 0 & 0 & 0 & 1, \end{pmatrix} \quad \Upsilon = \begin{pmatrix} \upsilon_1 & 0 \\ 0 & \upsilon_2 \end{pmatrix}.$$

Therefore, we have 16 equations in total, with 16 unknowns. Solving the equations for chosen in simulation values of the coefficients ($k_1 = 3$, $k_2 = 3$, $k_3 = 0.6$, $a_1 = 0.6$, $a_2 = 2$), we obtain:

$$S_0 = \begin{pmatrix} 0 & 1 \\ -3.6 & -2.6 \end{pmatrix}, \quad S_1 = \begin{pmatrix} 0 \\ 3 \end{pmatrix}, \quad J = \begin{pmatrix} -1 & 0 \end{pmatrix}, \quad O = \begin{pmatrix} 0 \\ 1 \end{pmatrix}, \quad B = \begin{pmatrix} 0 & -1 \\ -0.6 & 0.6 \end{pmatrix}, \quad \Upsilon = \begin{pmatrix} -1 & 0 \\ 0 & 0 \end{pmatrix}.$$

Then, we have the dynamics of ω, which must satisfy the LMIs in Theorem 3.3.1. From the given dynamics, we have the condition:

$$e^\top F \left(z_1^3 - \omega_1^3 \right) = (F_1 e_1 + F_2 e_2) \left(-e_1 (z_1^2 + \omega_1 z_1 + \omega_1^2) \right) \leq e^\top W e,$$

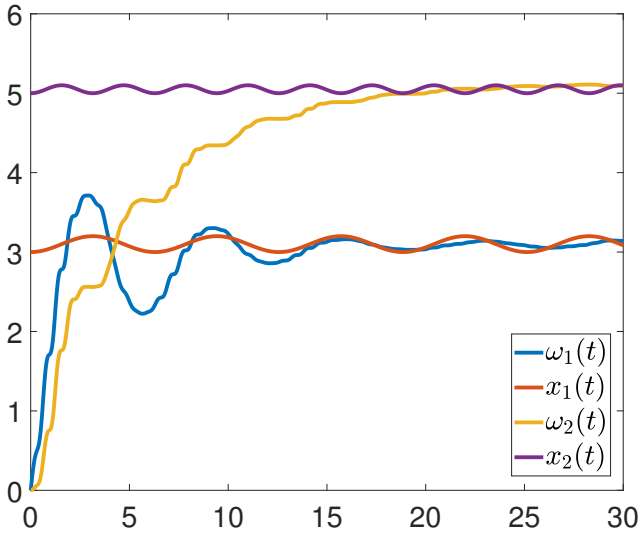

FIGURE 3.9: Example 2: nonlinear regression for a system given in a form (3.50).

which has to be satisfied locally in $z, \omega \in \mathbb{R}^2$ *by imposing the admissible upper limits on these variables. Assume that* $z_1^2 + \omega_1^2 \leq \eta$ *for some* $\eta > 0$*, then*

$$W = 0.5\eta \begin{pmatrix} -F_1 + 1.5F_2 & 0 \\ 0 & 1.5F_2 \end{pmatrix}.$$

Consider, for example, the following matrices:

$$F = \begin{pmatrix} 0.25 \\ 0 \end{pmatrix}, \quad W = \begin{pmatrix} -0.1875 & 0 \\ 0 & 0 \end{pmatrix},$$

$\gamma = 0.5$, $\eta = 1.5$ *and the solution of LMIs given by the solver is:*

$$P = \begin{pmatrix} 0.267 & 0.0547 \\ 0.0547 & 0.031 \end{pmatrix}, \quad \Xi = \begin{pmatrix} 0.384 & -0.006 \\ -0.006 & 0.027 \end{pmatrix}.$$

Finally, we build an observer for states x_3 *and* x_4 *from the expression* $\omega = \Pi x + \Upsilon D_0 x$*:*

$$\hat{x}_3 = \frac{\omega_1 - \upsilon_1 x_1}{p_1} = \omega_1 + x_1,$$
$$\hat{x}_4 = \frac{\omega_2 - \upsilon_4 x_2}{p_4} = \omega_2.$$

Fig. 3.8 demonstrates the convergence of the observer for unmeasured states, which successfully reduces the dimension of the observation problem from 4 to 2, in the considered case.

Example 6. *Consider the nonlinear regression equation* (3.50) *with* $d(t) = 0.1 \begin{pmatrix} \sin(t) & \sin(2t) \end{pmatrix}$, $t \in \mathbb{R}_+$*, error* $v \equiv 0$ *and:*

$$J(t) = \begin{pmatrix} 1 & \sin(t) \end{pmatrix}, \quad D_1(t) = \sin^2(5t), \quad f(t) = \arctan(t)$$

for $t \in \mathbb{R}_+$*, and constant parameters* $x(0) = \begin{pmatrix} 3 & 5 \end{pmatrix}^\top$ *to estimate. Then we build an observer of the form* (3.49)*, with* $\gamma = 0.75$*, and the conditions of the Theorem 3.3.3 are satisfied. Fig. 3.9 demonstrates the convergence of the estimates* $\omega(t)$ *to the time-varying parameter* $x(t)$*.*

Example 7. *Consider a discrete benchmark dataset from the example of Weisberg, 2005 which represents a so-called "sniffer", which measures the captured amount of hydrocarbon vapors* y_k *in the devices, specifically*

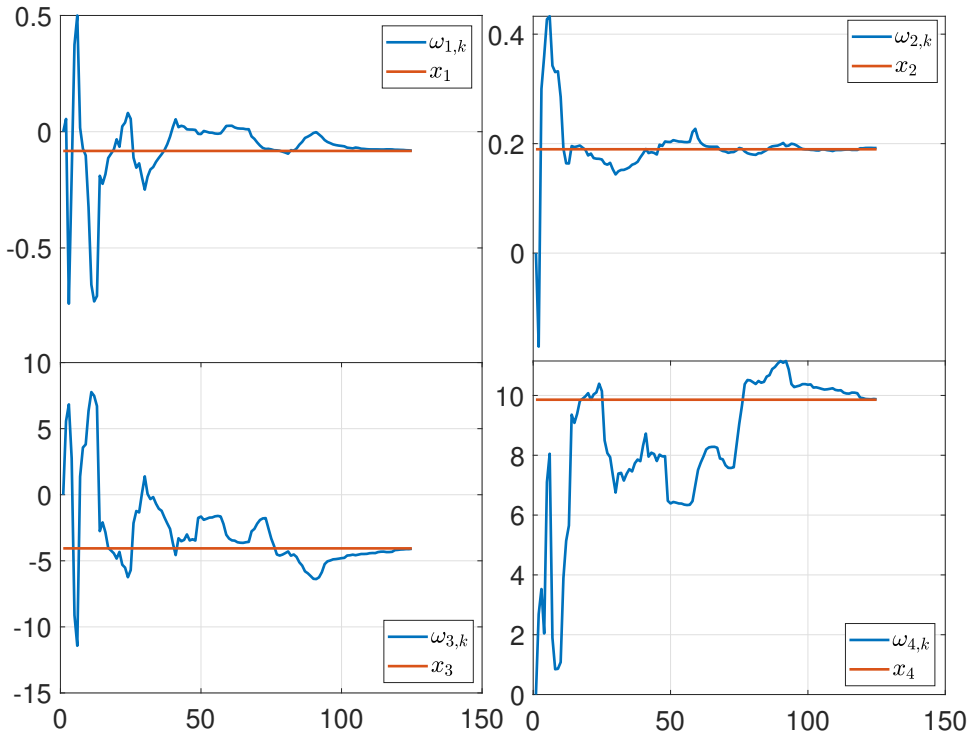

FIGURE 3.10: Parameter's convergence for Example 7. Real parameters in red, estimated parameters in blue

installed for this task into gasoline tanks. The dataset represents the laboratory experiment, controlling four different predictors: $a_{1,k}$ *as initial tank temperature,* $a_{2,k}$ *as gas temperature,* $a_{3,k}$ *as tank pressure and gas pressure* $a_{4,k}$*. To this end, the data can be represented as a linear regression equation* $y_k = a_{1,k}x_1 + a_{1,k}x_2 + a_{1,k}x_3 + a_{1,k}x_4$*, with parameters* x_1, x_2, x_3, x_4 *to be estimated.*

Set $D_{0,k} = \begin{pmatrix} a_{1,k} & a_{2,k} & a_{3,k} & a_{4,k} \end{pmatrix}$*, then the parameter observer take the form (.3), which leads us to the estimator. In general, there is no unique or optimal way to define* Γ_k*, the choice has to depend on the regression method. Therefore, let us apply the Recursive Least-Squares algorithm [Ljung, 1999]. We can define*

$$\Gamma_k := \left(\sum_{i=0}^{k} D_{0,i}^{\top} D_{0,i} \right)^{-1}, \tag{3.61}$$

then the final expression for the estimator will be as

$$\omega_{k+1} = \omega_k + \left(\sum_{i=0}^{k} D_{0,i}^{\top} D_{0,i} \right)^{-1} D_{0,k}^{\top} (y_k - D_{0,k}\omega_k). \tag{3.62}$$

Fig. 3.10 and 3.11 demonstrate the convergence of the estimator to the ideal parameters, obtained by a more sophisticated algorithm [Weisberg, 2005]. Of course, it is possible to improve the performance of the regression in different ways, but the point of this example is to show the applicability of the theory, presented in the manuscript.

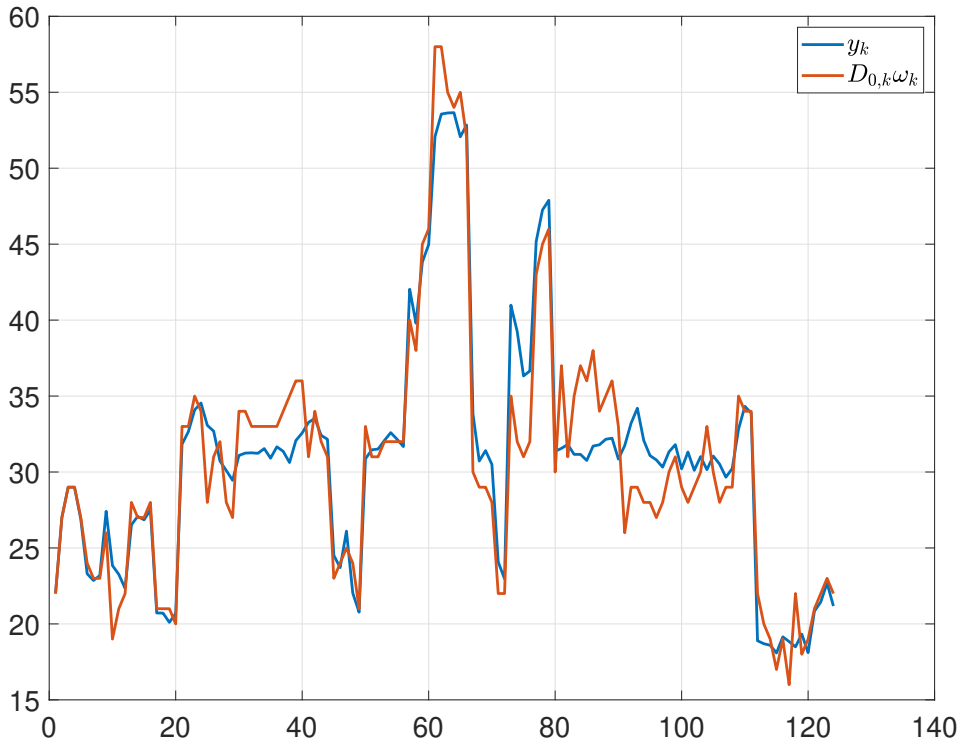

FIGURE 3.11: Given signal (blue) and estimated signal (red) for Example 7

Chapter 4

Design of reduced-order observers and regulators using nonlinear steady-state mapping

4.1 Introduction

In this chapter, we go back to a more classical problem statement of the output regulation theory, illustrated in Fig. 4.1. In the system Σ_1, there is no linear part in dynamics, which dominates the equation (which was considered in the previous chapter), but only a nonlinear function. Moreover, the system Σ_2 does not have to be of the same class as Σ_1 and does not take input from Σ_1. The system Σ_2 only generates the input, namely: it is a signal generator (or exosystem). These considerations do not make the mapping π necessarily linear since the PDE (1.9) cannot be transformed in an LME. However, this chapter aims to show that the nonlinear steady-state response as a solution of the PDE, can be found analytically for certain classes of systems.

More precisely, this chapter addresses the problem of finding the steady-state response for particular types of nonlinear systems inspired by recursive procedures, such as *backstepping* and *forwarding* [Sepulchre, Janković, and Kokotović, 1997] (See Section 4.2). Namely, we propose a way of determining steady-state solutions for systems based on the diagonal structure of its model.

The main idea of backstepping, introduced in [Kokotovic, 1992], consists of using the lower-triangular form of a system to make a step-by-step output passivation through time-derivative, starting from the first equation to the last one, where the stabilizing input is designed (*e.g.*, see [Nizami, Chakravarty, and Mahanta, 2017, Krishnamurthy, Khorrami, and Chandra, 2003, Haizhou et al., 2005, Kim and Kim, 2003]). Forwarding is a more recent method of stabilization [Sepulchre, Jankovic, and Kokotovic, 1997], which utilizes the upper-triangular form of systems. It has a similar iterative idea to backstepping, which works in the opposite direction: it uses the integration starting from the input and going forward (*e.g.*, see [Zhang et al., 2011, Boeren, Bruijnen, and Oomen, 2017]). *Interlaced systems* introduced in [Sepulchre, Janković, and Kokotović, 1997] combine both types of triangular dynamics in their subsystems. It is a large class of models that have restrictions only on the structure of their feedback and feedforward interconnections.

In this chapter, we use techniques similar to backstepping and forwarding to derive the steady-state solutions of such an interlaced system. One of our goals is to design a robust reduced-order observer with the

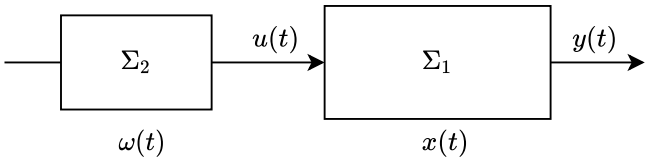

$$t \to \infty, x(t) \to \pi(\omega(t))$$

FIGURE 4.1: Connected systems

corresponding input to the system. This result could significantly improve the observer design for the considered classes of nonlinear systems without the hypothesis about uniform observability.

The outline of the chapter is as follows. First, the methods for analytical calculation of the steady-state solutions for two types of canonical forms of nonlinear systems are presented in Section 4.3. The observer design is then given in Section 4.4. In Section 4.5, the efficiency of the proposed solutions is illustrated in two examples.

4.2 Problem statement

Consider an interconnection of two nonlinear systems one of which is in a form similar to (1.1) but with disturbance and measurement noise, and the second one being (1.7):

$$\begin{cases} \dot{x} = F(x) + G(x,u) + d, \\ y = h(x) + v; \end{cases} \tag{4.1}$$

where $F : \mathbb{R}^n \to \mathbb{R}^n$ and $G : \mathbb{R}^n \times \mathbb{R} \to \mathbb{R}^n$ are smooth or real analytic maps, and the remaining functions are as in (1.1) with $m = 1$; $F(0) = 0$, $G(\cdot, 0) = 0$; $d \in \mathcal{L}_\infty^n$ is an unknown essentially bounded disturbance, $v \in \mathcal{L}_\infty^p$ is a measurement noise signal.

This chapter aims to design a robust reduced-order observer for classes of lower- or upper-triangular functions F and G in (4.1) using tools from the moment theory for nonlinear systems. The derived expressions of steady-state solutions will be used next to propose a robust reduced-order observer to reconstruct the state of (4.1), (1.7). We also assume that the form of the input signal ℓ can be chosen to ensure observability or detectability of (4.1), (1.7).

4.3 The steady-state response of Feedback and Feedforward systems in a disturbance-free case

Two particular classes of F and G are studied in this section.

4.3.1 Feedback (lower-triangular form) case

A particular case of (4.1) is given by a nonlinear single-input system in the canonical feedback form ($d = 0$):

$$\begin{aligned} \dot{z} &= \eta(z, \xi_1), && (4.2)\\ \dot{\xi}_1 &= f_1(\xi_1, z) + g_1(\xi_1, z)\xi_2, && (4.3)\\ &\vdots \\ \dot{\xi}_{\nu-1} &= f_{\nu-1}(\underline{\xi}_{\nu-1}, z) + g_{\nu-1}(\underline{\xi}_{\nu-1}, z)\xi_\nu && (4.4)\\ \dot{\xi}_\nu &= f_\nu(\xi, z) + g_\nu(\xi, z)u, && (4.5) \end{aligned}$$

with the same signal generator system as in (1.7), where $z : \mathbb{R}_+ \to \mathbb{R}^r$ is the zero dynamics state, $\xi = (\xi_1 \ \dots \ \xi_\nu)^\top \in \mathbb{R}^\nu$ and $x = (z^\top \ \xi^\top)^\top \in \mathbb{R}^{\nu+r}$, $n = \nu + r$; and the functions $\eta : \mathbb{R}^{r+1} \to \mathbb{R}^r$, $f_i, g_i : \mathbb{R}^{r+i} \to \mathbb{R}$ for $i = 1, \dots, \nu$ are smooth. The conditions providing a representation of (4.1) in the form (4.2)-(4.5) can be checked in [Sepulchre, Janković, and Kokotović, 1997].

Remark that the input u of (4.2)-(4.5) appears solely in the state equation for ξ_ν. Hence, inspired by the backstepping idea, if $\xi_1 = \pi_1(\omega)$ is fixed, then an input function $\ell(\omega)$ can be designed in such a way that it assigns π_1 as the steady-state solution of this interconnected system. Thus, using the theory of output regulation, we can formulate the conditions for the existence of a steady-state solution for (1.7)-(4.5):

Proposition 4.3.1. *For any smooth function $\pi_1 : \mathbb{R}^q \to \mathbb{R}$, let a smooth function $\rho : \mathbb{R}^q \to \mathbb{R}^r$ be the steady-state solution of* (4.2) *under substitution $\xi_1 = \pi_1(\omega)$. Then there always exists the input function $\ell : \mathbb{R}^q \to \mathbb{R}$ such*

that $\pi(\omega) = (\pi_1(\omega) \ \dots \ \pi_\nu(\omega))^\top$ *is the steady-state solution of the interconnected system* (1.7)-(4.5) *provided that* $g_i(\underline{\pi}_i(\omega), \rho(\omega)) \neq 0$ *for all* $i = 1, \dots, \nu$ *and* $\omega \in \mathbb{R}^q$.

Proof. We can set $\xi_1 = \pi_1(\omega)$, which is the first steady-state solution of the system (4.5), then $z = \rho(\omega)$ is the corresponding steady-state of the zero dynamics (4.2). To find the remaining components of π and the respective input function ℓ, let us use the output regulation theory, which states that the equation (1.9) must be satisfied. Consequently, we obtain

$$\begin{aligned}
\frac{\partial \pi_1(\omega)}{\partial \omega} s(\omega) &= f_1(\pi_1(\omega), \rho(\omega)) + g_1(\pi_1(\omega), \rho(\omega))\pi_2(\omega), \\
&\vdots \\
\frac{\partial \pi_{\nu-1}(\omega)}{\partial \omega} s(\omega) &= f_{\nu-1}(\underline{\pi_{\nu-1}}(\omega), \rho(\omega)) + g_{\nu-1}(\underline{\pi_{\nu-1}}(\omega), \rho(\omega))\pi_\nu(\omega), \\
\frac{\partial \pi_\nu(\omega)}{\partial \omega} s(\omega) &= f_\nu(\pi(\omega), \rho(\omega)) + g_\nu(\pi(\omega), \rho(\omega))\ell(\omega).
\end{aligned}$$

Since the considered form of (4.5) is lower-triangular (feedback based), and only the last equation depends on the input, the components π_i and the input ℓ can be found step by step from the top system as follows:

$$\begin{aligned}
\pi_2(\omega) &= \frac{\frac{\partial \pi_1(\omega)}{\partial \omega} s(\omega) - f_1(\pi_1(\omega), \rho(\omega))}{g_1(\pi_1(\omega), \rho(\omega))}, \\
&\vdots \\
\pi_\nu(\omega) &= \frac{\frac{\partial \pi_{\nu-1}(\omega)}{\partial \omega} s(\omega) - f_{\nu-1}(\underline{\pi_{\nu-1}}(\omega), \rho(\omega))}{g_{\nu-1}(\underline{\pi_{\nu-1}}(\omega), \rho(\omega))}, \\
u = \ell(\omega) &= \frac{\frac{\partial \pi_\nu(\omega)}{\partial \omega} s(\omega) - f_\nu(\pi(\omega), \rho(\omega))}{g_\nu(\pi(\omega), \rho(\omega))},
\end{aligned}$$

where $g_i(\underline{\pi}_i(\omega), \rho(\omega)) \not\equiv 0$ according to the imposed conditions. □

Note that the conditions of Proposition 4.3.1 do not imply any attractivity of the derived steady-state solution $x(t) = \pi(\omega(t))$ for (1.7)-(4.5), only its existence is established.

Remark 4.3.1. *In Proposition 4.3.1, it is assumed that the zero dynamics has a well-defined respective steady-state solution* ρ. *Such an additional hypothesis has a counterpart in the backstepping method, where for the system stabilization, it is usually assumed that the zero dynamics is input-to-state stable [Sepulchre, Janković, and Kokotović, 1997]. Here, to find steady-state solutions for* ξ, *we need to settle the same property for* z.

4.3.2 Feedforward (upper-triangular form) case

Let us consider a nonlinear single-input system in the feedforward canonical form ($d = 0$) [Sepulchre, Janković, and Kokotović, 1997]:

$$\begin{aligned}
\dot{\zeta}_1 &= \widetilde{f}_1(\zeta_1) + \widetilde{g}_1(\overline{\zeta}_2, z, u), && (4.6) \\
&\vdots \\
\dot{\zeta}_{\mu-1} &= \widetilde{f}_{\mu-1}(\zeta_{\mu-1}) + \widetilde{g}_{\mu-1}(\zeta_\mu, z, u), && (4.7) \\
\dot{\zeta}_\mu &= \widetilde{f}_\mu(\zeta_\mu) + \widetilde{g}_\mu(u) && (4.8) \\
\dot{z} &= \widetilde{\eta}(z, \zeta_\mu, u) && (4.9)
\end{aligned}$$

with the same signal generator (1.7), where $z : \mathbb{R}_+ \to \mathbb{R}^r$ is the zero dynamics state, $\zeta = \begin{pmatrix} \zeta_1 & \dots & \zeta_\mu \end{pmatrix}^\top \in \mathbb{R}^\mu$ and $x = (z^\top \ \zeta^\top)^\top$, $n = \mu + r$; the functions $\widetilde{\eta} : \mathbb{R}^{r+2} \to \mathbb{R}^r$, $\widetilde{f}_i : \mathbb{R} \to \mathbb{R}$ and $\widetilde{g}_i : \mathbb{R}^{\mu-i+r+1} \to \mathbb{R}$ are real analytic for

$i = 1, \ldots, \mu$ taking zero value for zero argument. Due to the upper-triangular structure of the system (4.6)-(4.9), the control propagates from the last equation for ζ_μ till ζ_1, allowing the steady-state solutions to be iteratively calculated. For instance, the equation (1.9) for the variable ζ_μ can be written as follows:

$$\frac{\partial \pi_\mu(\omega)}{\partial \omega} s(\omega) = \widetilde{f}_\mu(\pi_\mu(\omega)) + \widetilde{g}_\mu(\ell(\omega)) \tag{4.10}$$

provided that the control signal $u = \ell(\omega)$ is fixed (for a real analytic function ℓ). For a given s and any initial condition $\omega(0) \in \Gamma = \{w \in \mathcal{W} : w_q = 0\}$, where $\mathcal{W} \subset \mathbb{R}^q$ is a neighborhood of the origin, the signal generator (1.7) has a solution ω that is defined at least locally in time. Assuming that

$$\forall \omega \in \Gamma \setminus \{0\} : s_q(\omega) \neq 0, \tag{4.11}$$

there is a real analytic solution $\pi_\mu : \mathcal{W} \to \mathbb{R}$ of the output regulation equation (4.10) according to Theorem 1.3.1 (since (4.11) implies that (4.10) can be completed by initial conditions making this Cauchy problem non-characteristic). The same procedure can be repeated/forwarded for the rest of the system:

Proposition 4.3.2. *Let* (4.11) *be satisfied. For any real analytic* $\ell : \mathbb{R}^q \to \mathbb{R}$*, let* π_μ *be a solution of* (4.10) *and* $\rho : \mathbb{R}^q \to \mathbb{R}^r$ *be the steady-state solution of* (4.9) *under substitution* $\zeta_\mu = \pi_\mu(\omega)$ *and* $u = \ell(\omega)$*. Then there exists a real analytic steady-state mapping* $\pi(\omega) = \begin{pmatrix}\pi_1(\omega) & \ldots & \pi_\mu(\omega)\end{pmatrix}^\top$*,* $\omega \in \mathcal{W}$*, of the interconnected system* (1.7),(4.6)-(4.9) *with* $\pi(0) = 0$*.*

Proof. By choosing $\ell(\omega)$ such that $\pi_\mu(\omega)$ satisfies (4.10), we obtain $\rho(\omega)$ from (4.9). For the remaining $\pi_i(\omega)$, $i = 1, \ldots, \mu - 1$, we have the following equations from (1.9):

$$\begin{aligned}
\frac{\partial \pi_1(\omega)}{\partial \omega} s(\omega) &= \widetilde{f}_1(\pi_1(\omega)) + \widetilde{g}_1(\overline{\pi}_2(\omega), \rho(\omega), \ell(\omega)), \\
&\vdots \\
\frac{\partial \pi_{\mu-2}(\omega)}{\partial \omega} s(\omega) &= \widetilde{f}_{\mu-2}(\pi_{\mu-2}(\omega)) + \widetilde{g}_{\mu-2}(\overline{\pi}_{\mu-1}(\omega), \rho(\omega), \ell(\omega)), \\
\frac{\partial \pi_{\mu-1}(\omega)}{\partial \omega} s(\omega) &= \widetilde{f}_{\mu-1}(\pi_{\mu-1}(\omega)) + \widetilde{g}_{\mu-1}(\pi_\mu(\omega), \rho(\omega), \ell(\omega)),
\end{aligned}$$

which all yield the form of (4.10) and the same condition of being non-characteristic for the initial values $\pi_i(\omega) = 0$ for $\omega \in \Gamma$ (since the system is in the upper-triangular form, $\pi_1(\omega), \ldots, \pi_{\mu-1}(\omega)$ can be found iteratively from the last equation to the first). Then, according to Theorem 1.3.1, these first order quasi-linear PDEs have unique analytic solutions $\pi_i : \mathcal{W} \to \mathbb{R}$, $i = 1, \ldots, \mu - 1$. □

Here again, we need to assume the existence of the steady-state solution ρ for the zero dynamics (4.9), while in the forwarding method, the input-to-state stability hypothesis is used (compare to Remark 4.3.1 for the lower-triangular case). Similarly, Proposition 4.3.2 establishes the existence of the steady-state solutions, but not their attractiveness to surrounding solutions.

4.4 Reduced-order observer design

To show the utility of the presented results to the analytical derivation of a steady-state solution, consider the problem of state estimation for a nonlinear system. The considered model is a combination of both studied

systems, the upper- and the lower-triangular ones (with disturbances d_i, v):

$$\begin{aligned}
\dot\zeta_1 &= \widetilde{f}_1(\zeta_1)+\widetilde{g}_1(\overline{\zeta}_2,z)+d_1,\\
&\vdots\\
\dot\zeta_{\mu-1} &= \widetilde{f}_{\mu-1}(\zeta_{\mu-1})+\widetilde{g}_{\mu-1}(\overline{\zeta}_\mu,z)+d_{\mu-1},\\
\dot\zeta_\mu &= \widetilde{f}_\mu(\zeta_\mu)+\widetilde{g}_\mu(\xi_1,z)+d_\mu \qquad (4.12)\\
,\dot\xi_1 &= f_1(\underline{x}_{\mu+1},z)+g_1(\underline{x}_{\mu+1},z)\xi_2+d_{\mu+1},\\
\dot\xi_2 &= f_2(\underline{x}_{\mu+2},z)+g_2(\underline{x}_{\mu+2},z)\xi_3+d_{\mu+2}, \qquad (4.13)\\
&\vdots\\
\dot\xi_{\nu-1} &= f_{\nu-1}(\underline{x}_{\mu+\nu-1},z)+g_{\nu-1}(\underline{x}_{\mu+\nu-1},z)\xi_\nu+d_{\mu+\nu-1},\\
\dot\xi_\nu &= f_\nu(x,z)+g_\nu(x,z)u+d_{\mu+\nu},\\
\dot z &= \eta(z,\xi_1),\\
y &= h(z,x)+v.
\end{aligned}$$

A system in such a form is called interlaced. Variables $\zeta\in\mathbb{R}^\mu$ correspond to the state of the upper-triangular part, variables $\xi\in\mathbb{R}^\nu$ describe the state of the lower-triangular part; $x=(\zeta^\top\ \xi^\top)^\top\in\mathbb{R}^n$ and $n=\mu+\nu$, $z\in\mathbb{R}^r$ is the state of zero dynamics; $y\in\mathbb{R}^p$ is the output available for measurements. We assume that all nonlinear functions in (4.13) satisfy the requirements on regularity needed to use propositions 4.3.1 and 4.3.2, *i.e.*, they all are real analytic and admit the zero solution, h is globally Lipschitz continuous. The signal generator is considered in the linear form to simplify the observer design:

$$\dot\omega = A\omega,\ u=\ell(\omega), \qquad (4.14)$$

where as before $\omega:\mathbb{R}_+\to\mathbb{R}^q$, a neutrally stable matrix $A\in\mathbb{R}^{q\times q}$ is chosen in a way that the condition (4.11) is satisfied:

$$\forall\omega\in\Gamma\setminus\{0\}:[0\dots0\ 1]A\omega\neq0. \qquad (4.15)$$

Our goal is to design a robust reduced-order observer for (4.13), (4.14) using steady-state solutions $\pi(\omega)$ and $\rho(\omega)$, as established before and assuming that they describe the steady-state solutions of this system. Note that there is no restriction imposed on the uniform observability of (4.13) (*i.e.*, observability for all admissible inputs u). We assume below that the input function ℓ is properly set to ensure state estimation. In such a setup, it is enough to design an observer for the generator (4.14) and calculate the asymptotic estimates of the steady-state solutions.

Thus, we start with the next hypothesis:

Assumption 4.4.1. *Assume*

1. *the condition* (4.15) *holds;*
2. *for any real analytic* $\pi_{\mu+1}:\mathbb{R}^q\to\mathbb{R}$ *there is the corresponding steady-state solution* $\rho:\mathbb{R}^q\to\mathbb{R}^r$ *of the zero dynamics under substitution* $\xi_1=\pi_{\mu+1}(\omega)$.

Under Assumption 4.4.1, the conditions of propositions 4.3.1 and 4.3.2 are satisfied for the system (4.13), (4.14), with $d=0$. Due to the structure of (4.13), for any $\pi_{\mu+1}$ and the related ρ, the steady-state solution $\underline{\pi}_\mu$ can be derived following the forwarding guidelines in the proof of Proposition 4.3.2. Next, the steady-state solution $\overline{\pi}_{\mu+2}$ can be calculated following the backstepping procedure of Proposition 4.3.1, together with the input function $\ell:\mathbb{R}^q\to\mathbb{R}$. Thus, all steady-state solutions $\pi:\mathbb{R}^q\to\mathbb{R}^n$ can be derived, for which we assume the following:

Assumption 4.4.2. *Let* 1) *the function* $\pi_{\mu+1}$ *be chosen such that* $h(\rho(\omega),\pi(\omega))=C\omega$, *where the pair* (A,C) *is detectable;*

2) *the system* (4.13) *be δISS for* $u = \ell(\omega)$*, for any solution* ω *of* (4.14) *with respect to the input* d*.*

Under these restrictions, the following theorem formulates the main result of the chapter:

Theorem 4.4.1. *Let assumptions 4.4.1, 4.4.2 be satisfied,* $u = \ell(\omega)$*, and suppose there exist* $P = P^\top \in \mathbb{R}^{q\times q}$*,* $Q = Q^\top \in \mathbb{R}^{q\times q}$*,* $\Gamma = \Gamma^\top \in \mathbb{R}^{p\times p}$ *and* $U \in \mathbb{R}^{q\times p}$ *such that the linear matrix inequalities*

$$P > 0, \quad Q > 0, \quad \Gamma > 0,$$
$$\begin{pmatrix} A^\top P - C^\top U^\top + PA - UC + Q & -U \\ -U^\top & -\Gamma \end{pmatrix} \leq 0$$

have a solution. Then

$$\dot{\hat{\omega}} = A\hat{\omega} + L(y - C\hat{\omega}), \quad \hat{x} = \pi(\hat{\omega}), \quad \hat{z} = \rho(\hat{\omega}) \tag{4.16}$$

is a global robust asymptotic reduced-order observer for the system (4.13), (4.14) *with* $L = P^{-1}U$*, where* $\hat{\omega}(t) \in \mathbb{R}^q$*,* $\hat{x}(t) \in \mathbb{R}^n$ *and* $\hat{z}(t) \in \mathbb{R}^r$ *are the estimates of* $\omega(t)$*,* $x(t)$ *and* $z(t)$*, respectively.*

Proof. According to Assumption 4.4.1, the system (4.13) has steady-state solutions π and ρ for any $\pi_{\mu+1}$ with the corresponding input ℓ (by propositions 4.3.1 and 4.3.2). Assumption 4.4.2 states that the function $\pi_{\mu+1}$ was selected in a way that the measured output y is a linear function of the generator state ω while being projected on the steady-state solution, and in addition, $\pi(\omega)$ and $\rho(\omega)$ are steady-state solutions to which $x(t)$ and $z(t)$ converge when $t \to +\infty$, respectively, for the assigned input $u = \ell(\omega)$. Therefore, we can write that we measure $y = C\omega + \varepsilon + v$, where $\varepsilon : \mathbb{R}_+ \to \mathbb{R}^p$ is a bounded error representing the convergence of solutions of (4.13) to the steady-state ones, $\varepsilon = h(z,x) - h(\rho(\omega),\pi(\omega))$. To analyze the behavior of $e = \omega - \hat{\omega}$, whose dynamics take the form:

$$\dot{e} = (A - LC)e + L(\varepsilon + v),$$

let us select a quadratic Lyapunov function candidate $V(e) = e^\top Pe$, where P is given in a formulation of the theorem. Denote $\widetilde{v} = \varepsilon + v$, then we have:

$$\dot{V} = \begin{pmatrix} e \\ \widetilde{v} \end{pmatrix}^\top \begin{pmatrix} A^\top P - C^\top U^\top + PA - UC + Q & -U \\ -U^\top & -\Gamma \end{pmatrix} \begin{pmatrix} e \\ \widetilde{v} \end{pmatrix} - e^\top Qe + \widetilde{v}^\top \Gamma \widetilde{v}.$$

According to the formulation of the theorem, the matrix above is non-positive. Then, we obtain:

$$\dot{V} \leq -e^\top Qe + \widetilde{v}^\top \Gamma \widetilde{v}.$$

After straightforward calculations, we can obtain the estimate on the behavior of e as follows:

$$\|e(t)\| \leq \sqrt{\frac{\lambda_{\min}(P)}{\lambda_{\max}(P)}} e^{-0.5\frac{\lambda_{\min}(Q)}{\lambda_{\max}(P)}t} \|e(0)\| + \sqrt{\frac{\lambda_{\max}(\Gamma)\lambda_{\max}(P)}{\lambda_{\min}(P)}} \|\widetilde{v}\|_\infty.$$

The error ε possesses an estimate from Definition 1.3.7

$$\|\varepsilon(t)\| \leq \beta(\|\varepsilon(0)\|, t) + \gamma(\|d\|_\infty),$$

for any $\varepsilon(0) \in \mathbb{R}^n$ and d, for some $\beta \in \mathcal{KL}$ and $\gamma \in \mathcal{K}$ and the disturbance d is considered to be essentially bounded. Therefore the error e is ISS with respect to $\widetilde{v}$,[Sontag and Wang, 1995,Sontag and Wang, 2000]. Then, the estimation for x and z can be chosen as in (4.16). □

4.5 Examples

Two examples are given to illustrate the considered problematics.

Example 8. Interlaced system (academic example). *Consider the following interconnected dynamics:*

$$\begin{cases} \dot{x}_1 = -x_1 + x_2^2 x_3 + d, \\ \dot{x}_2 = -x_2 + x_3 + d, \\ \dot{x}_3 = -x_3^3 + x_4 + d, \\ \dot{x}_4 = -x_4 + (1 + x_3^2)u + d, \\ y = x_3 + v, \end{cases} \qquad \begin{cases} \dot{\omega}_1 = \omega_2, \\ \dot{\omega}_2 = -\omega_1, \\ u = \ell(\omega), \end{cases} \tag{4.17}$$

where $d(t) = 20\sin(100t)$, and v is a white noise signal. We can consider state x_3 as an internal input to the top subsystem (for (x_1, x_2)) from the bottom one (for (x_3, x_4)). The top subsystem is upper-triangular, which means that we can use the feedforward approach to find the steady-state solutions of the system by the procedure described above. Let us assign $x_3 = \omega_1$. Since the second equation is linear on both x_2 and x_3, we can present

$$x_2 \quad = \quad b_1\omega_1 + b_2\omega_2,$$

where b_1 and b_2 are the coefficients to be found. Then, substituting x_3 in the second equation,

$$b_1\omega_2 - b_2\omega_1 = -(b_1\omega_1 + b_2\omega_2) + \omega_1,$$

we obtain the values for b_1 and b_2:

$$b_1 = \frac{1}{2},\ b_2 = -\frac{1}{2}.$$

Next, we substitute x_2 and x_3 in the first equation, and we can see that the dependence of x_1 on ω is cubic. Hence, we can present x_1 as a cubic polynomial:

$$x_1 \quad = \quad a_1\omega_1^3 + a_2\omega_2^3 + a_3\omega_1^2\omega_2 + a_4\omega_2^2\omega_1,$$

where the coefficients a_i can be calculated solving the corresponding system of linear equations

$$\left(a_1 - a_3 - \frac{1}{4}\right)\omega_1^3 + (a_2 + a_4)\omega_2^3 + \left(3a_1 - 2a_4 + a_3 + \frac{1}{2}\right)\omega_1^2\omega_2 + \left(2a_3 - 3a_2 + a_4 - \frac{1}{4}\right)\omega_2\omega_1^2 = 0,$$

which leads to the following values:

$$a_1 = \frac{1}{40},\ a_2 = -\frac{7}{40},\ a_3 = -\frac{9}{40},\ a_4 = \frac{7}{40}.$$

Therefore, according to Proposition 4.3.2, the steady-state solutions $x = \pi(\omega)$ for the feedforward subsystem is given by

$$\begin{aligned} \pi_2 &= \frac{1}{2}\omega_1 - \frac{1}{2}\omega_2, \\ \pi_1 &= \frac{1}{40}\omega_1^3 - \frac{7}{40}\omega_2^3 - \frac{9}{40}\omega_1^2\omega_2 + \frac{7}{40}\omega_2^2\omega_1. \end{aligned}$$

After obtaining π_1, π_2, we can move to the feedback subsystem (x_3, x_4). To find π_3 and π_4, we use Proposition 4.3.1. Recall that $x_3 = \pi_3(\omega) = \omega_1$, using the PDE (1.9) *for the third equation we can easily find π_4:*

$$\pi_4 \quad = \quad \omega_2 + \omega_1^3.$$

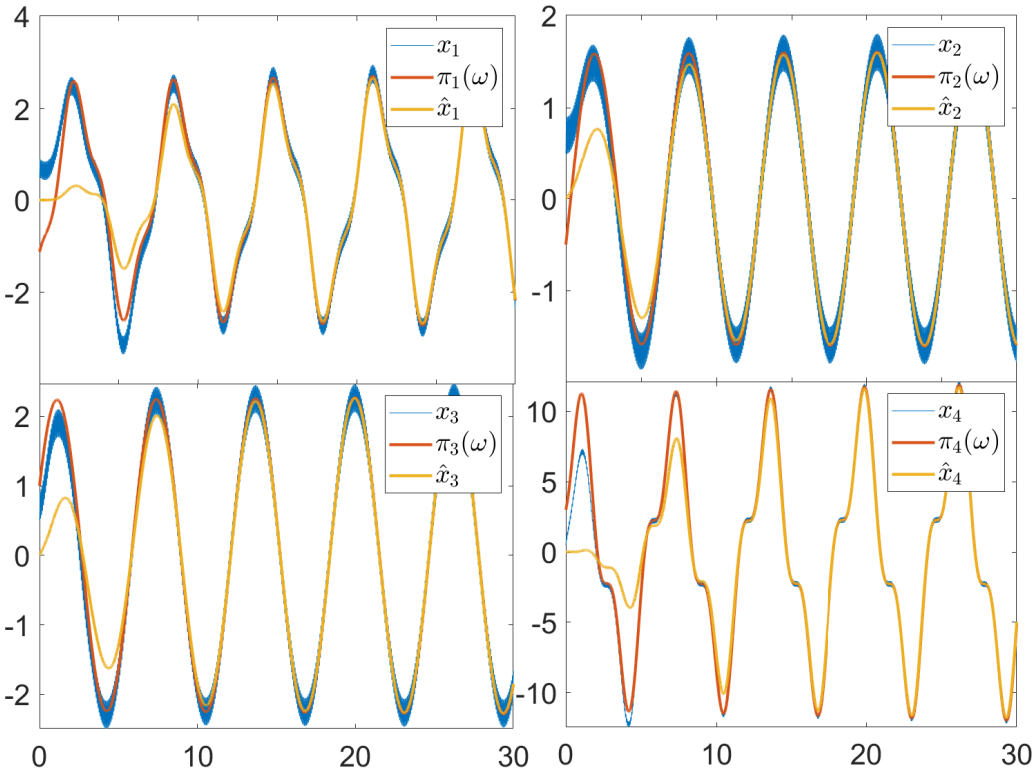

FIGURE 4.2: Simulation results for Example 8. Initial conditions: $x_i(0) = 0.5, i = 1..4, \omega_1(0) = 1, \omega_2(0) = 2, \hat{\omega} = 0$;

Substituting it in (4.17) *gives us the form of the input, which is required for* π_3 *and* π_4 *to be steady-state solutions of the feedback subsystem:*

$$u = \frac{-\omega_1 + 3\omega_1^2\omega_2}{1+\omega_1^2}.$$

Finally, we have all the equations for the steady-state response of (4.17)*:*

$$\begin{aligned}
\pi_1 &= \frac{1}{40}\omega_1^3 - \frac{7}{40}\omega_2^3 - \frac{9}{40}\omega_1^2\omega_2 + \frac{7}{40}\omega_2^2\omega_1, \\
\pi_2 &= \frac{1}{2}\omega_1 - \frac{1}{2}\omega_2, \\
\pi_3 &= \omega_1, \\
\pi_4 &= \omega_2 + \omega_1^2.
\end{aligned}$$

Next, we can design the observer (4.16) *suggested by Theorem 4.4.1 (assuming all conditions of the theorem are satisfied). We have in this example:*

$$A = \begin{pmatrix} 0 & 1 \\ -1 & 0 \end{pmatrix} \quad C = \begin{pmatrix} 1 & 0 \end{pmatrix}$$

and we can find such L, P, Q *and* Γ *that* $A - LC$ *is Hurwitz and the LMIs in the theorem are satisfied. For instance:*

$$L = P^{-1}U = \begin{pmatrix} 0.6245 \\ 0.125 \end{pmatrix}, \quad P = \begin{pmatrix} 1.03 & -0.206 \\ -0.206 & 1.03 \end{pmatrix}, \quad \Gamma = 1.03, \quad Q = \begin{pmatrix} 0.412 & 0 \\ 0 & 0.206 \end{pmatrix}.$$

The steady-state response and the results of estimation for the system is shown in Fig. 4.2. As we can see,

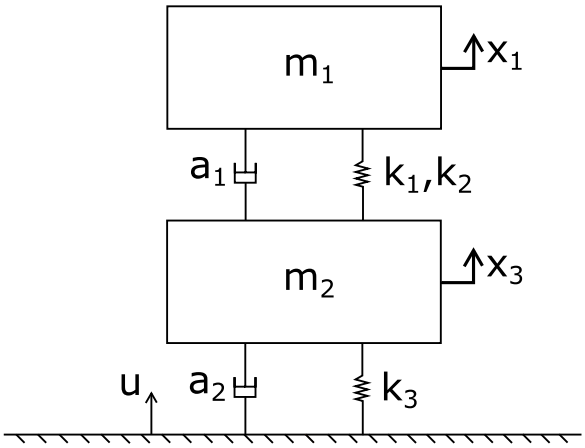

FIGURE 4.3: Schematics for Example 9

despite the uncertainties acting on the system, the estimates converge well to the region near the steady-state solution of the system and near the true state.

Example 9. Mass-spring system. *To demonstrate a rather practical application, consider a simple mechanical system of two masses connected vertically by a spring with nonlinear stiffness and a linear damper. The bottom mass is also attached to a fixed platform via spring with linear stiffness and a linear damper, and some perturbation u acts at bottom mass (Fig. 4.3). Then, the system dynamics will be as follows:*

$$\begin{cases} \dot{x}_1 = x_2, \\ \dot{x}_2 = -k_1(x_1 - x_3) - k_2(x_1 - x_3)^3 - a_1(x_2 - x_4), \\ \dot{x}_3 = x_4, \\ \dot{x}_4 = k_1(x_1 - x_3) + k_2(x_1 - x_3)^3 + a_1(x_2 - x_4) - k_3 x_3 - a_2 x_4 + u, \\ y = x_3 + v, \end{cases}$$

where x_1, x_2 are the position and velocity of a top mass, x_3, x_4 are the position and velocity of a second one, k_1, k_2, k_3 are the spring stiffness coefficients, a_1, a_2 are damper coefficients and an input u is some external force or disturbance, acting on a second mass.

Similar simplified representation can be applied, for example, to active suspension models [Kaddissi, Saad, and Kenne, 2009], where the top mass represents a quarter-car, and the bottom mass represents a tire, moving on some nonlinear (perturbed) road.

The task 2a). *Let us assume we want our bottom mass (tire) to follow a certain reference trajectory, produced by a simple signal generator (for example one with dynamics from the previous example) and we want to obtain a representation of our dynamics in terms of generator states ω_1, ω_2. This can be done by finding the proper input $u(\omega)$, using Propositions 4.3.1 and 4.3.2.*

However, the given system is not in the required interlaced form, and we need to do the substitution $y_1 = x_1$, $y_2 = x_2$, $y_3 = x_1 - x_3$, $y_4 = x_2 - x_4$. Then, we have following dynamics:

$$\begin{cases} \dot{y}_1 = y_2, \\ \dot{y}_2 = -k_1 y_3 - k_2 y_3^3 - a_1 y_4, \\ \dot{y}_3 = y_4, \\ \dot{y}_4 = +k_1 y_3 + k_2 y_3^3 + a_1 y_4 - k_3(y_1 - y_3) - a_2(y_2 - y_4) + u. \end{cases}$$

Now we can clearly see that the top subsystem is in upper-triangular form, which allows us to find $y_1(\omega)$ and $y_2(\omega)$ using Proposition 4.3.2, having only $y_3(\omega)$. Next logical step is to find $u(\omega)$ by a feedback-like procedure, using the Proposition 4.3.1.

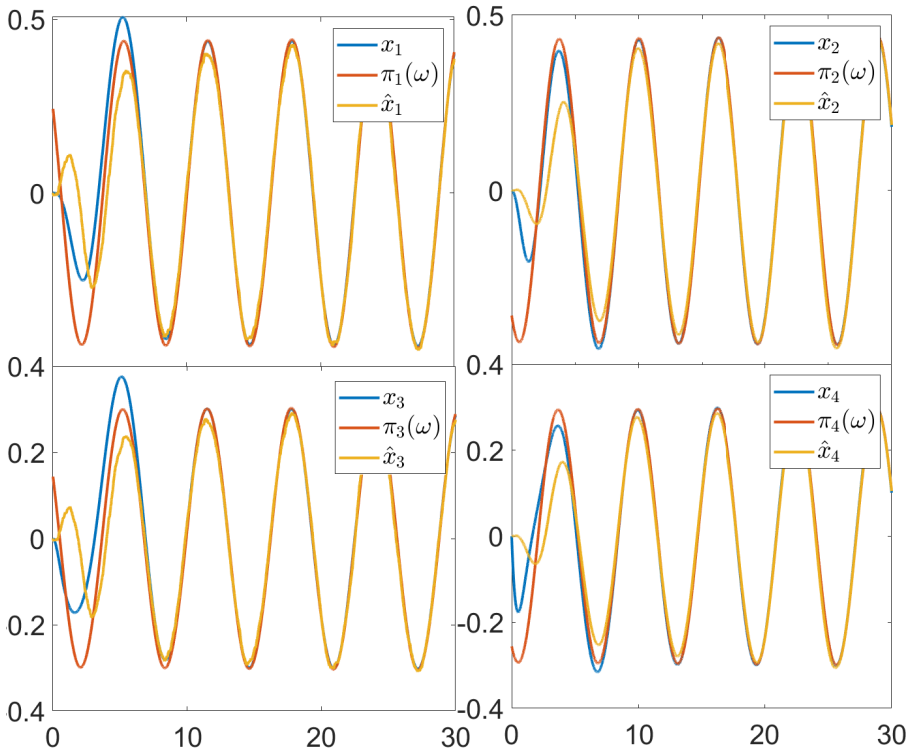

FIGURE 4.4: Simulation results for Example 9. Initial conditions: $x_i(0) = 0$; $\omega_1(0) = 0.1, \omega_2(0) = 0, \hat{\omega} = 0$. Coefficients: $k_1 = k_2 = 3, k_3 = 0.6, a_1 = 0.6, a_2 = 2$.

Therefore, let us assign $y_3(\omega) := \omega_1 + \omega_2$, *then* $y_4(\omega) = -\omega_1 + \omega_2$ *and substitute them in the equation for* y_2*:*

$$\dot{y}_2 = -k_1(\omega_1 + \omega_2) - k_2(\omega_1 + \omega_2)^3 - a_1(-\omega_1 + \omega_2).$$

Expressions for $y_1(\omega)$ *and* $y_2(\omega)$ *can be found by integrating the linear part* $\dot{y}_2^{\text{lin}} = \ddot{y}_1^{\text{lin}} = -k_1(\omega_1 + \omega_2) - a_1(-\omega_1 + \omega_2)$, *and for the nonlinear part by finding the coefficients of cubic function* $y_i(\omega) = y_i^{\text{lin}} + p_{i1}\omega_1^3 + p_{i2}\omega_1^2\omega_2 + p_{i3}\omega_1\omega_2^2 + p_{i4}\omega_2^3$, $i = 1, 2$. *For our case, the dynamics are as follows:*

$$y_1 = y_1^{\text{lin}} - k_2\left(\frac{4}{3}(\omega_2\omega_1^2 - \omega_1\omega_2^2) - \frac{11}{9}(\omega_1^3 + \omega_2^3)\right) := y_1^{\text{lin}} - k_2\tau_1,$$
$$y_2 = y_2^{\text{lin}} + k_2\left(\frac{4}{3}(\omega_1^3 + \omega_2^3) + (\omega_2\omega_1^2 + \omega_1\omega_2^2)\right) := y_2^{\text{lin}} + k_2\tau_2.$$

Next, we substitute $y_1(\omega)$, $y_2(\omega)$, $y_3(\omega)$ *in the equation for* y_4, *and* $u(\omega)$ *can be simply found as:*

$$u(\omega) = (\omega_1 + \omega_2)(1 - k_1(2 - k_3) - a_1a_2 - k_3) - 2k_2(\omega_1 + \omega_2)^3 + (\omega_1 - \omega_2)(a_1(2 - k_3) + a_2(1 - k_1)) - k_2k_3\tau_2 + k_2a_2\tau_1.$$

The final step to find $\pi(\omega)$ *is to go back to substitution, we have a steady-state solution* $\pi(\omega)$ *as follows:*

$$\begin{cases} \pi_1 = x_1(\omega) = \phi_1 \\ \pi_2 = x_2(\omega) = \phi_2 \\ \pi_3 = x_3 = y_1(\omega) - y_3(\omega) = y_1^{\text{lin}} - k_2\tau_1 - (\omega_1 + \omega_2) \\ \pi_4 = x_4 = y_2(\omega) - y_4(\omega) = y_2^{\text{lin}} + k_2\tau_2 - (\omega_2 - \omega_1) \end{cases}$$

Fig. 4.4 shows that the dynamics of x under chosen excitation input u indeed converges to a steady-state solution $\pi(\omega)$.

The task 2b)*. Let us assume that the system receives some reference signal u, which we do not measure and the system dynamics follows it. Instead, we measure the output of the initial system affected by some white measurement noise:* $Y = (x_1 - x_3) + v$*. Because of damping, our mechanical system is asymptotically stable and the signal generator oscillates, by design.*

The observer would take the form of (4.16)*, with the matrices A and C as follows:*

$$A = \begin{pmatrix} 0 & 1 \\ -1 & 0 \end{pmatrix}, \quad C = \begin{pmatrix} 1 & 1 \end{pmatrix}.$$

And we can find such L, P, Q *and* Γ *that* $A - LC$ *is Hurwitz and the LMIs in the theorem 4.4.1 are satisfied, for instance for*

$$L = \begin{pmatrix} 0.33 & 0.6 \end{pmatrix}^\top.$$

Fig. 4.4 shows the convergence of an observer to the given steady-state solution of the system.

Chapter 5

Conclusions and Future Work

5.1 Pointing Task

The results presented in Chapter 2 demonstrate the potential of the designed model and the tools for its identification. However, it leaves much room for improvement. Human motion dynamics are generally nonlinear and highly uncertain (it contains varying parameters, exogenous and endogenous perturbations). Hence, advanced robust-adaptive estimation and identification algorithms are essential in this domain, constituting a good benchmark for applying cut-edge technologies. A related issue is that a trade-off is necessary between the complexity and validity of the model used for estimation and the possibility of designing a corresponding observer procedure. For many existing pointing movement models, as in [Aranovskiy et al., 2020; Bullock and Grossberg, 1988; Meyer et al., 1988], it is challenging to design a reliable identification method (due to, for instance, the switched nature of the model and its nonlinearity). That is why in Chapter 2, we revisited the modeling theory for pointing and developed new tools for identification.

In Chapter 2, it has been observed that the identification based on a linear time-invariant second-order model does not work well in the high-velocity ballistic phase yet. This motivates proposing a switched model with different dynamics in the correction and ballistic phases. This model can be considered a simplified version of the one given by [Aranovskiy et al., 2020]. For the new model, the endpoint is well predicted at the velocity peak, but the idea of improving the correction phase dynamics to make it accurate even earlier is nevertheless relevant. How to correctly describe the ballistic phase in the model is a question for future research. For example, some interesting ideas were published recently in [Berret and Jean, 2020]. Using more data from trials of well-experienced users can help better understand the model's accuracy and limitations.

Another problem is the model's sensitivity to the data, which implies that sometimes the velocity profile requires an intensive tuning of the differentiator (thus, a high-frequency device should be acquired for better tuning). Although the velocity profile obtained from the differentiator is smooth enough, the acceleration is still noisy. Careful preliminary filtering of the sensor data may also improve accuracy.

The approach developed for the online identification of the pointing transfer function shows good performance, and increasing the degree of the polynomial applied for approximating the PTF leads to a more precise estimation. If more trials are used for the identification of the coefficients, then the better the accuracy.

Our identification framework's bottleneck is the necessity to measure or calculate the mouse velocity and acceleration. The homogeneous differentiator in [Perruquetti, Floquet, and Moulay, 2008] provides a relatively good solution to this problem. Also, instead of differentiating x_m or V_{mx}, it is appealing to use another sensor, like in [Antoine, Malacria, and Casiez, 2018] with an inertial accelerometer. This accelerometer can provide more precise data with a much higher frequency. For comparison, the mouse optical sensor can run up to 1 kHz, while even a cheap inertial accelerometer can write data with sampling up to 16 kHz. Then the only restriction would be the USB-port transmission capability. Fusing the two approaches can lead to better identification and noise reduction.

5.2 Estimation of Interconnected Systems

The second chapter of the thesis was dedicated to an estimation and control problem of certain classes of nonlinear systems. One of which being Persidskii systems and the second being interlaced systems.

Regarding Persidskii systems, it appears that under certain assumptions the steady-state of the interconnection is linear. In Section 3.2 of Chapter 3, using tools from nonlinear model reduction by moment matching, the steady-state solution of the interconnection of such systems was established. Having the derived expressions of invariant solutions and imposing conditions on their global or local attractiveness, a reduced-order observer and a trajectory tracking controller were designed, considering the additional disturbances. The presented framework allows a relaxation of the uniform observability condition to be achieved by setting up an appropriate input. The stability of the error dynamics in the ISS framework (concerning the measurement and state perturbations) was proven, where the conditions were constructively formulated using appropriate LMIs. Several examples illustrate the efficiency of our results.

In Chapter 3, Section 3.3, we simplify the design of reduced-order observers for a particular class of systems of the presence of disturbances, avoiding solutions of PDEs that arise in the conventional invariant manifold methodology (see [Astolfi and Ortega, 2003]). The resulting solution is explicit and more constructive than existing results on nonlinear observer design. We have shown two possible applications of our approach in discrete- and continuous-time cases: nonlinear robust reduced-order observer and a particular case of nonlinear regression. Two examples, one representing a mechanical system and another one being an academic case for nonlinear regression, demonstrated the applicability of our results in this work.

In Chapter 4, two particular forms of interconnected systems were investigated. The analytical expression for the steady-state solution in a disturbance-free scenario was found. Existence conditions for such solutions were provided, and the result was applied for a robust reduced-order observer design for an interlaced system. The main advantage of the suggested approach is the order reduction of the observer. Two examples were provided in Section 4.5.

Generally speaking, in chapters 3 and 4, the applicability conditions of many theories, such as nonlinear model reduction by moment matching, output regulation for nonlinear systems, invariant manifold approach, immersion & invariance, *etc*, were significantly simplified for two classes of nonlinear systems. To some degree, the theory was developed, regarding the case of the reciprocal interconnection of two systems. It shows the potential of this direction in the analysis, especially regarding the observer design, based on the steady-state.

All the examples presented in chapters 3 and 4 show the efficiency of the dynamical system analysis based on methods involving steady-state solutions. Especially when it is possible to provide the analytical solution for this mapping, connecting two interconnected systems. Despite the classes of systems being limited, most examples are based on the dynamical models, which describe real-life processes and mechanical systems, including the bioreactor model, electrical circuit, two-link robot manipulator, and mass-spring system imitating the quarter-car with the tire. The list is not exhaustive but rather demonstrative that the presented approach has a potential for practical implementation in many experimental setups and is relatively simple to execute.

The methods presented in this thesis can be applied to various estimation and control problems indicating the results' potential. Some are parameter identification, observer design (including the case without uniform observability), tracking control, and synchronization.

The main direction for further research is to explore other classes of nonlinear systems for which the propositions in chapters 3 and 4 can be extended, avoiding coupled functions, partial derivatives function inversions, and other rather complicated tools and replacing them with LMIs, matrix equations, and estimation algorithms.

Bibliography

Angeli, D. (2002). "A Lyapunov approach to incremental stability properties". In: *IEEE Transactions on Automatic Control* 47.3, pp. 410–421.

Antoine, Axel, Sylvain Malacria, and Géry Casiez (2018). "Using High Frequency Accelerometer and Mouse to Compensate for End-to-end Latency in Indirect Interaction". In: *Proceedings of the 2018 CHI Conference on Human Factors in Computing Systems*, pp. 1–11.

Aranovskiy, Stanislav et al. (2016). "Performance enhancement of parameter estimators via dynamic regressor extension and mixing". In: *IEEE Transactions on Automatic Control* 62.7, pp. 3546–3550.

Aranovskiy, Stanislav et al. (2020). "A switched dynamic model for pointing tasks with a computer mouse". In: *Asian Journal of Control* 22.4, pp. 1387–1400.

Arcak, M. and P. Kokotovic (2001). "Nonlinear observers: a circle criterion design and robustness analysis". In: *Automatica* 37.12, 1923–1930.

Asano, Takeshi et al. (2005). "Predictive interaction using the delphian desktop". In: *Proceedings of the 18th annual ACM symposium on User interface software and technology*, pp. 133–141.

Astolfi, A. (2010). "Model Reduction by Moment Matching for Linear and Nonlinear Systems". In: *Analysis and Design of Nonlinear Control Systems*, pp. 429–444.

Astolfi, A. and R. Ortega (2003). "Immersion and invariance: A new tool for stabilization and adaptive control of nonlinear systems". In: *IEEE Transactions on Automatic control* 48.4, pp. 590–606.

Bernard, O. et al. (2001). "Dynamical model development and parameter identification for an anaerobic wastewater treatment process". In: *Biotechnology and Bioengineering* 75.4, pp. 429–438.

Bernuau, Emmanuel et al. (2013). "Verification of ISS, iISS and IOSS properties applying weighted homogeneity". In: *Systems & Control Letters* 62.12, pp. 1159–1167.

Berret, Bastien and Frédéric Jean (2020). "Stochastic optimal open-loop control as a theory of force and impedance planning via muscle co-contraction". In: *PLoS computational biology* 16.2, e1007414.

Berret, Bastien et al. (2021). "Stochastic optimal feedforward-feedback control determines timing and variability of arm movements with or without vision". In: *PLOS Computational Biology* 17.6, e1009047.

Besançon, G. (2007). *Nonlinear observers and applications*. Vol. 363. Springer.

Bitmead, R (1984). "Persistence of excitation conditions and the convergence of adaptive schemes". In: *IEEE Transactions on Information Theory* 30.2, pp. 183–191.

Blanch, Renaud, Yves Guiard, and Michel Beaudouin-Lafon (2004). "Semantic pointing: improving target acquisition with control-display ratio adaptation". In: *Proceedings of the SIGCHI conference on Human factors in computing systems*, pp. 519–526.

Blanch, Renaud and Michaël Ortega (2009). "Rake cursor: improving pointing performance with concurrent input channels". In: *Proceedings of the SIGCHI Conference on Human Factors in Computing Systems*, pp. 1415–1418.

Boeren, F., D. Bruijnen, and T. Oomen (2017). "Enhancing feedforward controller tuning via instrumental variables: with application to nanopositioning". In: *International Journal of Control* 90.4, pp. 746–764. DOI: 10.1080/00207179.2016.1219921.

Boutayeb, M. and M. Darouach (2000). "A reduced-order observer for non-linear discrete-time systems". In: *Systems & control letters* 39.2, pp. 141–151.

Bryan, Wm. L. (1892). "On the Development of Voluntary Motor Ability". In: *The American Journal of Psychology* 5.2, pp. 125–204. ISSN: 00029556. URL: http://www.jstor.org/stable/1410865.

Bullock, Daniel and Stephen Grossberg (1988). "Neural dynamics of planned arm movements: emergent invariants and speed-accuracy properties during trajectory formation." In: *Psychological review* 95.1, p. 49.

Casiez, Géry and Nicolas Roussel (2011). "No more bricolage! Methods and tools to characterize, replicate and compare pointing transfer functions". In: *Proceedings of the 24th annual ACM symposium on User interface software and technology*, pp. 603–614.

Chair, Z. and P. K. Varshney (1986). "Optimal data fusion in multiple sensor detection systems". In: *IEEE Transactions on Aerospace and Electronic Systems* 1, pp. 98–101.

Chapuis, Olivier, Renaud Blanch, and Michel Beaudouin-Lafon (2007). "Fitts' law in the wild: A field study of aimed movements". In.

Chapuis, Olivier, Jean-Baptiste Labrune, and Emmanuel Pietriga (2009). "DynaSpot: speed-dependent area cursor". In: *Proceedings of the SIGCHI Conference on Human Factors in Computing Systems*, pp. 1391–1400.

Chua, L. O. (1994). "Chua's circuit: an overview ten years later". In: *Journal of Circuits, Systems and Computers* 04.02, pp. 117–159. DOI: 10.1142/S0218126694000090.

Costello, Richard Gray (1968). "The surge model of the well-trained human operator in simple manual control". In: *IEEE Transactions on Man-Machine Systems* 9.1, pp. 2–9.

Efimov, D., N. Barabanov, and R. Ortega (2019). "Robustness of linear time-varying systems with relaxed excitation". In: *International Journal of Adaptive Control and Signal Processing*.

Efimov, Denis and Alexander Aleksandrov (2019). "Robust stability analysis and implementation of Persidskii systems". In: *2019 IEEE 58th Conference on Decision and Control (CDC)*. IEEE, pp. 6164–6168.

— (2021). "On analysis of Persidskii systems and their implementations using LMIs". In: *Automatica* 134, p. 109905.

Evan, L. C. (2010). *Partial Differential Equations*. Second. Vol. 19.R. Graduate Series in Mathematics. AMS.

Feldman, Anatol G (1986). "Once more on the equilibrium-point hypothesis (λ model) for motor control". In: *Journal of motor behavior* 18.1, pp. 17–54.

Finsler, P. (1936/37). "Uber das Vorkommen definiter und semidefiniter Formen in Scharen quadratischer Formen." In: *Commentarii mathematici Helvetici* 9, pp. 188–192.

Fitts, Paul M (1954). "The information capacity of the human motor system in controlling the amplitude of movement." In: *Journal of experimental psychology* 47.6, p. 381.

Forgione, M. and D. Piga (2021). "Continuous-time system identification with neural networks: Model structures and fitting criteria". In: *European Journal of Control* 59, pp. 69–81.

Francis, B.A. and W.M. Wonham (1976). "The internal model principle of control theory". In: *Automatica* 12.5, pp. 457–465. ISSN: 0005-1098. DOI: https://doi.org/10.1016/0005-1098(76)90006-6.

Fridman, L. et al. (2008). "Higher-order sliding-mode observer for state estimation and input reconstruction in nonlinear systems". In: *International Journal of Robust and Nonlinear Control: IFAC-Affiliated Journal* 18.4-5, pp. 399–412.

Gallant, A. R. (1975). "Nonlinear regression". In: *The American Statistician* 29.2, pp. 73–81.

Gori, Julien and Olivier Rioul (2020). "A feedback information-theoretic transmission scheme (FITTS) for modeling trajectory variability in aimed movements". In: *Biological Cybernetics* 114.6, pp. 621–641.

Grossman, Tovi and Ravin Balakrishnan (2005). "The bubble cursor: enhancing target acquisition by dynamic resizing of the cursor's activation area". In: *Proceedings of the SIGCHI conference on Human factors in computing systems*, pp. 281–290.

Haizhou, P. et al. (2005). "Experimental validation of a nonlinear backstepping liquid level controller for a state coupled two tank system". In: *Control Engineering Practice* 13.1, pp. 27–40. ISSN: 0967-0661. DOI: https://doi.org/10.1016/j.conengprac.2003.12.019. URL: https://www.sciencedirect.com/science/article/pii/S0967066103002946.

Han, C.-K. and J.-D. Park (2015). "Quasi-linear systems of PDE of first order with Cauchy data of higher codimensions". In: *Journal of Mathematical Analysis and Applications* 430.1, pp. 390–402. DOI: https://doi.org/10.1016/j.jmaa.2015.04.081.

Hogan, Neville (1984). "An organizing principle for a class of voluntary movements". In: *Journal of neuroscience* 4.11, pp. 2745–2754.

Hourcade, Juan Pablo et al. (2010). "Pointassist for older adults: analyzing sub-movement characteristics to aid in pointing tasks". In: *Proceedings of the sigchi conference on human factors in computing systems*, pp. 1115–1124.

Housfater, A. S., X.-P. Zhang, and Y. Zhou (2006). "Nonlinear fusion of multiple sensors with missing data". In: *2006 IEEE International Conference on Acoustics Speech and Signal Processing Proceedings*. Vol. 4. IEEE, pp. IV–IV.

Howell, A. and J.K. Hedrick (2002). "Nonlinear observer design via convex optimization". In: *Proceedings of the 2002 American Control Conference (IEEE Cat. No.CH37301)*. Vol. 3, 2088–2093 vol.3. DOI: 10.1109/ACC.2002.1023944.

Isidori, A. and C. I. Byrnes (1990). "Output regulation of nonlinear systems". In: *IEEE Transactions on Automatic Control* 35.2, pp. 131–140.

Izawa, Jun et al. (2008). "Motor adaptation as a process of reoptimization". In: *Journal of Neuroscience* 28.11, pp. 2883–2891.

Jiang, Z., A. Teel, and L. Praly (1994). "Small-gain theorem for ISS systems and applications". In: *Mathematics of Control, Signals and Systems* 7, pp. 95–120.

Kaddissi, C., M. Saad, and J.-P. Kenne (2009). "Interlaced Backstepping and Integrator Forwarding for Nonlinear Control of an Electrohydraulic Active Suspension". In: *Journal of Vibration and Control* 15.1, pp. 101–131.

Kambhampati, C., F. Garces, and K. Warwick (2000). "Approximation of non-autonomous dynamic systems by continuous time recurrent neural networks". In: *Proceedings of the IEEE-INNS-ENNS International Joint Conference on Neural Networks. IJCNN 2000. Neural Computing: New Challenges and Perspectives for the New Millennium*. Vol. 1, 64–69 vol.1.

Karagiannis, D. and A. Astolfi (2005). "Nonlinear observer design using invariant manifolds and applications". In: *Proceedings of the 44th IEEE Conference on Decision and Control*. IEEE, pp. 7775–7780.

Karagiannis, D., D. Carnevale, and A. Astolfi (2008). "Invariant manifold based reduced-order observer design for nonlinear systems". In: *IEEE Transactions on Automatic Control* 53.11, pp. 2602–2614.

Khalil, H. (2002). *Nonlinear systems*. Prentice-Hall.

Kim, K.-S. and Y. Kim (2003). "Robust backstepping control for slew maneuver using nonlinear tracking function". In: *IEEE Transactions on Control Systems Technology* 11.6, pp. 822–829. DOI: 10.1109/TCST.2003.815608.

Kim, Sunjun et al. (2020). "Optimal Sensor Position for a Computer Mouse". In: *Proceedings of the 2020 CHI Conference on Human Factors in Computing Systems*, pp. 1–13.

Kokotovic, P. V. (1992). "The joy of feedback: nonlinear and adaptive". In: *IEEE Control Systems Magazine* 12.3, pp. 7–17.

Korotina, Marina et al. (2020). "On parameter tuning and convergence properties of the DREM procedure". In: *2020 European Control Conference (ECC)*. IEEE, pp. 53–58.

Kowalevsky, S. von (1875). "Zur Theorie der partiellen Differentialgleichung". In: *Journal für die reine und angewandte Mathematik* 80, pp. 1–32.

Krishnamurthy, P., F. Khorrami, and R. S. Chandra (2003). "Global high-gain-based observer and backstepping controller for generalized output-feedback canonical form". In: *IEEE Transactions on Automatic Control* 48.12, pp. 2277–2283. DOI: 10.1109/TAC.2003.820226.

Lank, Edward, Yi-Chun Nikko Cheng, and Jaime Ruiz (2007). "Endpoint prediction using motion kinematics". In: *Proceedings of the SIGCHI conference on Human Factors in Computing Systems*, pp. 637–646.

Leondes, C. and L. Novak (1974). "Reduced-order observers for linear discrete-time systems". In: *IEEE Transactions on Automatic Control* 19.1, pp. 42–46.

Levant, Arie (2003). "Higher-order sliding modes, differentiation and output-feedback control". In: *International journal of Control* 76.9-10, pp. 924–941.

Li, C. et al. (2006). "Stability of genetic networks with SUM regulatory logic: Lur'e system and LMI approach". In: *IEEE Transactions on Circuits and Systems I: Regular Papers* 53.11, pp. 2451–2458.

Liberzon, M. (2006). "Essays on the absolute stability theory". In: *Autom Remote Control* 67, pp. 1610–1644.

Ljung, Lennart (1999). *System identification: theory for the user*. Prentice Hall PTR.

Luenberger, D. G. (1964). "Observing the state of a linear system". In: *IEEE transactions on military electronics* 8.2, pp. 74–80.

Lyapunov, Aleksandr Mikhailovich (1992). "The general problem of the stability of motion". In: *International journal of control* 55.3, pp. 531–534.

Martín, J Alberto Álvarez et al. (2021). "Intermittent control as a model of mouse movements". In: *ACM Transactions on Computer-Human Interaction (TOCHI)* 28.5, pp. 1–46.

Mei, W., D. Efimov, and R. Ushirobira (2020). "Towards state estimation of Persidskii systems". In: *59th IEEE CDC 2020 - Conference on Decision and Control*.

Meyer, David E et al. (1988). "Optimality in human motor performance: ideal control of rapid aimed movements." In: *Psychological review* 95.3, p. 340.

Moreno, J. and G. Besancon (2021). "On multi-valued observers for a class of single-valued systems". In: *Automatica* 123, p. 109334.

Müller, Jörg, Antti Oulasvirta, and Roderick Murray-Smith (2017). "Control theoretic models of pointing". In: *ACM Transactions on Computer-Human Interaction (TOCHI)* 24.4, pp. 1–36.

Narendra, K. S. and A. M. Annaswamy (2005). *Stable adaptive systems*. Dover Publications.

Nijmeijer, H. and I.M.Y. Mareels (1997). "An observer looks at synchronization". In: *IEEE Transactions on Circuits and Systems I: Fundamental Theory and Applications* 44.10, pp. 882–890. DOI: 10.1109/81.633877.

Nizami, T. K., A. Chakravarty, and C. Mahanta (2017). "Design and implementation of a neuro-adaptive backstepping controller for buck converter fed PMDC-motor". In: *Control Engineering Practice* 58, pp. 78–87. ISSN: 0967-0661. DOI: https://doi.org/10.1016/j.conengprac.2016.10.002. URL: https://www.sciencedirect.com/science/article/pii/S0967066116302325.

Oirschot, Hilde Keuning-van and Adrian JM Houtsma (2001). "Cursor displacement and velocity profiles for targets in various locations". In: *Proceedings of Eurohaptics*. Citeseer, pp. 108–112.

Oulasvirta, Antti et al. (2018). *Computational interaction*. Oxford University Press.

Padoan, A. and A. Astolfi (2020). "Singularities and Moments of Nonlinear Systems". In: *IEEE Transactions on Automatic Control* 65.8, pp. 364–3654.

Pasqual, Phillip T and Jacob O Wobbrock (2014). "Mouse pointing endpoint prediction using kinematic template matching". In: *Proceedings of the SIGCHI Conference on Human Factors in Computing Systems*, pp. 743–752.

Pavlov, A., N. Wouw, and H. Nijmeijer (2005). "Convergent Systems: Analysis and Synthesis". In: vol. 322. Springer, pp. 131–146.

Perruquetti, Wilfrid, Thierry Floquet, and Emmanuel Moulay (2008). "Finite-time observers: application to secure communication". In: *IEEE Transactions on Automatic Control* 53.1, pp. 356–360.

Persidskii, S. K. (1969). "Problem of absolute stability". In: *Autom. Remote Control* 1969, pp. 1889–1895.

Qian, Ning et al. (2013). "Movement duration, Fitts's law, and an infinite-horizon optimal feedback control model for biological motor systems". In: *Neural computation* 25.3, pp. 697–724.

Rajamani, R. and Y. M. Cho (1998). "Existence and design of observers for nonlinear systems: Relation to distance to unobservability". In: *International Journal of Control* 69.5, pp. 717–731.

Rigoux, Lionel and Emmanuel Guigon (2012). "A model of reward-and effort-based optimal decision making and motor control". In.

Rozado, David (2013). "Mouse and keyboard cursor warping to accelerate and reduce the effort of routine HCI input tasks". In: *IEEE Transactions on Human-Machine Systems* 43.5, pp. 487–493.

Ruiz, Jaime and Edward Lank (2009). "Effects of Target Size and Distance on Kinematic Endpoint Prediction". In.

— (2010). "Speeding pointing in tiled widgets: Understanding the effects of target expansion and misprediction". In: *Proceedings of the 15th international conference on Intelligent user interfaces*, pp. 229–238.

Sandy, T. et al. (2019). "Confusion: Sensor fusion for complex robotic systems using nonlinear optimization". In: *IEEE Robotics and Automation Letters* 4.2, pp. 1093–1100.

Scarciotti, G. and A. Astolfi (2017a). "Data-driven model reduction by moment matching for linear and nonlinear systems". In: *Automatica* 79, pp. 340–351.

— (2017b). “"Nonlinear Model Reduction by Moment Matching"”. In: *Foundations and Trends in Systems and Control* 4.3-4, pp. 224–409.

Senanayake, Ransalu, Ravindra S Goonetilleke, and Errol R Hoffmann (2015). “Targeted-tracking with pointing devices”. In: *IEEE Transactions on Human-Machine Systems* 45.4, pp. 431–441.

Sepulchre, R., M. Jankovic, and P. V. Kokotovic (1997). “Integrator forwarding: A new recursive nonlinear robust design”. In: *Automatica* 33.5, pp. 979–984. ISSN: 0005-1098. DOI: https://doi.org/10.1016/S0005-1098(96)00249-X. URL: https://www.sciencedirect.com/science/article/pii/S000510989600249X.

Sepulchre, R., M. Janković, and P.V. Kokotović (1997). *Constructive Nonlinear Control*. Communications and Control Engineering. Springer London. ISBN: 9783540761273. URL: https://books.google.fr/books?id=JKIeAQAAIAAJ.

Sontag, E. and Y. Wang (1995). “On Characterizations of Input-to-State Stability with Respect to Compact Sets”. In: *IFAC Proceedings Volumes* 28.14, pp. 203–208.

— (2000). “Lyapunov Characterizations of Input to Output Stability”. In: *SIAM Journal on Control and Optimization* 39.1, pp. 226–249.

Sontag, E. D. and Y. Wang (1997). “Output-to-state stability and detectability of nonlinear systems”. In: *Systems & Control Letters* 29.5, pp. 279–290.

Spong, M. W. (1987). “Modeling and control of elastic joint robots”. In.

Sundarapandian, V. (2006a). “Reduced order observer design for discrete-time nonlinear systems”. In: *Applied Mathematics Letters* 19.10, pp. 1013–1018.

— (2006b). “Reduced order observer design for nonlinear systems”. In: *Applied mathematics letters* 19.9, pp. 936–941.

Thau, F. E. (1973). “Observing the state of non-linear dynamic systems”. In: *International journal of control* 17.3, pp. 471–479.

Todorov, Emanuel (2004). “Optimality principles in sensorimotor control”. In: *Nature neuroscience* 7.9, pp. 907–915.

Todorov, Emanuel and Michael I Jordan (2002). “Optimal feedback control as a theory of motor coordination”. In: *Nature neuroscience* 5.11, pp. 1226–1235.

Todorov, Emanuel and Weiwei Li (2005). “A generalized iterative LQG method for locally-optimal feedback control of constrained nonlinear stochastic systems”. In: *Proceedings of the 2005, American Control Conference, 2005.* IEEE, pp. 300–306.

Wang, Jian, Denid Efimov, and Alexey A Bobtsov (2019). “Finite-time parameter estimation without persistence of excitation”. In: *2019 18th European Control Conference (ECC)*. IEEE, pp. 2963–2968.

Weisberg, Sanford (2005). *Applied linear regression*. Vol. 528. John Wiley & Sons.

Yakubovich, V.A. (2002). “Popov’s Method and its Subsequent Development”. In: *European Journal of Control* 8.3, pp. 200–208. DOI: https://doi.org/10.3166/ejc.8.200-208.

Yalçin, Müstak E, Johan AK Suykens, and Joos Vandewalle (2001). “Master–slave synchronization of Lur’e systems with time-delay”. In: *International Journal of Bifurcation and Chaos* 11.06, pp. 1707–1722.

Yassen, M.T. (2003). “Adaptive control and synchronization of a modified Chua’s circuit system”. In: *Applied Mathematics and Computation* 135.1, pp. 113–128. ISSN: 0096-3003. DOI: https://doi.org/10.1016/S0096-3003(01)00318-6.

Zhai, Shumin, Jing Kong, and Xiangshi Ren (2004). “Speed–accuracy tradeoff in Fitts’ law tasks—on the equivalency of actual and nominal pointing precision”. In: *International journal of human-computer studies* 61.6, pp. 823–856.

Zhang, X. et al. (2011). “Design of Stabilizing Controllers With a Dynamic Gain for Feedforward Nonlinear Time-Delay Systems”. In: *IEEE Transactions on Automatic Control* 56.3, pp. 692–697. DOI: 10.1109/TAC.2010.2097150.

Zhong, G.-Q. (1994). “Implementation of Chua’s circuit with a cubic nonlinearity”. In: *IEEE Transactions on Circuits and Systems I: Fundamental Theory and Applications* 41.12, pp. 934–941. DOI: 10.1109/81.340866.

Ziebart, Brian, Anind Dey, and J Andrew Bagnell (2012). "Probabilistic pointing target prediction via inverse optimal control". In: *Proceedings of the 2012 ACM international conference on Intelligent User Interfaces*, pp. 1–10.